Poster Session A (Dec. 1)

Poster Session B (Dec. 2)

Electrical potential oscillation induced by salt water oscillation

Kei Abe

Graduate School of Science, Chiba University
Chiba University, Yayoi-cho 1-33, Inage-ku, Chiba 263-8522, Japan

The electrical potential between two aqueous solutions, derived from the concentration gradient, has been frequently studied in electrochemistry such as diffusion potential.

In 1970, Martin found an interesting phenomenon [1]. When a small vessel, bored a vertical small hole at the center of the bottom, is filled with salt-water and partially submerged in a large vessel of pure-water, in the system oscillations are observed (Fig. 1(A)). The oscillation appears as an alternation between a downward jet of salt-water and an upward jet of pure-water through the small hole (Fig.1(B)).

While this oscillation is running, the electrical potential shows a rhythmic change of the flip-flop type. The electrical potential takes two certain values, although the neighborhood concentrations of the both electrodes have been keeping initial conditions. In addition, the oscillations of the flow and electrical voltage have the same periods and electrical potential depends on the direction of water flow but not on the rate of the flow (Fig. 2(B)). This electrical potential oscillation was discovered by Yoshikawa *et al*. and they suggested the potential is due to the diffusion potential described Henderson equation [2]. He also suggested this equation depends neither on the direction nor on rate of the solution flow.

We study the electrical potential with a downward or upward jet using several flow rate and different density of solutions, and would like to discuss the contribution of the solution flow and concentration gradient.

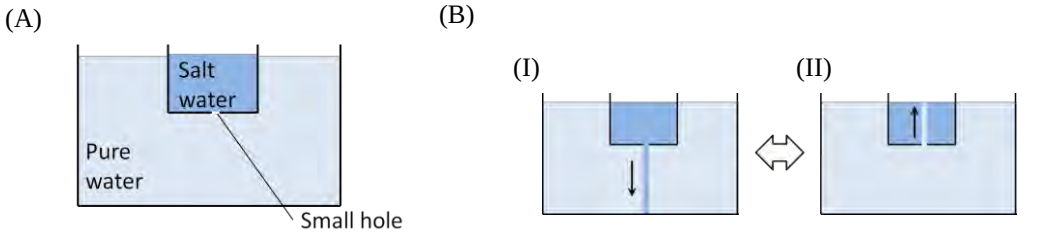

Fig. 1. (Color online) (A) Experimental apparatus for salt water oscillator. (B) Schematic representation of the oscillatory water flow, (I)Downward flow of salt-water, (II)Upward flow of pure-water.

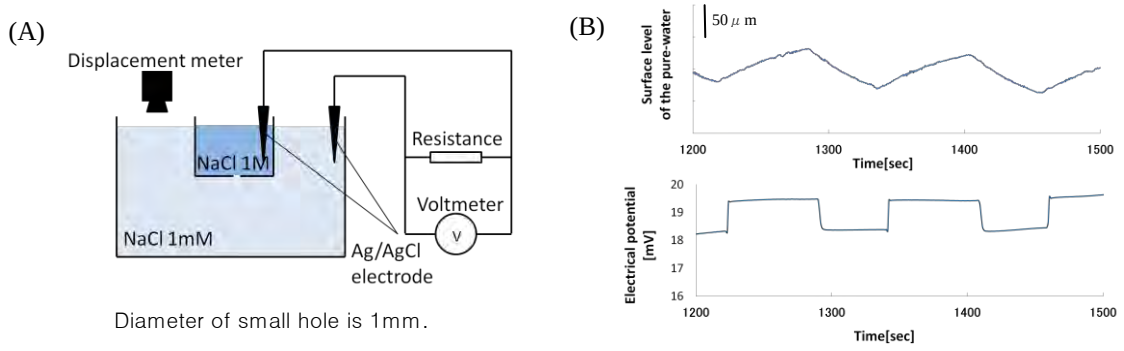

Fig. 2. (Color on line) (A) Experimental apparatus for the measurement of electrical potential (B) Experimental results of pure-water level and electrical potential between 1M salt-water and 1mM salt-water.

REFERENCES

[1] S. Martin, ”A hydrodynamic curiosity : The salt oscillator” , *Geophys. Fluid Dyn*. , 1, 143-160(1970).

[2] K. Yoshikawa, S. Maeda, and H. Kawakami, “Various oscillatory regimes and bifurcations in a dynamic chemical system at an interface” , *Ferroelectrics*, 86, 281-298 (1988).

Pattern Formation of Bacterial Colonies by Pseudomonas aeruginosa

Mina Arima, Ryuto Kumata, Jun-ichi Wakita, Tohey Matsuyama, and Mitsugu Matsushita

Department of Physics, Chuo University

When a small amount of *Pseudomonas(P.) aeruginosa* are inoculated on agar medium with nutrient, they increase and form a colony on the surface of agar medium. The colony varies its morphology depending on concentrations of agar and nutrient, and shows some characteristic patterns (Fig.1).

We are interested in the concentric-ring pattern of *P. aeruginosa* which is formed in the region A3 (Fig.1). In the previous study, we found that the growing front of the concentric-ring pattern repeated migration and consolidation phases changing its size oscillatory. Therefore we suppose that there is the relationship of bistability between the size and the mobility of bacterial collectives. In this study, we focus on the fluid-spreading pattern to investigate this relationship. The concentration of agar is lowered from the case of concentric-ring patterns, then the colonies grow very fast and expand to the edge of a laboratory dish (about 88mm in diameter) within a day.

We observe the growing process of the fluid-spreading patterns in the beginning of a colony expansion, because they spread out homogenously keeping the growing front stable in this stage. As a result, we have found that a colony begins to expand when the density of bacterial cells at an inoculation spot becomes high and stops its expansion when the density inside the growing colony becomes low. We wish to find the appropriate condition on which the colonies begin to expand uniformly to investigate the relationship of bistability between the size and the mobility of bacterial collectives.

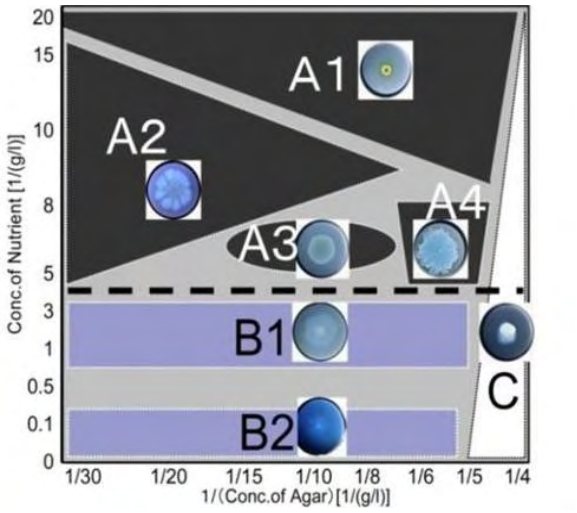

Fig.1 Morphological diagram of *P. aeruginosa* colonies.

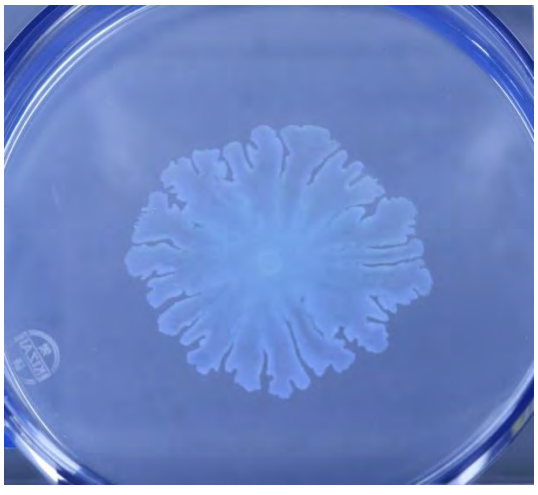

Fig.2 A fluid-spreading colony of *P. aeruginosa* during its growth.

REFERENCE

1. Y.Yanagawa, “Concentric-ring Colonies of Bacterial Species *Pseudomonas aeruginosa*”, master’s thesis (2010), Chuo University.

Simulation of three-dimensional granular materials with polyhedral discrete elements

Jian Chen Hans-Georg Matuttis

Department of Mechanical Engineering and Intelligent Systems,
Graduate School of Informatics and Engineering,
The University of Electro-Communications, Chofugaoka 1-5-1, Chofu-shi, Tokyo, Japan

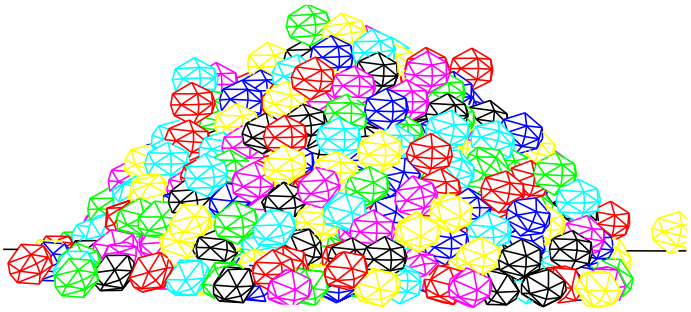

Fig. 1 Heap formation in three dimensional space on a flat floor [1].

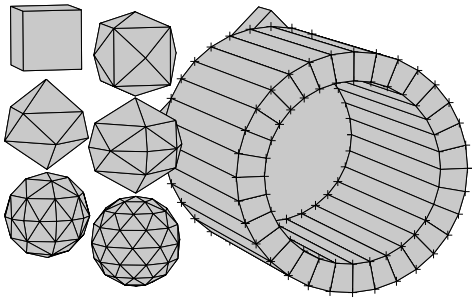

Fig. 2 Particle shapes used in the simulation of the rotating drum [2].

The discrete element method (DEM) has been widely used in the field which allows simulations of complex behavior of granular materials without constitutive laws. In the last years, it has become increasingly clear that the dynamics (competition between rolling and sliding) of non-spherical granular materials is governed essentially by the deviations of the particle shape from ideal spheres, i.e. by the roughness and by the elongation.

We developed a DEM program for polyhedral granular materials with a contact force model which takes into account the whole geometry of the overlap polyhedron between non-deformed poly- hedral particles [1]. The contact point is defined as the center of mass of the overlap polyhedron and the normal of the contact area is defined as the average of the area-weighted normals of the contact triangles which are formed by the center of mass of the overlap polyhedron and the generated vertices (the intersection points of two polyhedra). The volume of the overlap polyhedron is used as a measure for the elastic force and its changes for the damping force in normal direction. The characteristic length is defined to model the contact force, with which in the elastic force model, the continuum-mechanical sound velocity can be recovered for a space-filling packing of cubic blocks. The two- dimensional Cundall-Strack model is generalized for three dimensions as the approximation for friction.

Simulation results for heaps show more realistic high angles of repose than any penetration length based simulations with either round or polyhedral particles [1]. As verification, consistent results have obtained from the developed DEM code and the experiments for quasi-two-dimensional heaps with respect to density distribution patterns and the existence of pressure dip in the simulation [3]; consistent results have also been obtained from the investigation of the dynamics of avalanches inside rotating by the DEM code and the corresponding experiments [2]. With our polyhedral DEM code, a larger phenomenology is accessible than either with round particles or with penetration length based force model.

REFERENCES

1. J. Chen, A. Schinner and H.-G. Matuttis, "Discrete Element Simulation for Polyhedral Granular Particles", *Theoretical and Applied Mechanics Japan*, **59**, p. 335-346 (2010)
2. J. Chen, T. Matsuyama, E. Seo and H.-G. Matuttis, "Micro-avalanches of granular particles inside rotating drums: a numerical and experimental study", *Journal of the Physical Society of Japan*, to be submitted
3. J. Chen and H.-G. Matuttis, "Study of Quasi Two Dimensional Granular Heaps", *Theoretical and Applied Mechanics Japan*, **60**, to appear (2011)

Simple models for Quorum sensing

W. Y. Chiang[1], Yue-Xian Li[2] and, Pik-Yin Lai[1]

[1]*Dept. of Physics and Center for Complex Systems, National Central University, Chung-Li, 320 Taiwan*

[2] *Dept. of Mathematics and Dept. of Zoology, University of British Columbia, Vancouver, Canada*

Quorum sensing refers to the change in the cooperative behavior of a collection of elements in response to the change in their population size or density. This behavior can be observed in chemical and biological systems. These elements/cells are coupled via chemicals in the surrounding environment. Here we focus on thechange of dynamical behavior, in particular from quiescent tooscillatory, as the cell population changes. For instance, the silent behavior of the elements can become oscillatory as the systemconcentration/population increases. In this work, two simple modelsare constructed that can produce the essential representativeproperties in quorum sensing. The first is an excitable/oscillatory phase model, which is probably the simplest model one can construct to describe quorum sensing. Using the mean-field approximation, the parameter regime for quorum sensing behavior can be identified, analytical results for the detailed dynamical properties, including the phase diagrams, are obtained and verified numerically. The second model consists of FitzHugh-Nagumo elements coupled to the signaling chemicals in the environment. Nonlinear dynamical analysis of this mean-field model exhibits rich dynamical behaviors, such as infinite period bifurcation, super-critical Hopf, fold bifurcation and sub-criticalHopf bifurcations as the population parameter changes for differentthe coupling strengths. Analytical result is obtained for the Hopfbifurcation phase boundary. Furthermore, two elements coupled viathe environment and their synchronization behavior for these twomodels is also investigated. For both models, it is found that the onset of oscillations is accompanied by the synchronized dynamics of the two elements. We further consider the effect of diffusion of the signaling chemicals with a spatial concentration profile, and analyze the bifurcation due to the onset of quorum sensing. Possible applications and extension of these models are also discussed.

Noise effect on force measurement on a particle confined in a thermo-osmotic trap

Mark Nolan P. Confesor[1], Pik-Yin Lai[1] and C.K. Chan[1,2]

[1]*Department of Physics and Graduate Institute of Biophysics, National Central University, Jhongli City 320, Taiwan*
[2]*Institute of Physics, Academia Sinica, Nankang, Taipei 115, Taiwan*

Multiplicative noise such as due to the presence of spatially dependent diffusion coefficient can give rise to different result for different force measurement approach. The force obtained from equilibrium-distribution approach and by drift approach differs by a factor of the drift induced by the spatially varying diffusion [1]. Here we investigate this effect further by having a particle in thermo-osmotic trap [2]. We measure the force by both the equilibrium and drift method. For the radial trapping force the two approaches give equal result. However much deviation is seen for the force along the z-axis such that even the functional form of the force is not the same.

REFERENCES

1. Volpe, G. *et al.* "Influence of Noise on Force Measurements", *Phys. Rev. Lett.*, 104, 170602 (2011).
2. Jiang, H.R. et al. "Maniuplation of colloids by Nonequilibrium Depletion Force in Temperature Gradients", *Phys. Rev. Lett.*, 102, 208301 (2009).

Model of the heaping in vibrated suspensions under slip/non slip switching boundary condition

Hiroyuki Ebata, Masaki Sano

Department of Physics, Graduate school of Science,
The University of Tokyo, Tokyo, 113-0033, Japan

There has been growing interests in instabilities and rheological properties of non-Newtonian fluids, including surface instabilities induced by vertical vibration. Various surface instabilities are found in vertically vibrated suspension, for example, heaping [1], stable hole, expanding hole and replicating hole. Dense suspensions have interesting rheological features, such as yield stress, shear thinning and shear thickening and so on. It is important to reveal which rheological features are crucial for the surface instabilities in dense suspensions. We focus on the heaping in vibrated non-density matched suspension and propose a model of heaping. When the non-density matched suspension is vertically vibrated, the flat surface become unstable and deformation of surface grows to form heaps (see Fig. 1). In our model, we assume that the boundary condition changes as the direction of the gravity changes. In the experiment, granules are heavier than surrounded fluid. Therefore, if gravity $g(t)$, which includes inertial force due to vibration, works downward, granules are pushed on the bottom wall. On the other hand, if the gravity $g(t)$ works upward, granules should unstick from the bottom wall. Thus, we assume that suspension slips on the wall if $g(t)>0$ and suspension sticks on the wall if $g(t)<0$. This condition is written as following.

$$u_w = \beta\theta(g(t))\tau_w$$

where u_w, β, and τ_w are velocity on the wall, slip length and shear stress on the wall, respectively. $\theta(x)$ is step function of x and $g(t)=g(-1+\Gamma\sin\omega t)$. To derive the model equation, we use incompressible Navier-Stokes equations, lubrication approximation and Stokes approximation. Then time evolution equation of fluid layer becomes following.

$$\eta\partial_t h = -\partial_x\left\{\left(\frac{1}{3}h^3 + \beta\theta(g(t))h^2\right)\left(\rho g(t) + \sigma\partial_x^2\right)\partial_x h\right\} \qquad (1)$$

where h, η, ρ and σ are depth of the layer, viscosity, density and surface tension, respectively. We calculate Eq. (1) with periodic boundary condition. If the acceleration Γ is sufficiently large, flat surface become unstable and steady deformation appears and grows to form heaps (see Fig. 2). From the linear stability analysis of Eq. (1), we find that the onset acceleration is independent of the vibration frequency ω. We also find convection like flow in the heaping. These results are comparable to the experimental result. We will also show the result of the non-Newtonian case.

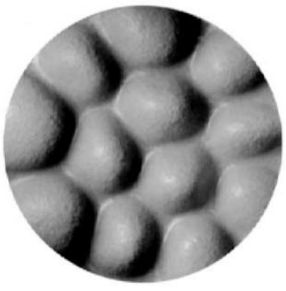

Fig.1 Heaping in the experiment [1]

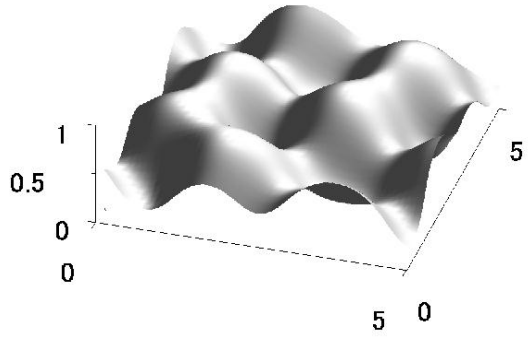

Fig.2 Surface instability found in Eq. (1)

REFERENCES

1. J.M. Schleier-Smith and H.A. Stone, Phys. Rev. Lett. **86**, 3016 (2001).

Oscillatory Instability of Slow Crack Propagation in Rubbers under Large Deformation

Daiki Endo

Department of Physics, Graduate School of Science,
Tohoku University, Aramaki Aza-Aoba 6-3, Aobaku, Sendai, Miyagi, Japan

When a rubber balloon is ruptured, oscillatory crack patterns in macroscopic scales can be seen quite robustly [1]. This phenomenon draws much attention of investigators. Recently, Deegans et al. have performed an excellent experiment of the rapid fracture of rubber sheets by stretching and rupturing the sheet under biaxial strain in the air, and have demonstrated the transition from a straight crack pattern to oscillatory one depending on applied biaxial strain [2]. After that experiment, the wavy crack pattern and the transition in rubber sheets are reproduced by the numerical simulations with some models [3, 4], and several possible factors behind the instability, such as hyperelasticity, viscoelasticity, and nonlocal elasticity are suggested.

However, the mechanism of the oscillating instability is still not understood due to difficulty in treating a fast crack dynamics on which inertia is significant. Hence, if we could design an experiment where the crack propagation speed is quite reduced, we might be able to find an alternative approach to the oscillatory crack propagation in rubber films. Therefore, we propose a slow fracture experiment in which a rubber film is stretched and ruptured on a highly viscous oil. In this experimental system, we are able to control the crack propagation speed by changing the viscosity of the oil and the inertial effects of the rubber can be negligible in the overdamping limits. Note that the rubber film has a cylindrical shape and applied strain is always uniaxial for convenience of experiments. In the experiment, we have found an oscillatory instability of crack propagation when the applied uniaxial strain becomes smaller than a characteristic value. The transition from a straight pattern to oscillatory one arises around at a strain where strong nonlinear elasticity of the rubber film appears. We, therefore, expected that nonlinear elasticity may be a key factor for the crack pattern instabilities. To examine this expectation, we have conducted numerical simulations based on the neo-Hookean model showing the nonlineality at large strains. By comparing the results with those from the usual linear elastic model, we show the nonlinear elasticity is the essential factor to induce oscillatory instabilities.

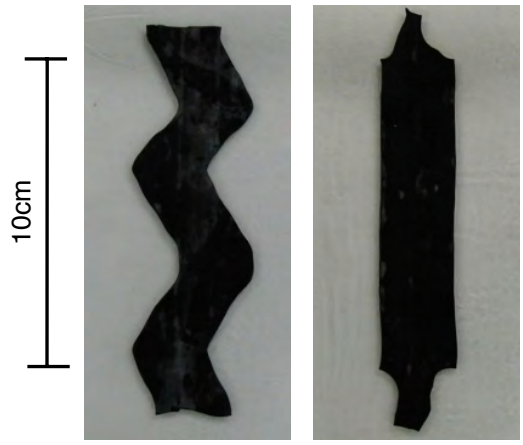

Fig.1 Rubber films after rupture. A typical oscillatory pattern(left) and straight one(right) have been left by crack propagation.

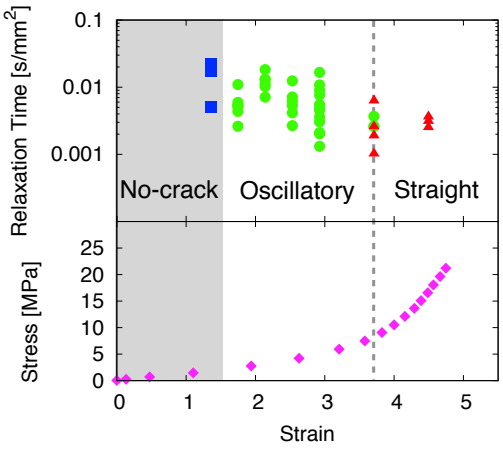

Fig.2 Crack pattern diagram(upper) and stress-strain curve of rubber films(lower). Relaxation time gives an indication of the intensity of the resistance from the oil.

REFERENCES

1. A. Stevenson and A. Thomas, J. Phys. D **12**, 2101 (1979).
2. R. Deegan, P. Petersan, M. Marder, and H.Swinney, Phys. Rev. Lett. **88**, 014304 (2002).
3. H. Henry and H. Levine, Phys. Rev. Lett. **93**, 105504 (2004).
4. W. Wang and S. Chen, Phys. Rev. Lett. **95**, 144301 (2005).

Modeling Competition of More than Two Languages

Ryo Fujie[1,2], Naoki Masuda[3,4], and Kazuyuki Aihara[1,2,3]

[1]*FIRST, Aihara Innovative Mathematical Modelling Project, Japan Science and Technology Agency, 4-6-1 Komaba, Meguro-ku, Tokyo 153-8505, Japan*

[2]*Institute of Industrial Science, The University of Tokyo, 4-6-1 Komaba, Meguro-ku, Tokyo 153-8505, Japan*

[3]*Department of Mathematical Informatics, The University of Tokyo, 7-3-1 Hongo, Bunkyo-ku, Tokyo 113-8656, Japan*

[4]*PRESTO, Japan Science and Technology Agency, 4-1-8 Honcho, Kawaguchi, Saitama 332-0012, Japan*

Language competition is an example of consensus problems. Recent interests in this problem have been triggered by the model proposed by Abrams and Strogatz (AS-model) [1] to account for the data of extinction of endangered languages. Many of studies dealing with this problem assume that agents prefer the majority as described by, for example, the standard majority rule. Although "the preference for the majority" and "the aversion to the minority" result in the same dynamics in two options (e.g., languages) case, they may cause different dynamics in the case of more than two options.

We extend the AS-model, which was originally proposed for two options, to the case of n options ($n \geqq 3$). Each agent is assumed to select the option according to the preference for the majority rule (model 1) or the aversion to the minority rule (model 2). The time evolution of share of option i is expressed as

$$\dot{x}_i = \sum_{j \neq i} P_{ji} x_j - \sum_{j \neq i} P_{ij} x_i, \tag{1}$$

$$P_{ji} = \begin{cases} s_i x_i^a & \text{for model 1,} \\ (1-s_j)(1-x_j)^a & \text{for model 2,} \end{cases} \tag{2}$$

where a is a parameter and s_i is the strength of option i. We show numerically and analytically that the coexistence conditions are independent of n ($\geqq 2$) in model 1. In model 2, however, the n option system ($n \geqq 3$) can reach the coexistence state for the parameter values that result in the monopoly state when $n=2$.

This research is partially supported by the Aihara Innovative Mathematical Modelling Project, the Japan Society for the Promotion of Science (JSPS) through the "Funding Program for World-Leading Innovative R&D on Science and Technology (FIRST Program)," initiated by the Council for Science and Technology Policy (CSTP).

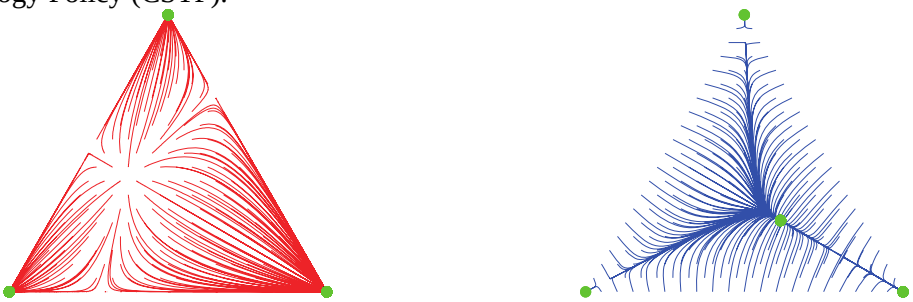

Fig.1 (Color Online) Population dynamics of competition of three options in model 1 (left) and model 2 (right) with a=1.3, s_1=s_2=0.3, and s_3=0.4.

REFERENCES

1. Abrams, D. M. and Strogatz, S. H. "Linguistics: Modelling the dynamics of language death", *Nature*, 424, 900(2003).

Text Structure Analysis in the Framework of Complex Network

Sho Furuhashi

Department of Physics, Graduate School of Science, Tohoku University,
Aza-Aoba, Aramaki, Aoba-ku, Sendai, Miyagi, Japan

Human written language is one of important examples of complex systems in nature. The character of human written language has been examined within the framework of complex network.

Words are simple elements of this system and combine in accordance with syntax. If we consider words as nodes and their relationships as links, this system can be represented as network. By using the network representation, we can investigate the character of their relationships (co-occurrence, syntactic dependency and semantic dependency) and compare the similarities between different languages (e.g., English [1] and Chinese [2]). Previous studies reported that these networks exhibit small-world and scale-free features.

In this poster, we focus on the relationships among sentences in texts in order to characterize human writing. In discourse analysis, contextual sentence relationship of text is often studied. To the contrary, we analyze network structures constructed from co-occurrence between sentences.

We used a tagged corpus, Balanced Corpus of Contemporary Written Japanese (Monitor Edition), and public-domain texts stored in Gutenberg. We considered human written language as a directed network in which sentences are nodes and two nodes are linked if they are neighbors in texts. In this network, we labelled nodes not with original sentences but with the sequences of parts of speech consisting of them. Note that if different sentences have a same sequence of parts of speech, they are regarded as same nodes. Links have directions showing the appearance order of nodes in texts and a quantity denoting the frequency of the transition between two nodes (link weight). Moreover, in Japanese, we simplified sentences by using their dependency trees and reconstructed networks (Reconstructed Japanese in Fig. 1). We analyzed the networks and tried to find the character of text structure.

As a result, we found that these sentence co-occurrence networks have similar features to word co-occurrence networks. For example, degree and link weight distribution follow power-law in form (Fig. 1). These results indicate that text structure has same statistical features through different hierarchical levels.

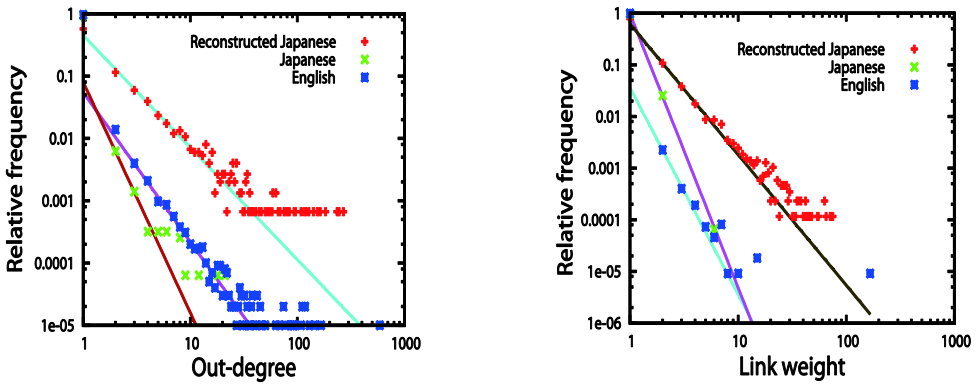

Fig. 1. The distribution of out-degree and link weight.

REFERENCES

1. A. P. Masucci and G. J. Rodgers, “Network properties of written human language”, *Phys. Rev. E*, 74, 026102 (2006).
2. Long Sheng and Chunguang Li, “English and Chinese languages as weighted complex networks”, *Physica A*, 388, 2561 (2009).

Simple gene networks models show cell differentiation behavior

Yusuke Goto[1], Shuji Ishihara[1,2], and Kunihiko Kaneko[1]

[1]*Department of Basic Science, University of Tokyo,Komaba, Meguro-ku, Tokyo 153-8902, Japan,* [2]*PRESTO, Japan Science and Technology Agency, Kawaguchi, Saitama, Japan*

In globally coupled chemical reaction network models gene network models, “differentiation” was observed [1,2]. In these models, cell to cell interactions enable coexistence of different cell states. The preceding works studied models with a large degrees of freedom. Here, we show a simplest model with a dynamical mechanism for such “differentiation” .

We considered a globally coupled gene regulatory network model composed of two genes x and y,as

$$\frac{dx_i}{dt} = \frac{1}{1+\exp[-40(J_{xx}x_i + J_{xy}y_i - c_x)]} - x_i$$

$$\frac{dy_i}{dt} = \frac{1}{1+\exp[-40(J_{yx}x_i + J_{yy}y_i - c_y)]} - y_i + D(\frac{1}{N}\sum_{k=1}^{N} y_k - y_i)$$

Jij: regulation of i gene by j gene
(1: activation 0: no regulation
-1: inhibition)
N: total cell number
i: cell number (i=1, 2,...,N)

We numerically studied all possible patterns of Jij, and examined whether they show differentiation or not. We found four differentiation types.Three of them were explained by known mechanisms; multi attractor, Turing instability, and oscillation death.

The other example we found shows coexistence of two different amplitude oscillation (Fig.1). Here, gene expression dynamics of a single cell shows oscillation near saddle-node bifurcation. By the influence of cell to cell interaction, phase desynchronization occurs, which drives a part of cells to go through bifurcation. In this process, diffusion term plays two important roles. Driving force to desynchronization and change in an effective bifurcation parameter.

We expect that this “desynchronization induced bifurcation” generally occurs in globally coupled oscillators near saddle-node bifurcation. We will provide some other simple models which show this type of differentiation.

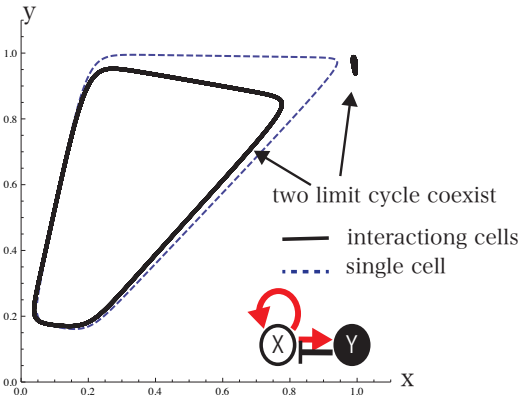

Fig1. gene network which shows coexistence of two different amplitude oscillation and steady states of cells with (without) interaction.

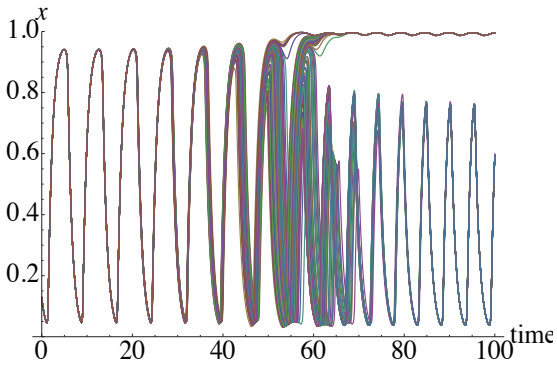

Fig2. dynamics of x gene expressions of 200cells.

REFERENCES

1. Furusawa. C. and Kaneko. K. “Emergence of Rules in Cell Society: Differentiation, Hierarchy, and Stability”, *Bull.Math.Biol.*60, 9070034(1998)
2. Suzuki, N., Furusawa, C., and Kaneko, K.”Oscillatory Protein Expression Dynamics Endows Stem Cells with Robust Differentiation Potential”, *PLoS One*, in press

A theoretical exploration of temperature compensation of Kai-protein-based circadian clock

Tetsuhiro Hatakeyama, Kunihiko Kaneko

Department of Basic Science, College of Arts and Sciences,
The University of Tokyo, Komaba 3-8-1, Meguro-ku, Tokyo, Japan

The circadian clock satisfies three criteria: persistence in constant conditions, phase resetting by light dark signals, and temperature compensation of the period, which is our concern here. In general, the period of chemical oscillator is very much sensitive to kinetic rate constants, which increase strikingly with temperature. Thus, the temperature compensation is an uncommon property of biochemical oscillators. Here, we propose a novel mechanism for this temperature compensation. Traditionally, “balance model” has often been adopted to explain the temperature compensation, where series of counterbalanced biochemical reactions in the core of clock are assumed to undergo equal and opposing changes against the temperature change. However, such “balance model” requires a delicate balance among temperature-dependent reactions and is unlikely to be robust to mutations or any fluctuations. Furthermore, Kondo and his colleagues recently demonstrated that the period of circadian oscillation of Kai-proteins indeed is temperature compensated (Nakajima, et al., 2005). By simulating a model with phosphoration/dephosphoration cyclic reactions (extended from van Zon, et al., 2007), we first demonstrated the temperature compensation of the period indeed works over a broad range of temperatures, without the need for tuning parameters in the reactions. We then unveiled the mechanism for it as enzyme-limited sequential reactions. We also showed that the oscillation is entrained to an external temperature cycle as seen in the experimental result (Yoshida, et al., 2009).

REFERENCES

1. M. Nakajima, K. Imai, H. Ito, T. Nishiwaki, Y. Murayama, H. Iwasaki, T. Oyama, T.Kondo (2005) "Reconstitution of circadian oscillation of cyanobacterial KaiC phosphorylation in vitro" Science 308, 5720: 414-415.
2. van Zon JS, Lubensky DK, Altena PR, ten Wolde PR. (2007) “An allosteric model of circadian KaiC phosphorylation” Proc Natl Acad Sci U S A. 04(18):7420-5.
3. T. Yoshida, Y. Murayama, H. Ito, H. Kageyama, T. Kondo. (2009) “Nonparametric entrainment of the in vitro circadian phosphorylation rhythm of cyanobcaterial KaiC by temperature cycle” Proc Natl Acad Sci U S A. 106(5):1648-53.

Randomization process of the flying arrangement within bird flocks

Yoshinori Hayakawa

Center for Information Technology in Education
Tohoku University, Kawauchi 41, Aoba-ku, Sendai, Japan

Bird flocks exhibit a rich variety of collective motion. For instance, we can often see *aerial acrobat* of large population of wild starlings even in the urban areas in Japan. Although structure and motion of such flocks seems to be self-organized in a decentralized manner, actual control mechanism of individual birds and rules of interactions have not been known, and understandings for them are still speculative.

For quantitative study of such complex dynamics, we conduct field measurements of airborne starlings in the northern region of Miyagi prefecture in Japan. To estimate the three-dimensional position of each individual, we developed a portable stereogrammetry system[1]. The distance resolution was ± 5 cm for the objects located 50 m away from the cameras, when the target object has an area of 64 x 64 pixels, at frame rate of 30 fps. The acquired movies are decomposed into a series of still images, and processed with an image processing software. The software automatically detects the moving object on the images and carries out matching of the objects in the stereo pairs. For better estimate of distance, it calculates the amount of the shift to a sub-pixel accuracy by using phase correlation.

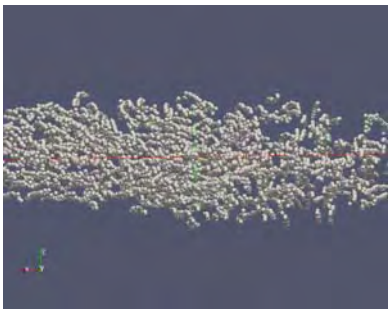

Fig.1 Front view of 3D trajectories of individual birds in a flock of starling. Duration of time is 1.1 s. Diameter of sphere corresponds to 6 cm in real scale.

From the positional data of individuals (e.g., Fig. 1), we calculate the local density in flock at position **r** and time t as $\rho(\mathbf{r},t)$. In practice, we divide the space into equal cubic region of 20 cm on the side, and the estimate $\rho(\mathbf{r},t)$ as the number density in the cubes. Note that the size of the cube is comparable to the body size of starling. From the density distribution, we estimate the spatio-temporal correlation function $C(\mathbf{x},\tau)$. Fig. 2 shows the typical profile of $C(\mathbf{x},\tau)$ for several time differences τ. Density autocorrelation $C(\mathbf{x},0)$ has a single sharp peak, so that there is no apparent correlation in the internal structure of flock, which is consistent to the results for neighbor distributions. Within a short time step comparable to the video frame rate, the sharp peak of coherence remains with some positional shift indicating simple translation of individuals in one direction. For a longer time difference τ, the profile of correlation becomes broader and the corresponding peak value decreases. It turned out that the peak value obeys a power law as $C^* \sim \tau^{-a}$, where $a \approx 3/2$ in the intermediate time scale shorter than seconds. By fitting the profile with a Gaussian form, we evaluate the root mean square distance of the mutual positional change. Its effective diffusion coefficient was of the order of 1 m^2/s. Our results suggest that individual birds in the flock behave like a Brownian tracer particles in a translational coordinate.

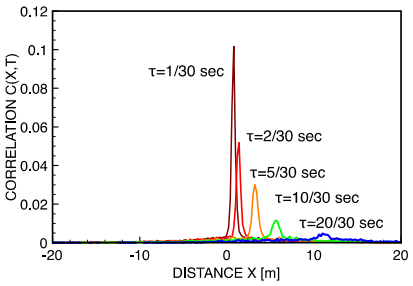

Fig.2 Fast decay of the spatio-temporal correlation.

If there are some social interactions that yield a preferable distance to neighbours as in intermolecular forces, a density wave can be excited depending on the conditions as a collective mode of the system. The randomization process of mutual arrangement, which is revealed by the present study, might be necessary for the stabilization of structure of flocks.

REFERENCES

1. *Spatiotemporal Dynamics of Skeins of Wild Geese*, Yoshinori Hayakawa, Europhysics Letters 89, 48004 (2010).

Size Frequency Distribution of Japanese Names

Ryo Hayakawa[1] and Tsuyoshi Mizuguchi[1, 2]

[1]*Department of Mathematical Sciences, School of Engineering,*

Osaka Prefecture University, 1-1 Gakuen-cho, Nakaku, Sakai, Osaka, 599-8531, Japan

[2]*JST, PRESTO, 4-1-8 Honcho, Kawaguchi, Saitama, 332-0012, Japan*

Size frequency distribution of the family names shows a power law behavior in several countries and areas [1] [2], where frequency ***n***(***s***) is a number of names having size ***s***. We focus on the case for the first names, and data obtained from Directory Database of **Re**search **a**nd **D**evelopment Activities (ReaD) are analyzed statistically. It is shown that the size frequency distribution of the first names also exhibits a power law behavior in rare name region with most of the same exponent as that of the family names (Fig.1).

Naming process of one person is different between his/her family name and first name, i.e., there is a rule that one person generally inherits his/her father's family name while there is no such a rule for the first name. The latter is chosen 'freely' such as an existing name or a completely new one that has never existed. Despite the difference of naming process, why do they exhibit a similar relationship in the size frequency distribution?

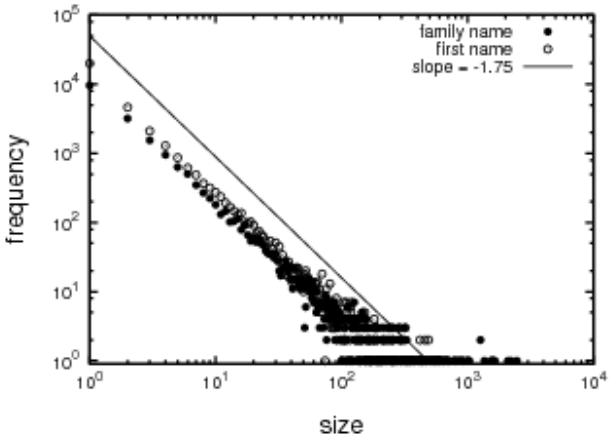

Fig.1 Size frequency distribution of the family names (・) and the first names (○) in ReaD. Both of them show power law behavior in rare name region with most of the same exponent.

To clarify this problem, we suggest a model consisting of a population having first names determined by Yule process. Power law behavior of the size frequency distribution is reproduced quantitatively by numerical simulation of this model.

REFERENCES

1. Miyazima, S. *et al*, "Power-law distribution of family names in Japanese societies", *Physica A*, **278**, 282 (2000).
2. Baek, S. K. , Kiet, H. A. T. , and Kim, B. J. , "Family name distributions: Master equation approach", *Phys. Rev. E*, **76**, 046113 (2007).

Collective Motion and Phase Transitions of Symmetric Camphor Boats in 1-D

Eric Heisler, Nobuhiko J. Suematsu[A], Akinori Awazu, Hiraku Nishimori

Dept. of Mathematical and Life Sciences, Hiroshima University,
1-3-1 Kagamiyama, Higashihiroshima, Hiroshima, Japan
[A]Meiji Institute for Advanced Study of Mathematical Sciences (MIMS),
1-1-1 Higashimita, Tamaku, Kawasaki, Japan

A model describing an ensemble of symmetric camphor boats moving in a one dimensional, circular channel displays several different patterns of collective behavior. Similar systems containing asymmetric boats have been studied previously and are explained further in [1]. A simple schematic of the system is shown in the figure to the right.

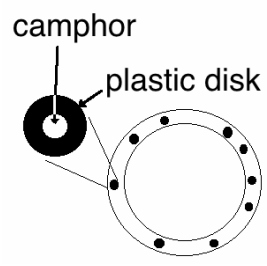

Depending on the viscous resistance in the system, the boats may exhibit: a) unidirectional flow, b) group oscillation, c) individual oscillation, d) evenly spaced, stationary patterns. These can be seen in Fig.1 and are listed in order of increasing viscosity.

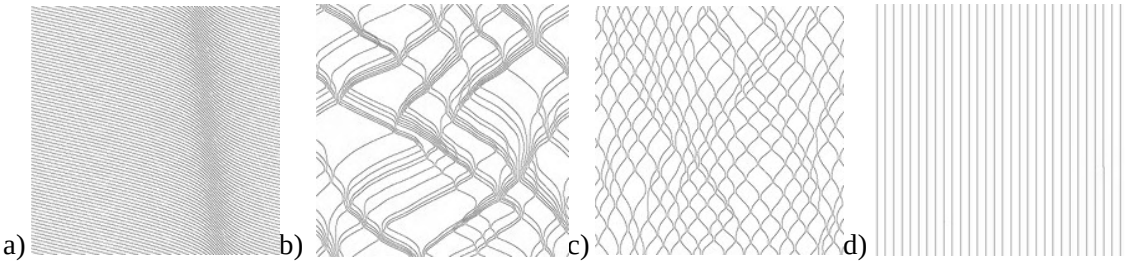

Fig.1 Space-time diagrams for a)unidirectional flow, b)group oscillation, c)individual oscillation, d)stationary pattern. The vertical axis is time.

Due to the oscillatory nature of the motion, a natural choice of order parameter is the average amplitude of oscillation, or more precisely, the average distance travelled between changes in direction. This value clearly shows distinct behavior for each phase as seen in Fig.2. The degree of synchronization, measured here as the zero-lag cross correlation of the velocity of neighboring boats, is also useful for distinguishing the two types of oscillation.

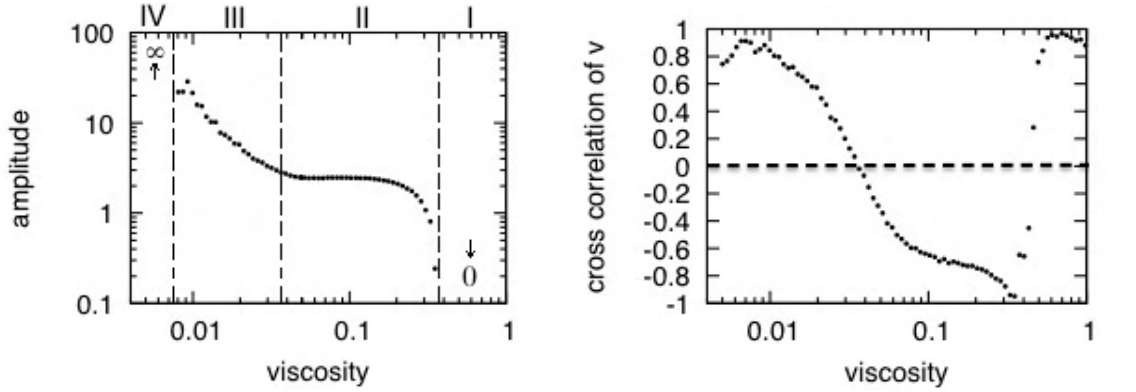

Fig.2 Average amplitude and cross correlation of velocity.

REFERENCES

1. Suematsu N. J. *et al.* "Collective Behavior of Inanimate Boats", *Phys. Rev. E*, 81, 056210 (2010).

Percolation analysis of the Cosmic Microwave Background radiation

Masaya Higuchi, Naoki Kobayashi, Jun-ichi Wakita, Yoshihiro Yamazaki[1], Hiroto Kuninaka[2], Makoto Katori, Mitsugu Matsushita, Satoki Matsushita[3], and Lung-Yih Chiang[3]

Department of Physics, Chuo University, Kasuga, Bunkyo-ku, Tokyo, Japan
[1] *Department of Physics, Waseda University, Okubo 3-4-1, Shinjuku-ku, Tokyo, Japan*
[2] *Department of Education, Mie University, Kurima-Machiya-cho, Tsu, Mie, Japan*
[3] *Institute of Astronomy and Astrophysics, Academia Sinica, Taipei, R.O.C.*

The Cosmic Microwave Background (CMB) radiation is the thermal radiation (black-body radiation) emitted about 380,000 years later after the birth of the universe. The average of the temperature distribution is 2.725 [K], and its fluctuation is important in order to elucidate the structure of the early universe and how the universe has been formed.

The set of isothermal loops on the CMB sky map has the property that the size of a loop changes significantly owing to the change in the threshold temperature to draw isothermal loops. [1] The relation between a threshold temperature and the size of a loop is similar to the relation between occupation probability and the size of a percolation cluster.

In order to study this percolation problem on the CMB sky map, we estimate the percolation threshold p_c and the critical exponent β defined by the scaling relation:

$$P(p) \sim (p - p_c)^{\beta} \ (p \geq p_c) \ ,$$

where $P(p)$ is the probability that a given site belongs to the percolation cluster. The values of p_c and β for the CMB sky map are 0.53 and 0.44, respectively. [2](Fig.1, Fig.2) These values are not consistent with the values for the site percolation on a square lattice: $p_c \cong 0.59$ and $\beta \cong 0.14$. [3] As a reference, we generate the percolation cluster on the HEALpix coordinate, numerically. [4] The results of the numerical simulations will be also discussed in this presentation.

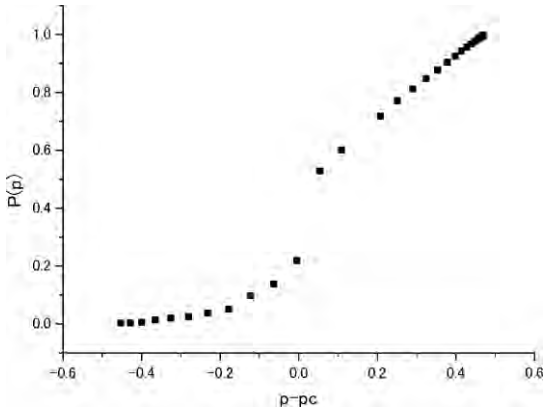

Fig. 1: *P(p)* obtained from the CMB sky map. It is clear that *P(p)* is changing at the percolation threshold p_c.

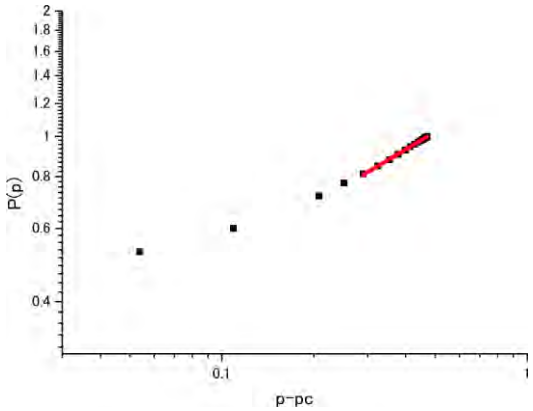

Fig. 2: Log – log plots of *P(p)* vs (p-p_c). The solid line indicates $\beta \cong 0.44$

REFERENCES

1. Kobayashi, N. Yamazaki, Y., Kuninaka, H., Katori, M., Matsushita, M., Matsushita, S., and Chiang, L.-Y., "Fractal Structure of Isothermal Lines and Loops on the Cosmic Microwave Background", *J. Phys. Soc. Jpn.*, **80**, 074003 (2011).
2. Ritsuko Nakahira: Master's thesis (2011. Chuo university)
3. Dietrich Stauffer and Amnon Aharony: *Introduction to Percolation Theory* (Taylor & Francis 1992)
4. http://healpix.jpl.nasa.gov/

Molecular dynamics simulation of gas-liquid flow of a binary Lennard-Jones particle system

Hajime Inaoka[A], Satoshi Yukawa[B], and Nobuyasu Ito[C]

Information Technology Center, The University of Tokyo, Tokyo, Japan [A]
Graduate School of Science, Osaka University, Osaka, Japan [B]
Graduate School of Engineering, The University of Toky, Tokyo, Japan [C]

Gas-liquid flow is a very important physical phenomenon for both the applied physics and the fundamental physics. For example, a regime of gas-liquid flow called spray flow is applied to many industrial processes, such as spray combustion, spray cooling, spray coating, and so on. Gas-liquid flow caused by boiling process is utilized in boilers and heat exchangers. It is also essential to understand the behaviour of gas-liquid flow to study natural phenomena such as volcanic eruptions. Thus, if we can simulate gas-liquid flow numerically by a computer, the technique is useful for both the industrial applications and the fundamental science.

Molecular dynamics simulation is one of the most promising methods to study the behaviour of gas-liquid flow, because it reproduces complex gas-liquid flows from microscopic mechanisms without introducing any artificial rules. We proposed a molecular dynamics model of gas-liquid flow composed of two types of Lennard-Jones particles. These two types of particles are called liquid particles and gas particles, respectively. By using a shock-tube-like configuration, we studied the behaviour of the gas-liquid flow caused by explosively rapid depressurization of the mixture of the liquid particles and the gas particles. The model reproduces a spray flow when the initial number density of the liquid particles is low, while it reproduces a network flow when the density is higher.

We showed that the regimes of the flow reproduced by the model depend on the initial number densities of the liquid particles and the gas particles. We showed that there is a transition from a spray flow to a network flow with the increase of the initial particle number density of the liquid particles and, at the transition point, the droplet size distribution follows a power-law distribution. In this way, the transition from a spray flow to a network flow involves similar physical phenomena to those seen in the phase transition of a model of percolation [1].

One of the main aims of a research of gas-liquid flow is to study the relation between physical quantities and flow regimes. A picture in which flow regimes are plotted in a parameter space of physical quantities such as temperature and flow velocity is called a “regime map.” To draw a regime map of the explosive flows of binary Lennard-Jones particles, we must first determine both the configurations of the flow regimes and the local physical quantities in a system. By measuring physical quantities such as particle number densities, temperature, flow velocity, pressure, and so on, and describe them as functions of position z measured along the tube and observation time t, we found that these physical quantities $Q(z,t)$ follow scaling relations $Q(z,t)=F(z/t)$ with a scaling function $F(\zeta)$. We also found that configurations of flow regimes along a tube also follow a similar scaling relation to those of the physical quantities. Since both the physical quantities and the configurations of flow regimes follow the scaling relations, we assume that the flow regime at a certain point in a system is determined by the local physical quantities at the point. This assumption is essential to draw a regime map of the explosive flows. We can get clear regime map only when the assumption holds.

We successfully drew a set of regime maps of the simulated gas-liquid flows. And by the regime map, we conclude that three flow regimes, that is, spray flow, network flow, and bubble flow, are fully determined by local physical quantities of the liquid and the gas particle number densities and the temperature [2].

REFERENCES

1. Hajime Inaoka, Satoshi Yukawa, and Nobuyasu Ito, “Spray flow-network flow transition of binary Lennard-Jones particle system”, *Physica A*, 389, 1500-1509, Jul. 2010.
2. Hajime Inaoka, Satoshi Yukawa, and Nobuyasu Ito, “Scaling relation and regime map of explosive gas-liquid flow of binary Lennard-Jones particle system”, *Physica A*, to appear.

Mechanical control of hexagonal cell packing in morphogenesis of the *Drosophila* wing

Shuji Ishihara[a,b] and Kaoru Sugimura[c,d]

[a] *Graduate School of Arts and Science, The University of Tokyo, Tokyo, Japan*
[b] *JST PRESTO, Japan*
[c] *iCeMS, Kyoto University, Kyoto, Japan*
[d] *RIKEN BSI, Japan*

In the course of animal development, tissues undergo deformation, which is driven by the mechanical forces regulated by the activity of constituent cells. Thus, to understand variety of morphologies of multi-cellular organisms one must elucidate physical process as well as molecular processes to determine the eventual forms of their bodies from embryos. Recent studies have clarified how geometrical changes of cells are coordinated via the activity and/or localization of force-generating molecular machineries within a cell [1]. On the other hand, it remains unclear how the mechanical interaction among cells and the resulting stress field of a tissue are organized to control cellular pattern formation. One of the difficulties to characterize mechanical processes of morphogenesis is the lack of proper experimental methods to directly measure andquantify the forces in the cell population inside the animal body.

Here we propose a novel method to estimate the forces from observed cell shapes. Consider that the geometry of epithelial cell population is represented by an assemblage of 2D polygons ('vertex model'). Forces in the cell population are described by the isotropic pressures of respective cells and tensions applied in the adherent surface between cells. By considering the geometrical forms of the cells, we obtained balance equations of the aforementioned forces. We can estimate the unknown values of forces by solving the balance equations, however, the number of conditions is less than that of unknowns. To overcome the difficulty, we applied an inverse problem technique using Bayesian statistics. Present method has several advantages. At first, it is applicable to variety of systems. Second, the method is noninvasive and it can capture the dynamics of force field. Thirdly, it can distinguish pressures and tensions among respective cells, thus we can compare estimated forces with molecular activities responsible for generating forces in each cell. Forth, several hundreds of cells are simultaneously estimated, thus we can approach for their relationship between cell level and tissue level kinetics.

Using our method, we studied mechanical basis of hexagonal packing (the increase of hexagonal cells in the *Drosophila* wing during the pupal stage) [2]. Our quantification of developmental changes of the stress distribution within a tissue and of corresponding rearrangements of cells provides a physical mechanism for cell packing: biased external forces acting on the tissue provide the directional information for local orientation of hexagonal cells which underlies the global hexagonalization. Our force estimation method will become a powerful tool in analyzing how information for orchestrating cellular behaviors during morphogenesis is encoded in distributions of forces within a tissue.

REFERENCES

1. Bertet, C. *et al.* "Myosin-dependent junction remodelling controls planar cell intercalation and axis elongation", *Nature*, 429, 667 (2004)
2. Classen, A.-K. *et al.* "Hexagonal Packing of *Drosophila* Wing Epithelial Cells by the Planar Cell Polarity Pathway" *Dev. Cell*, 9, 805 (2005)

Order-Disorder Transition in the Deformable Self-Propelled Particle System

Y. Itino[1] and T. Ohta[1]
[1] *Department of Physics, Kyoto University, Kyoto 606-8502, Japan*

We present here the novel order-disorder transition observed in the self-propelled particles (SPPs) system. The background of our study is the generally introduced single SPP system, where the deformation tensor S of the particle is coupled to the velocity v of itself [2].

$$\begin{aligned} \frac{d}{dt}v_\alpha &= \gamma v_\alpha - |\boldsymbol{v}|^2 v_\alpha - aS_{\alpha\beta}v_\beta \\ \frac{d}{dt}S_{\alpha\beta} &= -\kappa S_{\alpha\beta} + b\left(v_\alpha v_\beta - \frac{1}{2}|\boldsymbol{v}|^2 \delta_{\alpha\beta}\right) \end{aligned} \tag{1}$$

This one-particle system, when the parameters being modulated, exhibits various trajectories such as rotating motion, zig-zag motion, chaotic motion and helical motion (in 3D). As it allows immediate extension to the interacting many-particle system, we exploited a 2D numerical simulation in the straight motion parameter domain [3]. The interaction we introduced is short-ranged repulsive force, but its magnitude depends on the relative direction of elongation (equivalent to the deformation).

Initially prepared random state (Fig.1a), with the order parameter $\Phi = 0$, relaxes to the ordered state $\Phi = 1$ under lower density region (Fig.1c) as commonly seen in the SPP literature [1]. When we slowly compress the system to higher density, however, the system undergoes the transition to the disordered state (Fig.1d); without applying the external noise. In the reverse process under expansion, the system gets back to the ordered state. The transition point differs in the forward compress and the backward expansion.

Theoretically, the mean field approximation explains qualitative behavior as saddle-node bifurcation. And it is confirmed, in the simulation, that the anisotropic interaction explained above is crucial for the transition to occur.

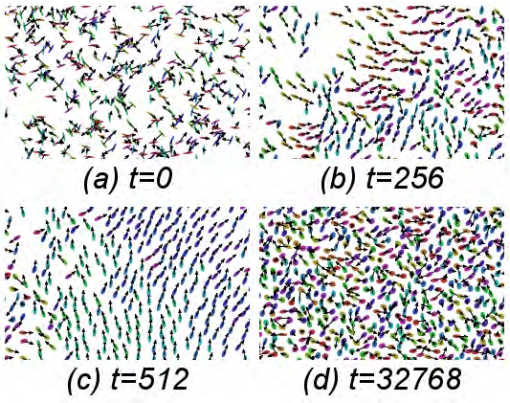

Figure 1: The figure shows typical snapshots of the part of $N = 8192$ particles system. Each arrow indicates the velocity, and the deformation is represented by the elliptical elongation.

References

[1] T. Vicsek, A. Czirók, E. Ben-Jacob, I. Cohen, and O. Shochet: *Phys. Rev. Lett.* **75**, 1226 (1995).
[2] T. Ohta and T. Ohkuma: *Phys. Rev. Lett.* **102**, 154101 (2009).
[3] Y. Itino, T. Ohkuma, and T. Ohta: *J. Phys. Soc. Jpn.* **80**, 033001 (2011).

Entropy pumping and finite time information thermodynamics

Sosuke Ito and Masaki Sano

Department of Physics, The University of Tokyo
7-3-1 Hongo, Bunkyo-ku, Tokyo, Japan

The ideas of Maxwell's demon have been discussed by many researchers. The relation between the information entropy and the work extracted under feedback control is lively discussed in the context of Maxwell's demon. Recently the second law was generalized under feedback control and this generalization was tested using a trapped Brownian particle [1]. In this experiment, by a non-equilibrium feedback manipulation of a Brownian particle on the basis of information about its location, an information-to-energy conversion has been achieved. In addition, feedback control of the Brownian motion has many useful applications ranging from a thermal noise cancellation in atomic force microscopy, to a cooling for investigating quantum effects in a mechanical system. This cooling by feedback control is called as entropy pumping [2].

We have studied fluctuations of a Brownian particle in one-dimensional Langevin system under feedback control. We have found a fundamental bound in cooling a Brownian particle in the presence of measurement errors which are not negligible in experimental settings. We have also found that this bound is determined by the balance between the information obtained by the measurement for feedback control and the information lost as a result of the relaxation [3]. The bound is determined by the relation,

$$\frac{T - T_{\mathrm{eff}}}{T} \leq \frac{\sum_i \langle I_i \rangle}{\tau} \frac{m}{\gamma}, \qquad (1)$$

where T is the temperature of a heat reservoir, T_{eff} is the effective temperature as the temperature of the Brownian particle, $\sum_i \langle I_i \rangle$ is the sum of the mutual information obtained within the time duration τ and m/γ is the relaxation time. Therefore the right-hand side of Eq. (1) is the information obtained in the relaxation time. The left-hand side of Eq. (1) has a form similar to the Carnot efficiency.

In this symposium, we generalize the result, Eq. (1). First we discuss N-dimensional Langevin system as a complex system. We show that the generalization of the result, Eq. (1), for the N-dimensional system has the same expression in a particular case. Second we discuss finite time information thermodynamics. In connection with the Carnot efficiency, it is acknowledged that the Curzon-Ahlborn efficiency determines the efficiency at maximum power of heat engines. Using the discussion of the Curzon-Ahlborn efficiency, we can discuss the information-to-energy conversion at maximum power. In our discussion, a factor 1/2 is essential to maximize the extracted work under feedback control. Furthermore we show that finite time information thermodynamics can be applied to entropy pumping. The result evaluating its finite time effect is the inequality,

$$\frac{T - T_{\mathrm{eff}}}{T} \leq \frac{1}{2} \frac{\sum_i \langle I_i \rangle}{\tau} \frac{m}{\gamma}. \qquad (2)$$

We construct two models of entropy pumping under feedback control including measurement errors and discuss the validity of Eq. (1) and Eq. (2) using numerical simulations.

REFERENCES

1. S. Toyabe. *et al.* "Experimental demonstration of information-to-energy conversion and validation of the generalized Jarzynski equality", Nature Physics **6**, 988 (2010).
2. K. Kim and H. Qian "Fluctuation theorems for a molecular refrigerator", Phys. Rev. E. **75,** 022102 (2007).
3. S. Ito and M. Sano "Effects of error on fluctuations under feedback control", Phys. Rev. E. **84**, 021123 (2011).

Quantitative observation of cell differentiation dynamics

Kyogo Kawaguchi & Masaki Sano

Department of Physics, University of Tokyo, Hongo 7-3-1, Bunkyo, Tokyo, Japan

Cell differentiation is a fundamental process in development and maintenance of multicellular life. Losing and regaining of multipotency through the differentiation and dedifferentiation process has not only been a long standing hot topic in medical research, but also has stimulated many physicist's challenge towards constructing general theoretical models of such robust, selfreproducing, and yet irreversible dynamics. On the other hand, single cell level fluctuations during differentiation have not been well studied, although such heterogeneity among cells must play a crucial roll in the mechanism to distribute stem cells and mature cells into a proper ratio. Thus, we expect new perspectives to rise through experimentally studying, 1. single cell level diversity, and 2. multi-cell level interactions during the differentiation and dedifferentiation process, leading to the formulation of a strong theoretical basis to understand general differentiation dynamics.

In this study, we use the human white blood cell line (HL60) to quantitatively analyze the morphological transitions that occur during differentiation. Observing HL60 through maturation to granulocytes, monocytes, and macrophage-like cells reveals the wide distribution in differentiation speed and diversity among inducing substances. In particular, we parameterize the 3D structure of nuclear segmentation during maturation of granulocytes, and consider its temporal relations to other known parameters of differentiation, such as cell shape, surface markers and phagocytosis rates. We also discuss on the phenomenological parameters of dedifferentiation dynamics.

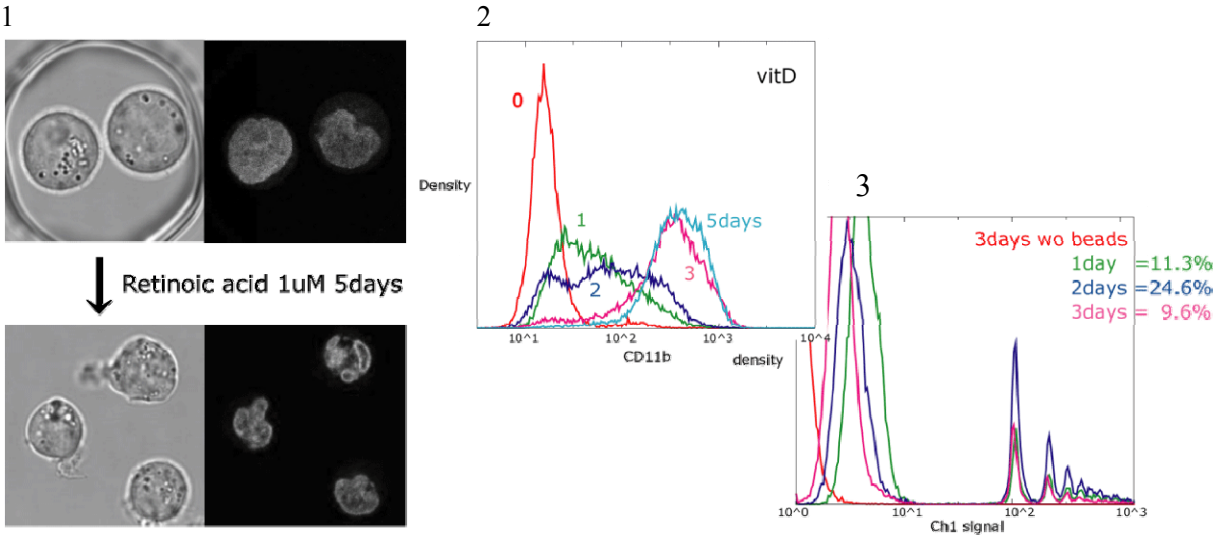

Fig.1 (left image) Confocal live imaging before and after differentiation of HL60 cells. Right-SYTO16 stain shows fluorescence of DNA (nuculeus). Retinoic acid induces HL60 to neutrophil-like cell morphology. Nuclear segmentation is clearly observed.

Fig.2 (centre figure, color online) Evolution of the distribution of CD11b expression (cell surface marker) from flowcytometry analysis. Vitamin D induces HL60 to monocyte-like cell morphology.

Fig.3 (right figure, color online) Evolution of phagocytosis assay data by flowcytometry. Distribution peaks indicate 1, 2, 3... fluorescent beads eaten by Vitamin D induced cells.

Droplet motion coupled with chemical reaction

Hiroyuki Kitahata

Department of Physics, Graduate School of Science, and PRESTO, JST,
Chiba University, Yayoi-cho 1-33, Inage-ku, Chiba, Japan

Droplets or objects can move spontaneously under nonequilibrium conditions. Such spontaneous motion has been investigated related to the motion of living organisms. We have studied several systems in which spontaneous motion is exhibited; a spontaneous motion of a droplet of the Belousov-Zhabotinsky (BZ) reaction medium, which exhibits chemical oscillation [1], an alcohol droplet motion on a alcohol aqueous solution, an oil droplet motion on a glass substrate in a surfactant aqueous solution, and so on. The mechanism of these spontaneous motions has wide variety, but we only consider the spontaneous motion driven by the interfacial tension gradient here.

The theoretical framework that can comprehensively describe the motions driven by interfacial tension gradient has not yet been established. Therefore, we have discussed theoretically on the spontaneous motion of a droplet with an interfacial tension gradient at its interface. We consider the coupling between hydrodynamic processes and interfacial tension change at a droplet interface under the approximation of the steady Stokes flow. The velocity of a droplet, as well as the flow field inside and outside of the droplet, can be calculated by the orthogonal function expansion of the interfacial distribution on a droplet interface. For example, in a three-dimensional system with axial symmetry, a spherical droplet moves at a velocity

$$v = -\frac{2}{3(3\eta_i + 2\eta_o)}\Gamma_1,$$

where η_i and η_o is the viscosity of the fluid inside and outside of the droplet, respectively. The interfacial tension profile, $\gamma(\theta)$, only depends on the angle, θ, from the symmetry axis. Here, $\gamma(\theta)$ can be expanded using Legendre polynominals $P_n(\cos\theta)$ as $\gamma(\theta) = \Sigma_{n=0}^{\infty}\Gamma_n P_n(\cos\theta)$. We adopt this result to the experimental ones on a droplet of BZ reaction medium, to prove its validity (see Figure 1) [5]. Then, we will discuss more detailed mechanism of the spontaneous motion of a droplet coupled with convection and/or deformation.

This work is the collaboration with Dr. Natsuhiko Yoshinaga (Kyoto Univ.), Dr. Ken H. Nagai (Univ. of Tokyo), and Dr. Yutaka Sumino (Aichi Univ. of Educ.).

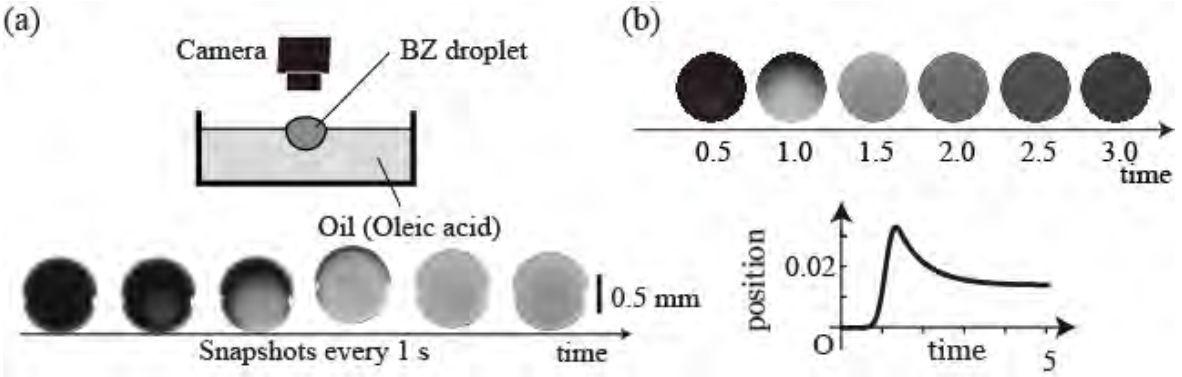

Fig.1 (a) Spontaneous motion of a BZ droplet. Snapshots every 1 s from above are shown. (b) Numerical results based on the steady Stokes flow coupled with reaction-diffusion-advection equation for BZ reaction. The time change in the concentration profile of a chemical compound and that in the position of the droplet are shown.

REFERENCES

1. Kitahata, H. *et al.* "Convective and periodic motion driven by a chemial wave", *J. Chem. Phys.*, 116, 5666 (2002).
2. Kitahata, H. *et al.* "Spontaneous motion of a droplet coupled with a chemical wave", *Phys. Rev. E.*, 84, 015101 (2011).

Time Development of a Growing String

So Kitsunezaki

Department of Physics, Graduate School of Human Culture,
Nara Women's University, Nara 630-8506, Japan

Growing is often a mean of migration for plants, such as growth of a vine. Rod shaped bacteria also grow like a string and extrude themselves to make a colony on a hard agar even when they hardly move[1]. The shape of such a growing string has been investigated as a problem of an elastic string in viscous fluid, typically formulated by assuming the length of the string as a constraint [2]. However actual strings do not always behave as an elastic string with a given length; they are soft and stretchable, or fold down for some cases.

In this study, we start from a chain of linear springs with bending forces and viscous drag forces on 2-dimensional space. We first indicate the center-manifold reduction to a continuum elastic string in the limit of the fixed length, and discuss folding of a string with the existence condition of the continuum limit. The method can be applied for a uniformly growing string and we obtain the reduced equations with a long range interaction depending curvatures,

$$L^4 \frac{\partial \phi}{\partial t} = -\phi'''' + \phi'^2 \phi'' - V\phi'' - 2V'\phi',$$
$$V'' - \phi'^2 V = (\phi'^2)'' - \phi''^2 - L^4,$$

where ϕ is an angle of tangent of a string with respect to the initial coordinate, and $L \equiv e^t$. These include no parameter after appropriate scaling of variables [3].

These equations are useful to calculate prolonged growth of a string. We next investigate the time development of this ideal string numerically, starting from a circular ring initially, as shown in Fig. 1. We find that the diameter of the string begins oscillation with its growth as in Fig. 2.

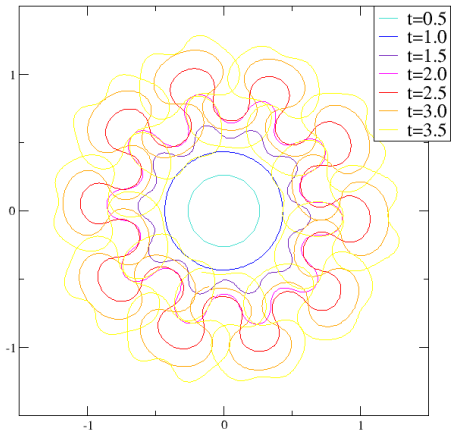

Fig. 1 Time development of the shape of a growing elastic string obtained numerically.

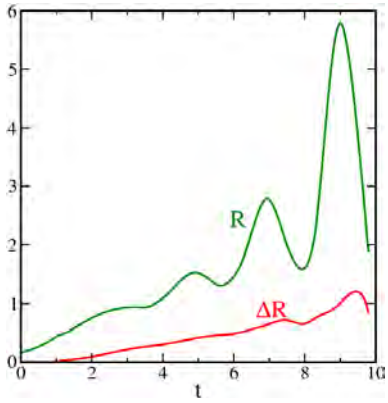

Fig. 2: Oscillation of the diameter of an ideal string appears with its growth.

REFERENCES

1. J. Wakita, H. Itoh, T. Matsuyama and M. Matsushita, "Self-Affinity for the Growing Interface of Bacterial Colonies", J.Phys.Soc.Jpn. 66, 67 (1997).
2. W. Wolgemuth, E. Goldstein and R.Powers, "Dynamic supercoiling bifurcations of growing elastic filaments", Physica D, 190, 266 (2004).
3. E. Ishikawa, Master thesis [in Japanese], Nara Women's University, (2009).

Fractal Structure of Isothermal Lines and Loops on the Cosmic Microwave Background

Naoki Kobayashi, Yoshihiro Yamazaki[1], Hiroto Kuninaka[2], Makoto Katori, Mitsugu Matsushita, Satoki Matsushita[3], and Lung-Yih Chiang[3]

Department of Physics, Chuo University, Kasuga, Bunkyo-ku, Tokyo, Japan
[1] *Department of Physics, Waseda University, Okubo 3-4-1, Shinjuku-ku, Tokyo, Japan*
[2] *Department of Education, Mie University, Kurima-Machiya-cho, Tsu, Mie, Japan*
[3] *Institute of Astronomy and Astrophysics, Academia Sinica, Taipei, R.O.C.*

The surprising feature of the Cosmic Microwave Background (CMB) radiation is its uniformity over the full sky. The recent development of measurements using artificial satellites has revealed, however, tiny but definite existence of temperature fluctuations, from which cosmologists are expecting to know the origin of large scale structures of galaxies and precise information that will be used for testing the Big Bang theory. In the present study, we discuss the temperature fluctuation of the CMB sky map from the viewpoint of fractal-pattern physics. In particular, we consider structures of fluctuations observed by the WMAP by producing a set of isothermal lines and loops on the sky map [1] (Fig. 1).

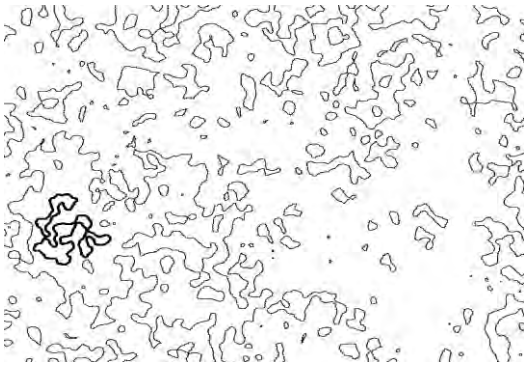

Fig. 1: Isothermal lines and loops of the CMB sky map at an average temperature (2.725 K). Thick line represents one of the single isothermal loops. See [1] for details.

To characterize "spatial" fluctuations of the CMB temperature shown in Fig.1, we evaluate the fractal exponents, such as the fractal dimension D_e of the entire pattern of isothermal loops, the fractal dimension D_c of a single isothermal loop, the characteristic exponent ζ in Korcak's law for the size distribution of isothermal loops, the Hurst exponent H_e for the profile of the CMB sky map, and the Hurst exponent H_c for a single isothermal loop. The two Hurst exponents are determined using the scaling relations for random rough surfaces [2, 3]. As a result of the fractal analysis, the Hurst exponent H_e is less than 1/2. Namely, the displacement of the isothermal lines and loops of the CMB radiation has antipersistent property, which is "noisier" than the usual Brownian motion.

In order to check the validity of our estimation, we perform the fractal analysis of two artificial sky maps simulated by a standard model in physical cosmology, the WMAP best-fit ΛCDM model, and by the Gaussian free field model of rough surfaces. We show that the obtained fractal dimensions and Hurst exponents for the ΛCDM model are consistent with those for the real CMB sky map.

One of the well-discussed topics regarding the recent progress in the conformal field theories and statistical physics of critical phenomena and random fractal patterns is the introduction of the Stochastic Loewner Evolution (SLE) by Schramm [4]. It should be noted that the fractal exponents $D_e \cong 1.39$ and $H_e \cong 0.23$ for the set of isothermal loops on the CMB sky map can be compared with the exponents of the phase boundary of the critical Ising model, $D_e = 11/8$ and $H_e = 1/4$. This corresponds to the SLE_3. This relationship between CMB and statistical physics will be also discussed.

REFERENCES

1. Kobayashi, N. Yamazaki, Y., Kuninaka, H., Katori, M., Matsushita, M., Matsushita, S., and Chiang, L.-Y., "Fractal Structure of Isothermal Lines and Loops on the Cosmic Microwave Background", *J. Phys. Soc. Jpn.*, **80**, 074003 (2011).
2. Matsushita, M., Ouchi, S., and Honda K., "On the Fractal Structure and Statistics of Contour Lines on a Self-Affine Surface", *J. Phys. Soc. Jpn*., **60**, 2109 (1991).
3. Kondev J. and Henley, C.L., "Geometrical Exponents of Contour Loops on Random Gaussian Surfaces", *Phys. Rev. Lett*. **74**, 4580 (1995).
4. Schramm, O., "Scaling limits of loop-erased random walks and uniform spanning trees", *Isr. J. Math*. **118**, 221 (2000).

A thermal diode and transistor utilizing gas-liquid transition

Teruhisa KOMATSU and Nobuyasu ITO

Department of Applied Physics, The University of Tokyo, Hongo, Bunkyo,

Tokyo 113-8656, Japan

We present ideas to make a simple thermal diode passively acting as a rectifier of heat current and a simple thermal transistor, a device to control heat current.

The key design of the diode is the size asymmetry of the areas in contact with two distinct heat baths as in Fig 1. The heat-conducting medium is liquid, inside of which gaslike regions are induced depending on the applied conditions.[1]

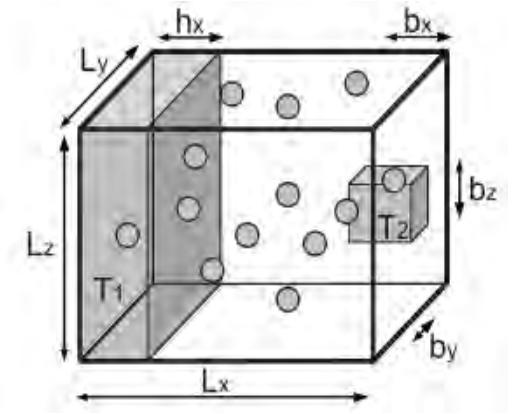

Fig.1 Setup of thermal diode

The key design of the transistor is the special arrangement of the three terminals as in Fig.2. The temperature at one end (gate temperature) is used as an input signal to control the heat current between the center (source/hot) terminal and another end (drain/cold) terminal. [2]

Simulating nanoscale systems of this diode and transistor, we demonstrate these systems work properly as expected.

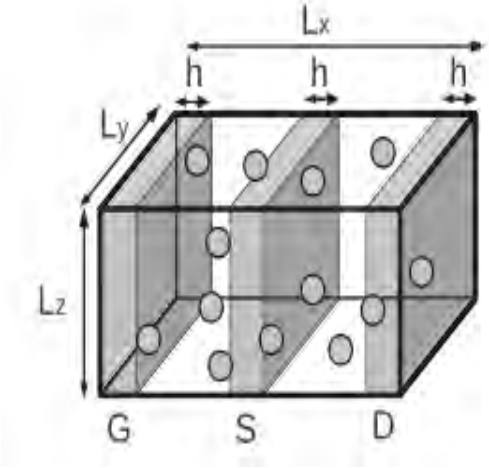

Fig2 Setup of thermal transistor

REFERENCES

1. Komatsu, T.S. and Ito, N. , “Thermal diode utilizing asymmetric contacts to heat baths”, Phys. Rev. E. **81** 010103(R) (2010)

2. Komatsu, T.S. and Ito, N. , “Thermal transistor utilizing gas-liquid transition”, Phys. Rev. E. **83** 012104 (2011)

Complex structure of air-water interfaces interacting collective motion of granular particles

Shin-ya Komura and Yoshihiro Yamazaki

Department of Physics, School of Advanced Science and Engineering, Waseda University, Okubo 3-4-1, Shinjuku-ku, Tokyo, Japan

A labyrinthine pattern of close-packed granules and air paths is spontaneously formed in a drying process of a mixture of water and granules which is sandwiched between two glass slides [1]. In the process, motion of air-water interfaces interacts with collective motion of granules. The granules are swept by advancing air-water interfaces and aggregated ahead of the interfaces. The aggregated granules become compact and interfere with advancement of the interfaces. By our numerical simulation with a model which simply describes the interaction, labyrinthine pattern which is quite similar to experimental one can be reproduced [2]. In the drying process, air paths extend with stick-slip motion of the interfaces. Furthermore, they wind, branch, and frequently join together. These behaviors cause the complex structure of the air paths which have branching and loop. In addition, the air-water interfaces have intricate structure.

In this presentation, we introduce our studies about shapes of the invading air regions and advancing air-water interfaces before air regions extend over the system with experimental and numerical approach. In the experiment, we use wheat starch for granules and took digital images of the system in drying process with a scanner and attempted to obtain the monochrome images of air regions from them with image processing. In the numerical simulation, we use the hybrid model, composed by a time evolution equation of a phase field describing air-water interfaces and an equation of granular particle motion [2], and obtained the images from the phase field.

As a result of the experiments and the simulations, the ratio of granules against water in the mixture affects the anisotropy of the growth and the compactness of the air paths. An example is shown in fig.1. In certain conditions, the outer air-water interface is self-similar fractal.

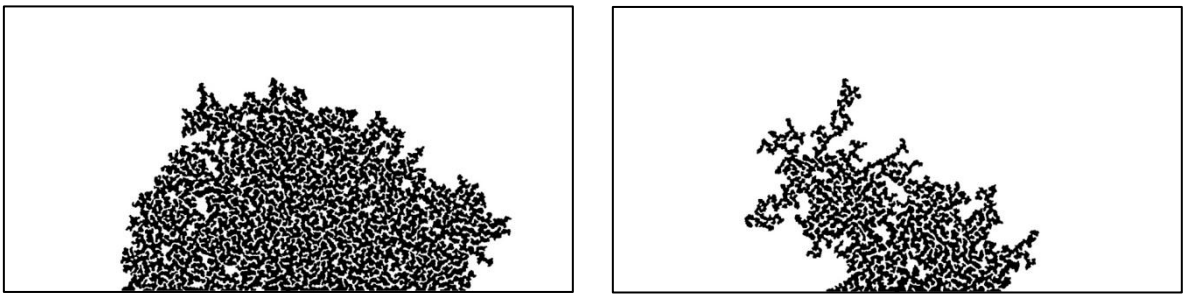

Fig.1 An example of difference in the shapes of air regions(black) by the density of granules in the numerical simulation. These figures were obtained in same condition except the occupied ratios of granular regions, 0.25(left) and 0.30(right). The air path in right image is more anisotropic and has more gaps between them than in left one. The outer air-water interface in the right image is self-similar fractal whose fractal dimension is about 1.63.

REFERENCES

1. Yamazaki, Y. and Mizuguchi, T., “Front Aggregation and Labyrinthine Pattern in the Drying Process of Two-Dimensional Wet Granular Systems”, *J. Phys. Soc. Jpn.*, 69, 2387, (2000).
2. Komura, S. and Yamazaki, Y., “Modelling for Collective Motion of Granular Particles Driven by Motion of Interfaces”, *J. Phys. Soc. Jpn.*, 76, 083801, (2007).

Structure of Cell Networks Critically Determines Oscillation Regularity

Hiroshi Kori[1, 2], Yoji Kawamura[3], Naoki Masuda[4, 2]

[1] *Division of Advanced Sciences, Ochanomizu Univeristy, Tokyo, Japan*
[2] *PRESTO, Japan Science and Technology Agency, Kawaguchi, Japan*
[3] *Institute for Research on Earth Evolution, Japan Agency for Marine-Earth Science and Technology, Yokohama, Japan*
[4] *Department of Mathematical Informatics, The University of Tokyo, Tokyo 113-8656, Japan*

Biological rhythms are generated by pacemaker organs, such as the heart pacemaker organ (the sinoatrial node) and the master clock of the circadian rhythms (the suprachiasmatic nucleus), which are composed of a network of autonomously oscillatory cells. Such biological rhythms have notable periodicity despite the internal and external noise present in each cell. Previous experimental studies indicate that the regularity of oscillatory dynamics is enhanced when noisy oscillators interact and become synchronized (The figure illustrates the enhancement of oscillation regularity in mathematical models). This effect, called the collective enhancement of temporal precision, has been studied theoretically using particular assumptions. In this study, we propose a general theoretical framework that enables us to understand the dependence of temporal precision on network parameters including size, connectivity, and coupling intensity; this effect has been poorly understood to date. Our framework is based on a phase oscillator model that is applicable to general oscillator networks with any coupling mechanism if coupling and noise are sufficiently weak. In particular, we can manage general directed and weighted networks. We quantify the precision of the activity of a single cell and the mean activity of an arbitrary subset of cells. We find that, in general undirected networks, the standard deviation of cycle-to-cycle periods scales with the system size N as $1/\sqrt{N}$, but only up to a certain system size N^* that depends on network parameters. Enhancement of temporal precision is ineffective when $N > N^*$. We also reveal the advantage of long-range interactions among cells to temporal precision.

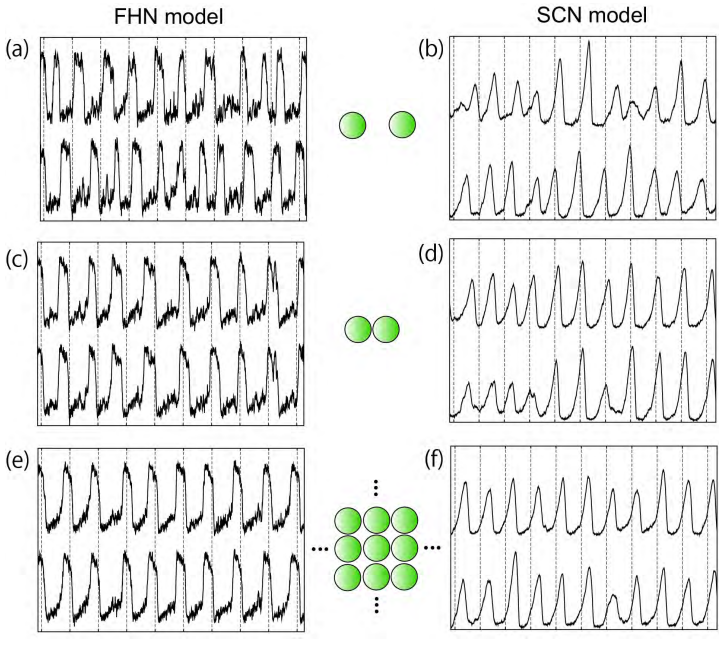

REFERENCES

1. H. Kori, Y. Kawamura, N. Masuda: “Structure of Cell Networks Critically Determines Oscillation Regularity”, arXiv: 1108.4790.

Mode bifurcation of bouncing dimer caused by chiral-asymmetry

Yoshitsugu Kubo[1], Shio Inagaki[2], and Kenichi Yoshikawa[1]

[1]*Department of Physics #1, Kyoto University*
Kitashirakawa, Sakyo, Kyoto 606-8502, Japan
[2] *Venture Business Laboratory, Kyoto University*
Yoshida-Honmachi, Sakyo, Kyoto 606-8501, Japan

It is known that an asymmetric particle such as a screw can move directionally when it is placed on vertically oscillated plate [1]. Even a symmetric dimer displays spontaneous ballistic motion without any anisotropic external field [2]. In these two cases, it was observed only directional or random motion. We investigate spin/orbital motion of a dimer by introducing chiral-asymmetry.

We use a dimer composed of two disks connected by a rigid rod. In order to introduce chiral-asymmetry, we drill holes in disks and rotate one disk against the another by the angle α as shown in Fig.1(a). We placed the dimer on sinusoidally vibrated plate. The plate is oscillated with frequency f and amplitude A. In this study, we fix f at 50Hz and vary A to study a dependence of dimer motion on dimensionless acceleration $\Gamma(=A(2\pi f)^2/g)$.

When we set the amplitude at 0.16mm, the dimer motion is shown in Fig.2(a). The dimer itself spins and the center of mass moves randomly (mode 1). Next we increase the amplitude to 0.17mm, and we observed an orbital motion (mode 2) as shown in Fig.2(b) . In both cases, the dimer spontaneously spins under vibrations. We found that center of mass of the dimer moves either randomly or orbitally dependent on Γ subcritically.

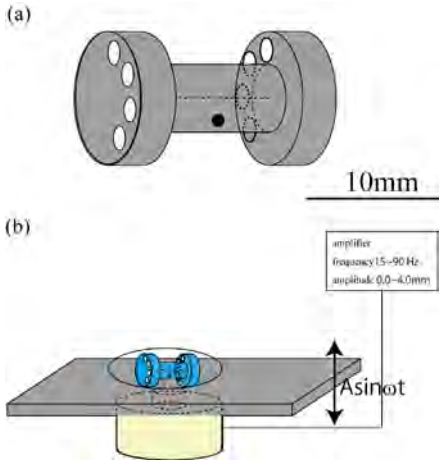

Fig1 (a) Schematic picture of a chiral-asymmetric dimmer. (b) Experimental set up.

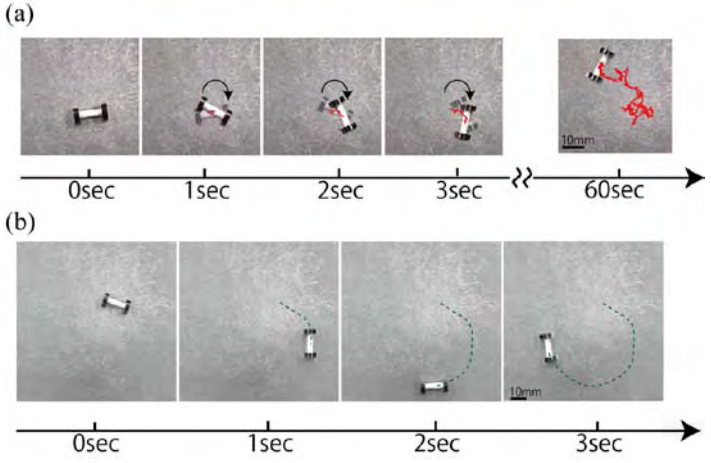

Fig2 (a) spin + random; f=50Hz, A=0.16mm
(b) spin + orbital; f=50Hz, A=0.17mm.

REFERENCES

1. Daizou Yamada. *et al.* "**Coherent dynamics of an asymmetric particle in a vertically vibrating bed**", *PRE*, 67, 040301 (2003).
2. S. Dorbolo. *et al.* "**Dynamics of a Bouncing Dimer**", *PRL*, 95, 044101 (2005).

Domain pattern formation in a ferromagnetic Bose-Einstein Condensate

Kazue Kudo[1] and Yuki Kawaguchi[2]

[1]*Ochadai Academic Production, Ochanomizu University, Tokyo, Japan*
[2]*Department of Physics, University of Tokyo, Tokyo, Japan*

Magnetic domain patterns appear in a ferromagnetic Bose-Einstein Condensate (BEC) as well as in a ferromagnet. Domain patterns in a ferromagnetic BEC are similar to those in a ferromagnet. However, the magnetization dynamics are influenced by the supercurrent of particles. We demonstrate the domain pattern dynamics of a ferromagnetic BEC in the presence and absence of the current of particles in numerical simulations [1]. We also discuss the characteristic lengths of domain patterns that have domain walls with and without finite magnetization.

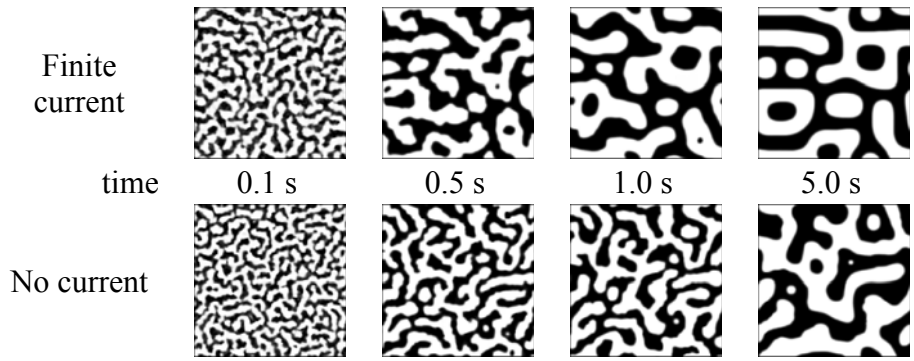

Fig.1 Snapshots of longitudinal magnetization in which white and black correspond to positive and negative values of the *z* component of magnetization.

The dynamics of a BEC are well described by the Gross-Pitaevskii (GP) equation. However, for the investigation of the magnetization dynamics, a hydrodynamic equation, which is expressed by spin variables, has an advantage. It provides the simple description that is useful to investigate the domain pattern formation in a ferromagnetic BEC. We introduce the hydrodynamic equation, which is derived from the GP equation, of a ferromagnetic BEC with dissipation originating from the energy dissipation of the condensate. The dissipative hydrodynamic equation has the same form as an extended Landau-Lifshitz-Gilbert (LLG) equation, which describes the magnetization dynamics of a conducting ferromagnet in which localized magnetization interacts with spin-polarized currents.

The analogy between the dissipative hydrodynamic equation and the extended LLG equation implies interesting connections between ferromagnetic BECs and conducting ferromagnets. It can provide suggestions on new experiments of a ferromagnetic BEC to investigate interesting phenomena that are observed in conducting ferromagnets.

REFERENCES

1. Kazue, K. and Kawaguchi, Y., "Dissipative hydrodynamic equation of a ferromagnetic Bose-Einstein condensate: Analogy to magnetization dynamics in conducting ferromagnets", *Phys. Rev. A*, 84, 043607 (2011).

Concentric-ring Colony Formation of *B. subtilis*

Ryuto KUMATA, Mina ARIMA, Jun-ichi WAKITA,
Tohey MATSUYAMA, and Mitsugu MATSUSHITA

Department of Physics, Chuo University

Bacteria inoculated on an agar plate surface form a two-dimensional colony pattern of macroscopic size. The colony patterns formed by *B. subtilis* are classified into five kinds depending on the condition of agar plate which is controlled by the concentrations of agar(*C*a) and nutrient(*C*n)(Fig.1). Here we focus on the concentric-ring pattern in the region C of the morphological diagram shown in Fig.1. This colony pattern is formed by the growing front repeating advancing (migration phase) and stop (consolidation phase) cyclically.

In our previous study, it was suggested that the local cell density at the growing front is related to the cyclical growth and there exists the threshold value of cell density independent of *C*a and *C*n, therefore we investigate the height profile (cell density) of the growing front at the beginning of a migration phase as a function of *C*a and *C*n.

The results that the height (cell density) of the tip of the growing front at the beginning of a migration phase is almost constant for *C*a, but is not constant in high concentration of *C*n. This result seems curious, since the cycle time which is defined by the sum of the migration and consolidation phase is confirmed to be constant for changing *C*a and *C*n. In this presentation, we will discuss this result.

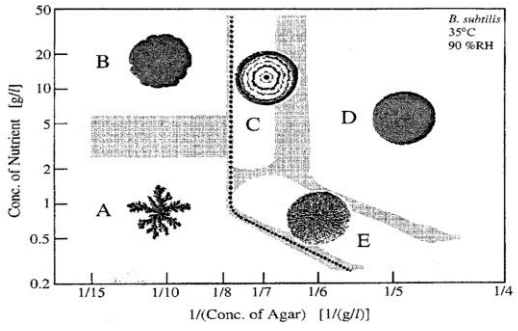

Fig.1 Morphorogy diagram of *B. subtilis* colonies.

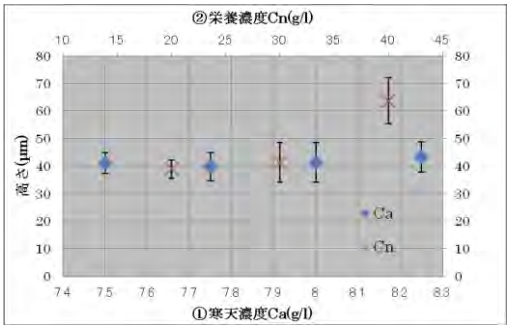

Fig.2 The height(cell density) dependence of the tip of the growing front on *C*a and *C*n.

REFERENCE

[1] H, Shimada et al. “Dependence of Local Cell Density of Concentric Ring Colony Formation by Bacterial Species Bacillus subtilis”, J, Phys. Soc. Jpn. **73**(2004) 1082-1089.

Statistical properties of height and weight of schoolchildren

Hiroto Kuninaka

Faculty of Education, Mie University,

Kurima-machiya 1577, Tsu city, Mie, Japan

The size distribution of human bodies is one of the important indices for the health condition of a given group. Although the growth of the human bodies is so complex, it is known that the size distribution is often approximated by the normal or lognormal distribution very well [1,2]. From the statistical distribution, we can guess whether the growth process of human bodies is approximately multiplicative or additive.

In this poster presentation, we investigate the statistical properties of height and weight of schoolchildren. Our analysis is based upon the statistical data of schoolchildren in Japan. Our previous results have revealed that the height distribution shows the transition from the lognormal distribution to the normal distribution around the age of 10-12 [1,2]. Although this result implies that the change in growth process around puberty might cause the clear transition, the mechanism of the transition is still unclear.

In addition, we have also found that the weight distribution of schoolchildren can be approximated by the superposition of some lognormal distributions [1,3]. This implies that the growth process of the heavier group might be different from those of other groups. The microscopic mechanism of the emergence of the superposition is one of our interests.

Some models are suggested for the description of the human growth [4]. In our poster, we will discuss whether such a model can reproduce the empirical size distribution and what is needed to be included in the models for the reproduction of the empirical size distributions.

This work is based upon the collaborative works with M. Matsushita (Chuo Univ.) and Y. Mitsuhashi (Chuo Univ.).

REFERENCES

1. Kobayashi, N. *et al.* “Statistical Features of Complex Systems –Toward Establishing Sociological Physics–”, *J. Phys. Soc. Jpn.*, 80, 072001 (2011).
2. Kuninaka, H., Mitsuhashi, Y., and Matsushita, M.: “Statistical properties of height of Japanese schoolchildren”, *J. Phys. Soc. Jpn*, 78, 125001 (2009).
3. Mitsuhashi, Y.: Master thesis (Chuo Univ. 2010).
4. Canessa, E.: “Modeling of body mass index by Newton’s second law”, J. Theor. Bio. 248, 646 (2007).

Crystal Growth and Morphology Change of Calcium Carbonate in Gel

Masakazu Kurashige, Mitsugu Matsushita

Dept. of Physics, Chuo University, 1-13-27, Kasuga, Bunkyo-ku, Tokyo 112-8551, Japan

Crystal growth of $CaCO_3$ was attempted in gelatin, agar and Na-metasilicate (water glass) gel by means of slowly reacting with ammonium carbonate and calcium chloride. Grown crystals were confirmed to be calcite and vaterite by X-ray diffraction. Morphology variety of these crystals was found with change of gel and solute conditions. Spherical polycrystalline particles characteristically appeared in higher gel concentrations.

Aqueous solutions of gel and ammonium carbonate were previously mixed and gelled at the bottom of test tubes, then formed additional gel layer as a buffer above mixture gel layer. Finally calcium chloride aqueous solutions were pored at the top of tubes, and were left in a constant temperature and humidity chamber at 15 degree C, 60%.

Almost the same size and morphology micro crystals were instantaneously formed in directly reacting ammonium carbonate and calcium chloride, while a variety in size and morphology was observed after reacting slowly in gel. The crystals having distinct facets tend to major at lower gel concentrations and higher solute concentrations. The facets tend to not clear at higher gel concentration and lower solute concentration. Spherical particles characteristically appeared in the latter case, and we found they were polycrystal by X-ray diffraction.

We argue the origin of the morphology change and spherical polycrystal formation in session.

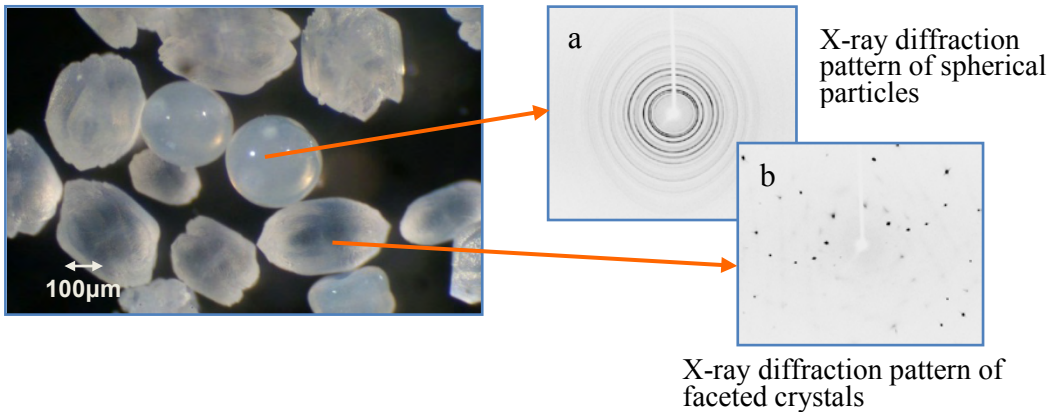

Fig.1 Single crystal X-ray diffraction for gelatin case; a spherical particle and a faceted crystal were picked up and measured respectively. (a) Spherical particle indicated polycrystal. (b) Faceted crystal indicated single crystal. Duration of growth: 28 days.

REFERENCE
Heinz K. Henisch, *Crystals in Gels and Liesegang Rings*, Cambridge University Press (1988)

Role of Delay in the Stochastic Birth and Death Process

Luis F. Lafuerza, Raúl Toral.

IFISC, Institute for Cross-Disciplinary Physics and Complex Systems, CSIC-UIB.

Complex systems are typically composed by many interacting elements, and very often a stochastic description is necessary to model them mathematically. Delay in the interactions is also common in those systems and their mathematical description. However, the combined effects of stochasticity and delay is not well understood.
Most theoretical approaches to this question have been based on stochastic differential equations or systems in discrete time. However, models with discrete variables but continuous in time are the natural description of many systems such as chemical reactions, population dynamics, epidemic spreading etc. In some cases this discreetness is a mayor source of fluctuations.
In this work, we study the combined effects of stochasticity and delay by mathematically analicing simple models that include both features. We use a master equation approach that considers discrete variables in continuous time.
In the case of delayed production [1] with state-dependent creation rate (feedback) we show that the delay can increase or decrease the fluctuations depending on the sign of the feedback. A negative feedback with large enough delay increases the fluctuations, contrary to the no-delay scenario.
We also analyze the case of distributed delay and show that as the delay becomes more spread, its effect decreases.
In the case of delay in the degradation [2], we solve the process exactly and show that, contrary to previous results, stochastic oscillations are not present and the system always has Poissonian character.

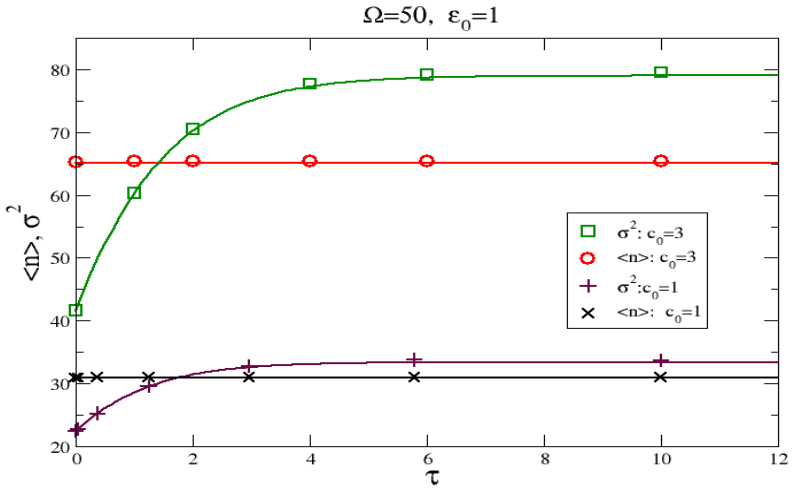

Average and variance as a function of the delay for delayed production with negative feedback, for two sets of parameters. The average is essentially independent of the delay, but the variance clearly increases with it.

References:
[1] Luis F. Lafuerza and Raúl Toral, Phys. Rev. E **84**, 021128 (2011).
[2] Luis F. Lafuerza and Raúl Toral, arXiv:1106.6306v2 (submitted).

Dramatic Reduction of Cardiac Alternans by small perturbations in pacing scheme

S. Sridhar[1], Duy-Manh Le[2], Y. J. Mi[2], S. Sitahbra[1], Pik-Yin Lai[2], and C. K. Chan[2, 3]

[1]*Institute of Mathematical Sciences, Chennai, India 300*

[2]*Department of Physics and Graduate Institute of Biophysics,*

National Central University, Jhongli City 320, Taiwan

[3]*Institute of Physics, Academia Sinica, Nankang, Taipei 115, Taiwan*

Abstract

Alternans response in cardiac tissue during fast periodic pacing can lead to conduction block, causing fatal cardiac failure. A novel method of pacing with feedback control is proposed to reduce the alternans and therefore the conduction block. The reduction is achieved by slight perturbation of the original alternans generating pacing period T by two pacing periods of $T-\varepsilon$ and $T+\varepsilon$, with $\varepsilon /T<<1$. That is: a very small alternating perturbation to the pacing period can dramatically suppress amplitude of the alternans to more than *90%.* Predictions and validity of this control method have been verified by both experiments performed with isolated heart preparations and numerical simulations. A nonlinear return map for this novel pacing scheme based on action potential duration restitution response is proposed to explain the working mechanism of the control. Furthermore, the optimal choice of ε for alternans reduction can be calculated analytically by nonlinear dynamic analysis.

References

1. Z. Qu, Y. Shiferaw, and J. N. Weiss, "Nonlinear dynamics of cardiac excitation-contraction coupling: An iterated map study", *PRE* 75, 011927 (2007).
2. Y. Shiferaw *et al.*, "Nonlinear dynamics of paced cardiac cells", *Ann. N.Y. Acad. Sci.* 1080, 376-394 (2006).
3. S. G. DILLY and M. J. LAB, "Electrophysiological alternans and restitution during acute regional ischemia in myocardium of anaesthetized pig", *J. Physiol*. 402: 315-333(1998).
4. J. J. Fox *et al.,* "Period-doubling instability and memory in cardiac tissue", *PRL* 89, 138101 (2002).

Stabilization of unstable state by interaction between a reaction-diffusion media and its environment

Hitoshi Mahara and Tomohiko Yamaguchi

Nanosystem Research Institute, National Institute of Advanced Industrial Science and Technology (AIST), Higashi 1-1-1, Ibaraki, Japan

Behaviours of biological system depend on its environment because the system is non-equilibrium system. On the other hands, its environment is influence by the system, too. Moreover, some biological systems change their environments in order to survive. For example, Tumour stimulates the surrounding arterial system because of lack of oxygen and then angiogenesis occurs around it. These phenomena imply that dynamics of the environment which is influenced by the system could be important factors for determine the fate of the system.

In general, the non-equilibrium systems are studied under the condition that its environment is constant. This condition is simple and useful to understand the mechanisms of non-equilibrium systems. However, influence of the above mentioned factor could not be discussed under this condition.

Here, we consider a nested system composed of two parts: a reaction-diffusion system and a continuous stirred tank reactor (CSTR). The reaction-diffusion media is immersed in the CSTR (Fig.1). Then the CSTR is an environment of the reaction-diffusion media. Both the media and the CSTR have chemical reaction dynamics and interact each other. Therefore, the environment of the media is not constant anymore.

In this poster, we will present some results of numerical calculation and linear analysis of this system. First, we will show the dynamics of both media and reactor. Form these results we can deduce that they are influenced by each other.

Second, we will present the difference between the results in the present case and in the case that the environment, i.e., the CSTR is constant. From the linear analysis, unstable state solution of the media can be realized because the environment of the media has dynamics. This unstable state solution is the unstable fixed point in the case that the CSTR is constant. This state cannot be realized in the case that the environment is constant.

Finally, we show that this unstable state brings other state that the media cannot show when the CSTR is constant.

We believe that these results give us some suggestion in order to discuss dynamics of nested systems, especially, hierarchical systems.

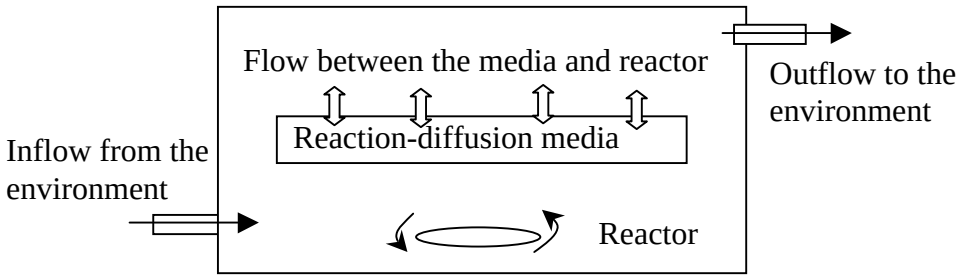

Fig.1: Schematic view of the nested system. The reaction-diffusion media is immersed in the continuous stirred tank reactor (CSTR). The CSTR is an environment of the media. The CSTR has also the environment.

Active stress and the contractile cytoskeleton

N. Yoshinaga
Fukui Center for Fundamental Chemistry
Kyoto University, Kyoto 606-8103, Japan

J. Prost
E.S.P.C.I. ParisTech
10 rue Vauquelin, 75231 Paris Cedex 05, France

P. Marcq
Laboratoire Physico-Chimie Curie
Institut Curie/CNRS/Université Pierre et Marie Curie
75248 Paris cedex 05, France
philippe.marcq@curie.fr

Abstract

In the cytoskeleton of animal cells, actin bundles and the actin cortex contract when myosin mini-filaments crosslink, and pull on, actin filaments. Crosslinked actin gels are elastic on timescales short compared to the typical unbinding time of crosslinkers. At mesoscopic lengthscales where hydrodynamics is relevant, we model contractility by an additionnal active stress term, and obtain a quantitative description of

(i) how stress fibers severed in the cell by laser ablation retract;

(ii) how traction forces exerted by cells in culture depend upon the rigidity of the substrate.

Resonance of Oscillatory Chemical Reactions

Masako Matsubara[1], Fumito Mori[2], Tetsuo Deguchi[1], Hiroshi Kori[1,3]

[1] *Department of Physics, Ochanomizu University, Tokyo, Japan*
[2] *Division of Advanced Sciences, Ochadai Academic Production, Ochanomizu University, Tokyo, Japan*
[3] *PRESTO, Japan Science and Technology Agency, Kawaguchi, Japan*

In this presentation, we report a study on a resonance phenomenon in periodically driven Brusselator model, given as

$$\dot{x} = a + x^2 y - bx - x,$$
$$\dot{y} = bx - x^2 y,$$

where x(t) and y(t) are concentrations of chemicals in the observed system. When a and b are constant, damped and limit-cycle oscillations are obtained. Here, we assume $b(t) = b_0 + \varepsilon \sin \Omega t$, where epsilon and Omega are the amplitude and the driving frequency of external periodic forcing. In this case, resonance occurs. The figure shows the dependence of oscillation amplitude on driving frequency Ω.

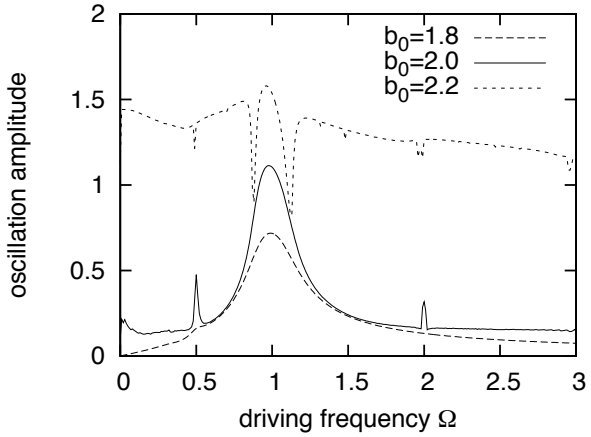

Fig.1

To understand the behavior, we analyze the correspond amplitude equation:

$$\frac{dA}{dt} = (\mu + i\omega_0)A - \beta |A|^2 A + \varepsilon e^{i\Omega t}.$$

REFERENCES

1. A. Förster: *J. Phys. Chem.*, Vol. **99**, No. 31, (1995).

Molecular Dynamics Study of Turbulence Generation

Shigenori Matsumoto, Takashi Shimada, Nobuyasu Ito

Department of Applied Physics, School of engineering, The University of Tokyo, 7-3-1 Hongo, Bunkyo, Tokyo 113-8656, JAPAN

Turbulence is important feature of flow for both science and engineering. In turbulent flow, vortex dynamics dominates. As a property of vortices, a hierarchic structure is well known. Especially, energy cascade from large to small vortex occurs. From these features, we must consider large scale flow to microscopic fluctuation in turbulent flow. Consequently, it is still hard to solve Navier Stokes equation for turbulent flow by direct numerical simulation[1] and so on. Furthermore, relation between molecular fluctuation and vortex dynamics in microscopic scale is not clear. We approach that relation and turbulence generation in molecular scale by molecular dynamics simulation.

To investigate microscopic structure in variety flows, a molecular dynamics method is a powerful approach. In this method, a motion of particle is calculated from the Newton's equation of motion exactly. Here, we consider elastic particles in a three dimensional system. Each particle feels a repulsive potential described as

$$V(r_i, r_{j,}) = \begin{cases} Y|\, r_i - r_j|^{5/2} & \text{if } |r_i - r_j| < \sigma \\ 0 & \text{otherwise} \end{cases},$$

where Y, r and σ denote Young's modulus, position and diameter of a particle, respectively. The elastic particle model has been simple and useful for simulating a fluid.

In our simulation, a thermal wall is imposed in z-direction. A particle randomly bounces back with a thermal velocity on the wall. Therefore it behaves as a non-slip boundary. In x- and y-direction, a boundary condition is periodic. Each particle is driven by a constant pressure gradient, g, on x-direction. Such flow is so-called Poiseuille flow. In this situation, the Navier-Stokes equation can be solved exactly for laminar flow.

As a result, we can obtain a velocity profile of Poiseuille flow and estimate a viscosity and a Reynolds number, Re. The Poiseuille flow becomes instable and then turbulence transition occurs for $Re > 5772.2218$[2], which is called a critical Reynolds number. For lower Re, our simulation shows similar results to fluid dynamics. For higher Re, we obtain vortex structure. Figure 1 shows snapshot of velocity fields. A size and a direction of cone shape correspond to a velocity amplitude and direction, respectively. We will show detail analysis results in our poster.

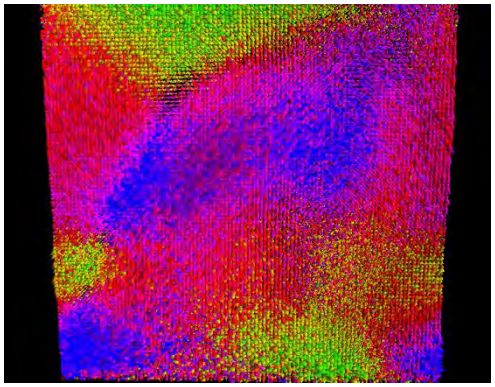

Fig.1 (Color Online) Snapshot of velocity field. Colors correspond to directions of velocity. Red, green and blue denote the direction of up or down, left and right, respectively. Top-left and bottom-right sparse areas correspond to the center of vortex.

REFERENCES

1. J. Kim, P. Moin and R. Moser, “Turbulence statistics in fully developed channel flow at low Reynolds number”, *J. Fluid Mech.*, 177, 133-166 (1987).
2. K. S. Gage and W. H. Reid, “The stability of thermally stratified plane Poiseuille flow”, *J. Fluid Mech.*, 33, 21 (1968).

Acoustic Emission from a plunged granular bed

Kazuhiro Matsuyama[1] and Hiroaki Katsuragi[2]

[1]*Department of Applied Science for Electronics and Materials, Kyushu University, 6-1 Kasugakouen, Kasuga, Fukuoka 816-8580, Japan*

[2]*Department of Earth and Environmental Sciences, Nagoya University, Furocho, Chikusa, Nagoya 464-8601, Japan*

The structure of grains network such as random close packing is a key to understand the granular physics. Network reconstruction by external force or deformation is also important, as well as static structure. The network structure is supported by friction at grains boundary and results in nonlinear rheological characteristics that are contrastive to the continuum media. In order to study the local grains network reconstruction, we performed the deformation experiment of a granular bed. An AE (Acoustic Emission) sensor (NF AE-900S-WB) is used to detect the local reconstruction or slip of grains network. A schematic drawing of the experimental system is shown in Fig. 1. A cylindrical container is filled with glass beads. The AE sensor is buried in the glass beads bed as shown in Fig. 1. A sphere object is plunged into the bed. The stroke and exerted force are measured by a universal testing machine (Shimadzu AG-100N), and the AE signal is also recorded. In Fig. 2, an example of AE signal is presented. Using the data, we divide the AE signal to each individual event, and measure the size distribution $N(s)$, where s is the maximum voltage of each AE event. The measured distribution is shown in Fig. 3. As can be seen in Fig. 3, $N(s)$ shows a power law behavior, and the exponent of fitted straight line is $\delta = 2.5$. We actually conduct the experiment with various grains sizes, intruder sizes, and intrusion rates. Through these systematic experiments, relation between the AE signal and the exerted force is discussed in the poster presentation.

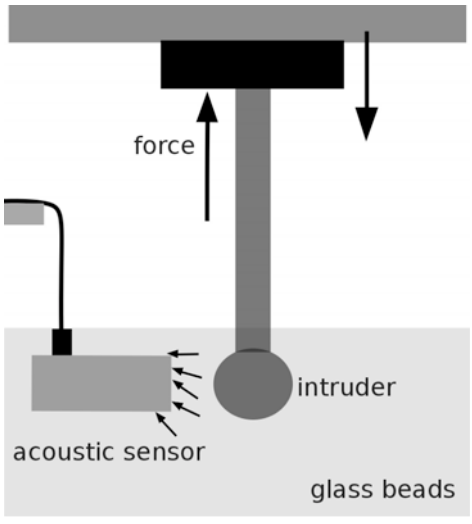

Fig. 1 Experimental apparatus. Glass beads are poured into a cylindrical container until 100 mm depth. The top surface of the glass beads layer is free and open to air. The AE sensor is buried at approximately 20 mm depth. The sphere intruder penetrates down to 70 mm depth. Instantaneous penetration depth and exerted force to the sphere, and AE signal are measured.

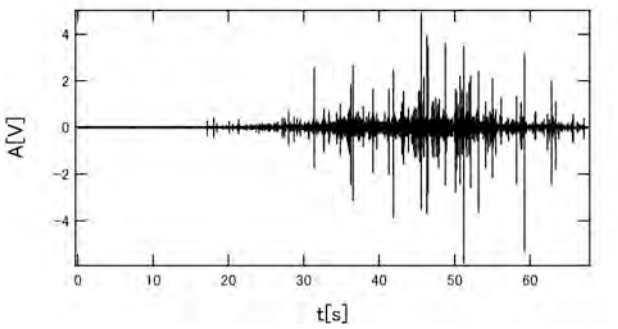

Fig. 2 An example of the AE signal during sphere intrusion. The intrusion rate is 1 mm/s.

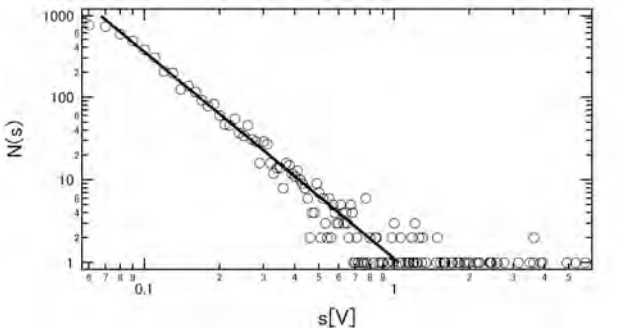

Fig. 3 Size distribution of AE events. A power law distribution with an exponent $\delta = 2.5$ can be observed.

Growth Rate Distribution for NH_4Cl Dendrite And its Scaling Structure

Hiroshi Miki and Haruo Honjo

Department of Applied Science for Electronics and Materials,
Interdisciplinary Graduate School of Engineering Sciences,
Kyushu University, Fukuoka, Japan

Dendrite is a typical pattern formed in nonlinear and nonequilibrium physics and observed in various systems such as crystallization and viscous fingering. It has a stem with its tip growing steadily and stably. Countless sidebranches grow behind the tip and complicated and hierarchical structures are formed (Fig.1). There are two main factors which dominate the growth of a dendrite; diffusion and anisotropy. Diffusion, as known in the diffusion-limited aggregation (DLA), makes a flat interface unstable and cause "the screening effect" – a longer branch screens off the diffusion field and therefore strongly suppresses the growth of shorter ones around it. On the other hand, anisotropy makes a tip stable. The combination and competition between these factors makes difficult understanding the growth process of dendrite.

The distribution of the growth rates on the interface is often expected to well characterize the growth process. For dendritic growth, due to the screening effect mentioned before, tips of the stem and some longer sidebranches substantially grow and the growth rates of the tips of many shorter sidebranches are extremely small. Therefore we expect the growth rate distribution to have a hierarchical structure reflecting the properties of dendritic growth.

We investigate the scaling properties of the growth rate distribution for a two-dimensional NH_4Cl dendritic crystal. NH_4Cl dendritic crystal growth is observed in supersaturated aqueous solution in a cell with a narrow space between two parallel grass plates. Images of the crystal are recorded using an inverted microscope and CCD camera. The images are binarized using an image processing software (Fig.1). The growth rates are evaluated by numerically solving the Laplace equation on lattice (Fig.2) and from them multifractal f-α spectrum is calculated. The distinction between the spectrum of the dendrite and that of DLA is discussed.

Fig.1 Binarized image of a NH_4Cl dendrite. Its fractal dimensions of area and perimeter length are 1.57 and 1.54, respectively.

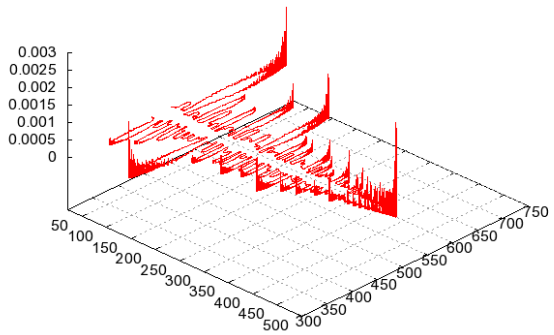

Fig.2 The growth rates on the interface of the dendrite of Fig.1.

Nucleation kinetics of bubble production in Lennard-Jones System

Masamichi J. Miyama and Nobuyasu Ito

Department of Applied Physics, School of Engineering,
The University of Tokyo, 7-3-1, Hongo, Bunkyo-ku, Tokyo, Japan.

We study the dynamics of bubble production in gas-liquid coexistence phase of Lennard-Jones particle systems by using molecular dynamics simulations. Bubble production is a kind of the relaxation and transient process to an equilibrium state accompanied by a gas-liquid transition, which is one of the first order transitions. The bubble production is essentially one of the non-equilibrium phenomena. As an ideal situation, we consider the case of homogeneous bubble production, which we can easily realize in numerical simulations.

In Lennard-Jones systems under the condition with the temperature and volume fixed, there is a gas-liquid coexistence region. By measuring the density dependence of bulk pressure, we can divide the coexistence region to two regimes: nucleation regime and spinodal decomposition regime. The boundary of two regimes is divided by the line where $dP/d\rho = 0$. Here, P is the bulk pressure and ρ is the density. In the nucleation regime, the kinetics of bubble production is divided by two steps: the nucleation step of critical bubble nuclei and the exponentially expansion step the nuclei. The key quantity for understanding the nucleation process is the nucleation rate J,

$$J = \frac{1}{L^3\langle t_w \rangle},$$

where L is the system size and t_w is the time until a critical nucleus is generated. However, according to [1], the system size dependence of nucleation time measured by numerical simulations performing the volume expansion process holds the relation

$$J = \frac{1}{L^3\tau}$$

where τ is the time appearing when we fit the cumulative distribution function of the nucleation time t_w as

$$F(t) \equiv P(t_w < t) = 1 - \exp\left[-\frac{t - t_0}{\tau}\right], t > t_0.$$

Here, the new characteristic time t_0 appears and in order to clarify t_0 more, in this study, we consider the different relaxation process from that used in [1]. Concretely, we change the temperature not the system volume, then, we discuss the difference of the statistics of bubble production time.

In our poster presentation, we present three results: the first, the nucleation rate does not depend on the method of manipulating parameters, but only on the parameter of the initial condition. Second, we have found the difference of the distribution of bubble production time between the nucleation regime and the spinodal decomposition regime. The last, we present the parameter dependence of nucleation rate and from this data we discuss the kinetics of bubble nucleation.

REFERENCES

1. Watanabe, H. *et al.* "Cumulative distribution functions associated with bubble-nucleation processes in cavitation", *Phys. Rev. E,* 82, 051604 (2010).

Low frequency magnetic field alters nitric oxide production in human endothelial cells

Hidetake Miyata, Nobuko Gan, Tsuyoshi Hondou

Department of Physics, Graduate School of Science
Tohoku University, Aramaki, Aoba-ku Sendai 980-8578, Japan

Low frequency electromagnetic fields (LFEMF) alter a number of physiological properties of the cell. For example, LFEMF promotes proliferation, apotosis, increases intracellular Ca ion concentrations and enhances DNA strand breaks.

We have studied the LFEMF effect on production of nitric oxide (NO) in human umbilical vein endothelial cells (HUVECs). HUVECs were exposed to or not exposed to 50 Hz, 1 mT sinusoidal magnetic field for one hour and NO in the cell culture medium was quantified with the fluorescence intensity of 4, 5- diaminofluorescein (Fig. 1A). The level of NO of exposed group was either significantly ($p < 0.05$) higher or lower than that of non-exposed (sham) group [1]. Previous studies by other groups have shown an increase in NO level in endothelial cells and immune cells after these cells were exposed to LFEMF. At present no clear explanation exists for the discrepancy, but we speculate that the balance of production and consumption of NO in the cell was altered by the LFEMF.

In HUVEC an enzyme called endothelial nitric oxide synthase (eNOS) constantly synthesizes NO from an amino acid L-arginine, but NO, a radical, is converted to other chemical species after reacting with molecular oxygen or other reactive oxygen species (Fig. 1B). Thus, NO level in the cytoplasm is kept at a constant level. If the change of the balance of production and consumption by LFEMF occurs, the level of NO can either increase or decrease depending on which process is promoted or inhibited. At present, the mechanism by which LFEMF affects the NO metabolism is unknown and the complex network of NO metabolism makes it difficult to predict the direction of LFEMF effect. Nevertheless, it will be interesting to pursue the big question of the mechanism of interaction of LFEMF with the cell through the study the effect of LFEMF on NO metabolism.

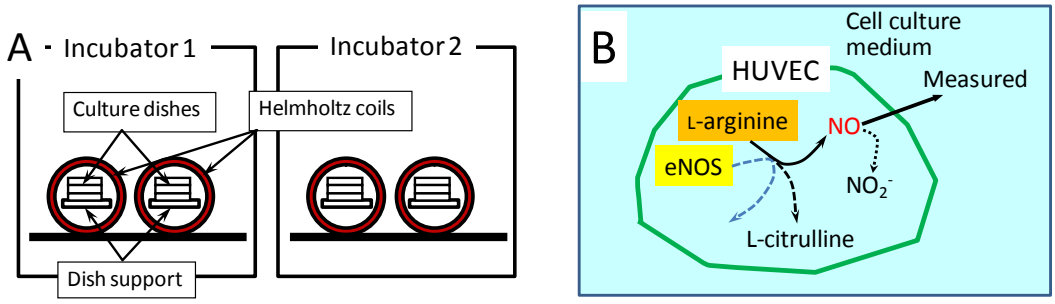

Fig. 1. A, A schematic representation of the arrangement of the Helmholtz coils and cell culture dishes in two CO_2 incubators. Helmholtz coils were used for exposure of cells to LFEMF. In one incubator coils were activated and in the other incubator coils were made inactive. The NO levels were compared between the two incubators.
B, A highly simplified scheme of NO metabolism in HUVEC. The NO produced form L-arginine is metabolized to other chemical species such as NO_2^-, but some NO penetrate the cell membrane and react with 4,5-diamionoflorescein, a fluorescence indicator for NO.

REFERENCES

1. Miyata, H., Ishizawa, S.-i. Ishido, M., Sugawara, K., Murase, M. and Hondou, T. "The effect of a 50-Hz sinusoidal magnetic field on nitric oxide (NO) production by human umbilical vein endothelial cells (HUVECs)", *J. Phys. Conf. Ser.*, in press.

Structure of genealogical network

Tsuyoshi Mizuguchi[1,2)], Yosuke Horiuchi[1)] and Satoru Morita[3)]

[1)] Department of Mathematical Sciences, Osaka Prefecture University,

1-1 Gakuen-cho Naka-ku Sakai 599-8531, Japan,

[2)] JST, PRESTO, 4-1-8 Honcho Kawaguchi, Saitama 332-0012, Japan,

[3)] Department of Systems Engineering, Shizuoka University,

3-5-1 Johoku Naka-ku, Hamamatsu 432-8561, Japan

Structure of genealogical trees of species with sexual reproduction is analyzed from the viewpoint of network. Biparental individuals including human beings have two parents, i.e., a mother and a father. Each of them has again two parents. Therefore, the number of the ancestors of each individual increases exponentially, 2^G for past G generation, and it exceeds the total population size at some era. To resolve this paradox, some ancestors inevitably play multiple roles in the list of one's ancestors. This repetition is exhibited by a complex structure of one's genealogical tree, i.e., a diagram of ancestors and connections between them which represent parent-child relation. Some statistical quantities are analyzed to characterize the structure of the tree for actual living populations, and it is clarified that the children number distribution and the sex ratio are important factor to determine the tree structure. The effect of mating system is also investigated.

Herding and Information Cascade

S. Mori[a], M. Hisakado[b] and T. Takahashi[c]

[a]*Department of Physics, Kitasato University*

[b]*Standard and Poor's*

[c]*Department of Behavioral Science, Hokkaido University*

We perform a sequential voting experiment to clarify how people decides based on others' choices. We gather 62 subjects and divide them into two groups and prepare two sequences of 31 subjects. The subject answers two-choice quiz sequentially with and without infomarion of the summary statistics of the previous r subjects. We change r in $\{0, 1, 2, 3, 5, 7, 9, \infty\}$, where $r = 0$ means the answer without any information and $r = \infty$ means the answer with the information of all previous subjects. As the summary statistics, we use how many subjects among r choose choice 1(0) and denote it as $C_1^r(resp.C_0^r)$. Fig.1 shows the distributions of the ratio of the correct answer for $r = 0$ and $r = \infty$. By observing others' choices, there occurs a drastic change and we see a two-peak structure in the latter case. We categorize the subjects into two classes –independent and herder. The subject in the former class knows the answer and the latter class means the subject who does not know the answer and can be affected by others' choice. We derive how the herder's probability of choosing one, we denote it as p_1, depends on C_1. Fig.2 shows the results for $r \in \{1, 5, 9, \infty\}$. Base on it, we introduce a stochastic model and study the possibility of the cascading transition [1].

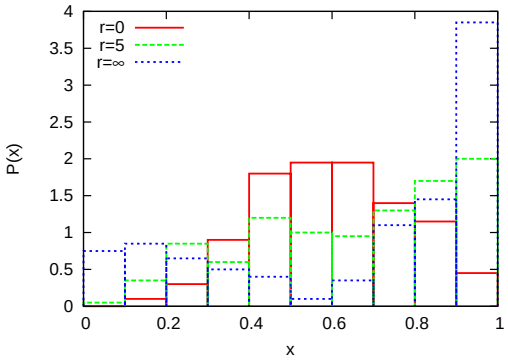

Figure 1: Plot od the distribution $P(x)$ of the ratio x of correct answer for $r = 0(red), 5(green)$ and $\infty(blue)$.

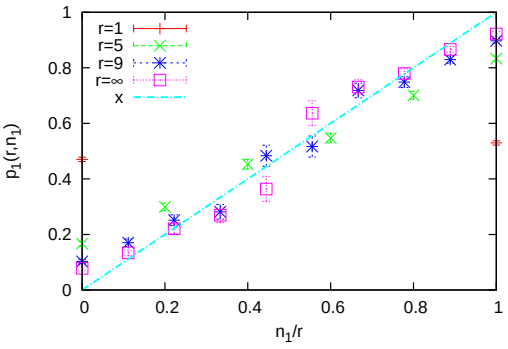

Figure 2: $p_1(r, n_1)$ vs n_1/r. We choose r as $r \in \{1, 5, 9, \infty\}$. We also plot $y = x$ to see fixed points.

References

[1] M. Hisakado and S. Mori, *Digital herders and phase transition in a voting model*, J.Phys.A,Math.Theor.44(2011)275204.

Period Variability for Noisy Coupled Phase Oscillators

Fumito Mori[1] and Hiroshi Kori[1,2]
mori.fumito@ocha.ac.jp
[1]Division of Advanced Sciences, Ochadai Academic Production, Ochanomizu University, Tokyo 112-8610, Japan
[2]PRESTO, Japan Science and Technology Agency, Kawaguchi 332-0012, Japan

Temporally precise oscillations; i.e., oscillations with small period variability, play an important role in many biological systems, including a biological clock for circadian rhythms, a cardiac pacemaker, and an electrical organ in weakly electrical fish. It is believed that temporally precise oscillations are derived from synchronization. Here, we emphasize that temporally precise oscillations are different in concept from synchronization, although they often appear at the same time.

Variability of oscillation periods is generally dependent on the check point, which is the term used to describe the beginning and end points of one cycle. For example, in the experimental data for circadian activity in mice [1], the variability of the periods between each onset of activity is smaller than that between each offset. However, this check-point dependence of period variability has received scant attention either experimentally or theoretically. To understand the phenomenon, we need a basic theory for a simple model. Although there are theoretical studies on the variability of periods in a coupled phase oscillator model [2], the model employed there can not show the check-point dependence of the variability because of its rotational symmetry.

We consider a coupled phase oscillator model without rotational symmetry given by

$$\begin{cases} \dot{\theta_1} = \omega + \kappa J(\theta_1, \theta_2) + \sqrt{D}\xi_1(t) \\ \dot{\theta_2} = \omega + \kappa J(\theta_2, \theta_1) + \sqrt{D}\xi_2(t), \end{cases} \tag{1}$$

θ_i and ω are the phase and the intrinsic frequency of the ith oscillator, respectively. $\xi_i(t)$ is i- and time-independent noise. The positive constants, κ and D, denote the coupling strength and the noise strength, respectively. The interaction $J(x, y)$ is a 2π-periodic function of x and y that drives synchronization. Note that this model is generally derived from weakly coupled limit-cycle oscillators [3].

To quantify the variability of periods, the coefficient of variation (CV) of periods is introduced as follows. The kth oscillation time of an oscillator, $t_k^{\theta_{\rm cp}}$, is defined as the time at which θ passes $2k\pi + \theta_{\rm cp}$ for the first time, where $\theta_{\rm cp}$ is a check-point phase. The oscillation period $\Delta t_k^{\theta_{\rm cp}}$ is defined by $\Delta t_k^{\theta_{\rm cp}} = t_k^{\theta_{\rm cp}} - t_{k-1}^{\theta_{\rm cp}}$. The CV is defined by the standard deviation of the period divided by the average period τ as follow: $\mathrm{CV}(\theta_{\rm cp}) = \sqrt{E[(\Delta t_k^{\theta_{\rm cp}} - \tau)^2]}/\tau$.

We analytically derived the CV as a periodic function of $\theta_{\rm cp}$. It is found that this periodicity has roots in the phase velocity and synchronization. Note that the CV is independent of $\theta_{\rm cp}$ for single oscillator systems. Our formula is in agreement with the numerical simulations, and provides valuable information about coupling as well as clarifying the relation between period variability and synchronization.

REFERENCES

[1] E. D. Herzog, S. J. Aton, R. Numano, Y. Sakaki and H. Tei, *J. Biol. Rhythms* **19**, 35 (2004).
[2] N. Masuda, Y. Kawamura and H. Kori, *New. J. Phys.* **12** 093007 (2010); H. Kori, Y. Kawamura, N. Masuda, arXiv:1108.4790v1.
[3] A. T. Winfree, *J. Theor. Biol.*, **16**, 15 (1967); Y. Kuramoto, *Chemical Oscillations, Waves, and Turbulence* (Springer, NewYork, 1984).

Instability of rivulet flowing inside pipe

Shin-ichiro Nagahiro

Department of Mechanical Engineering, Sendai National College of Technology, Miyagi, 981-1239, Japan

A water stream on a partially wetting surface flows straightly if the inertia of the flow is sufficiently larger than the Capillarity effect. In the case of small flow rate, contamination on the surface or fluctuations in the flow rate inherently brings about fluttering of the stream like a tube conveying fluid [1], or stationary meandering patterns [2]. In this report, we experimentally investigate a water rivulet flowing down inside a vertical acrylic pipe.

In our experimental setup, flow running down the pipe is produced by discharge from an upper container where distilled water is always overflowing to keep the constant water level. We used acrylic pipe whose length is 100cm and inner diameter d varies from 0.5 to 3cm. When the flow rate Q is small ($Q \cong 10$ml/min), we observe an irregular flow (Fig.1a). Similarly with the flow on a plate, meandering patterns appear inside the pipe if the flow rate exceeds a critical value (Fig.1b). We found another critical flow rate Q^* above that the meandering rivulet changes to a spiral (Fig.1c). If we see the spiral flow on the developed viewpoint, the water flows along a tilted straight line. Such a flow also appears on a partially wetting plate. However, no spiral pattern is observed when we put the flow outside the cylinder, thus the inertial effect may play an essential role to make spiral pattern.

The critical flow rate Q^* depends on the inner diameter of pipe, and reaches minimum value at $d \cong 10$cm. We also studied how the surface tension affects the behavior of the flow by adding a surfactant to the water. As the concentration of surfactant rises, the d dependence of Q^* tend to disappear, and the pitch length of the spiral is elongated.

We also discuss on the nature of the transition, and a simple model of rivulet meandering and spiral.

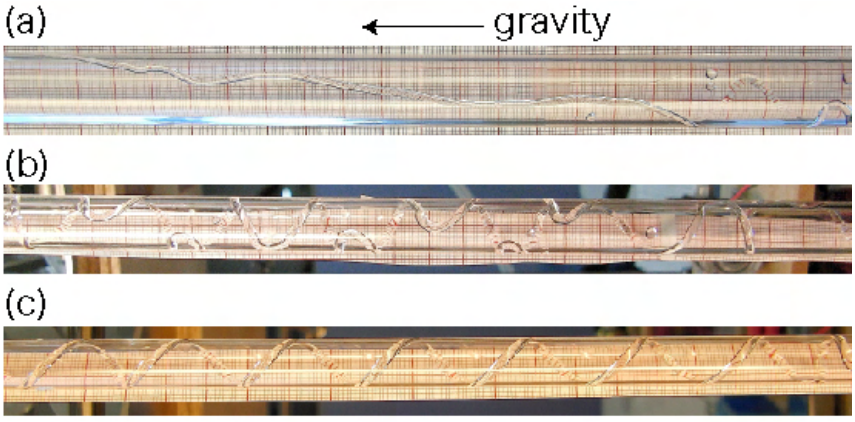

Fig.1 (Color Online) Rivulets inside acrylic pipe. .

REFERENCES

1. S. Shima and T. Mizyguchi “Dynamics of a Tube Conveying Fluid”, arXiv:nlin/0105038 (2001).
2. N. L. G-Piteria, A. Daerr and L. Kimat, “Meandering Rivulets on a Plane: A Simple Balance between Inertia and Capillarity”, Phys. Rev. Lett. **96**, 254503(2006), Bjorn Birnir, Keith Mertens, Vakhtang Putkaradze, and Peter Vorobieff “Meandering Fluid Streams in the Presence of Flow-Rate Fluctuations”, Phys. Rev. Lett. **101**, 114501(2008)

Spontaneous droplet motion induced by Marangoni effect

[1]Ken H. Nagai, [2,3]Hiroyuki Kitahata, [4]Yutaka Sumino, [5]Fumi Takabatake, [5]Masatoshi Ichikawa, [6]Natsuhiko Yoshinaga

[1]*Department of Physics, Graduate School of Science, The University of Tokyo, 7-3-1 Hongo, Bunkyo-ku Tokyo, 133-0033, Japan*
[2]*Department of Physics, Graduate School of Science, Chiba University, 1-33, Yayoi-cho, Inage-ku, Chiba 263-8522, Japan*
[3]*PRESTO, Japan Science and Technology Agency, 4-1-8 Honcho Kawaguchi, Saitama, 332-0012, Japan*
[4]*Department of Physics, Faculty of Education, Aichi University of Education, Aichi 448-8542, Japan*
[5]*Department of Physics, Kyoto University, Kyoto 606-8502, Japan*
[6]*Fukui Institute for Fundamental Chemistry, Kyoto University, Kyoto 606-8103, Japan*

There have been many studies about the motion of biological units. The way they obtain momentum from surroundings has attracted attention and many theoretical models have been proposed. Recently, the nonbiological systems that move spontaneously are actively studied as model systems for the biological motion. Spontaneous droplet motion induced by Marangoni effect is one of such systems [1]. Symmetry of interfacial tension field around a surfactant-containing droplet is broken due to the nonlinear effect by the Marangoni flow [2]. Compared to translational motion, it seems to be difficult to induce the rotational motion using interfacial tension for the following reason: Since the flow speed at the interface is proportional to the gradient of interfacial tension, the uniformly rotating flow around a circular droplet can not be induced without external torque.

We propose a system that shows spontaneous rotation of a droplet induced by the Marangoni effect, which is shown in Fig. 1. The critical Peclet number of our system was calculated as shown in Fig. 2. The theoretical results were compared with the experimental results in [3]. We also investigated the dynamics of the group of rotating droplets using a simple mathematical model. When the density of the droplet is appropriate, droplets accumulate and made the lattice of vortices.

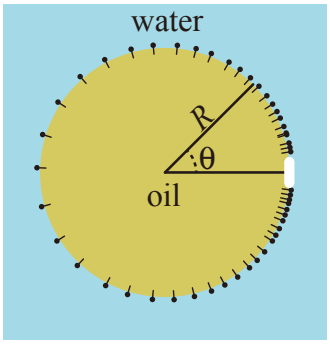

Fig. 0: Schematic diagram of the considered system. A oil droplet with a small particle is in water. The Marangoni flow is induced by the surfactant on oil-water surface.

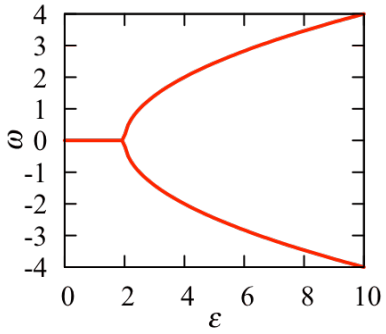

Fig. 2: Bifurcation of the motion. When the Marangoni flow is strong enough (ε is large enough), rotation speed, ω, is finite in the steady state.

REFERENCES

[1] K. Nagai, *et al.*, *Phys. Rev. E* (2005).
[2] M. Nagayama, *et al.*, *Physica D* (2004).
[3] F. Takabatake, *et al.*, *J. Chem. Phys.* (2011).

Memories of paste and their visualization as crack patterns

Akio Nakahara and Yousuke Matsuo

Laboratory of Physics, College of Science and Technology, Nihon University, Narashino-dai 7-24-11, Funabashi, Chiba 274-8501, Japan

A densely packed colloidal suspension with plasticity, called as a paste, remembers the direction of mechanical fields, such as vibration and flow. When a water-poor paste is vibrated at a stress just above the yield stress of the paste, the paste experiences a huge vibration just like an earthquake and remembers the direction of the vibration even after the vibration stops. The memories in pastes are visualized as morphology of desiccation crack patterns. When the paste has a memory of vibration, the lamellar crack pattern emerges as we dry the paste, with the direction of crack propagation all perpendicular to the direction of the initial vibration [1-2].

When a water-rich paste is vibrated, however, the paste is fluidized to form a flow pattern during the initial vibration. We find that a water-rich uncharged paste remembers the direction of flow while a water-rich charged paste cannot remember any flow patterns. The interactions between colloidal particles play important roles in making memories in pastes. When the water-rich uncharged paste remembers the flow pattern, the lamellar desiccation crack patterns emerge with the direction of crack propagation parallel to the direction of the flow induced by the initial vibration [3-5].

Memory effect of paste will be applied to many fields in science and technology. As we can imprint any flow patterns into pastes, we can design morphology of desiccation crack patterns and produce radial, lamellar, ring and spiral crack patterns [1, 3, 6].

This work was done in collaboration with Ooshida Takeshi, So Kitsunezaki, Michio Otsuki, Yuu Shinohara and Hiroshi Nakayama, and was supported by Grant-in-Aid for Scientific Research (KAKENHI) (B) 22340112 and (C) 21540388 and 23540452 of Japan Society for the Promotion of Science (JSPS).

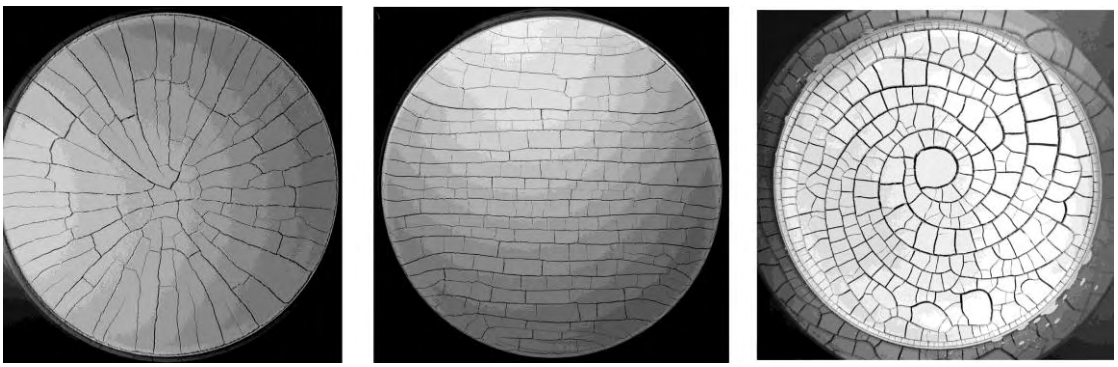

Fig.1 Various crack patterns produced by using memory effects of paste [1, 3].

REFERENCES

1. Nakahara, A. and Matsuo, Y. "Imprinting Memory into Paste and Its Visualization as Crack Patterns in Drying Process", *J. Phys. Soc. Jpn.*, 74, 1362 (2005).
2. Nakahara, A. and Matsuo, Y. "Imprinting memory into paste to control crack formation in drying process", *J. Stat. Mech.: Theory and Exp.*, P07016 (2006).
3. Nakahara, A. and Matsuo, Y. "Transition in the pattern of cracks resulting from memory effects in paste", *Phys. Rev.*, E74, 045102 (2006).
4. Nakahara, A., Shinohara, Y. and Matsuo, Y. "Control of crack pattern using memory effect of paste", *J. Phys: Conf. Ser.*, 319, 012014 (2011).
5. Matsuo, Y. and Nakahara, A. "Effect of interaction on the formation of memories in paste", submitted to *J. Phys. Soc. Jpn.*, *arXiv*:1101.0953v1 [cond-mat.soft].
6. "Desiccation cracks", *Physics Today*, vol. 60, no. 9, p. 116 (2007).

The effect of polymer adsorption on the non-equilibrium transport of colloidal particles

Nakayama Yohei and Sano Masaki

Department of Physics, the University of Tokyo, 7-3-1 Hongo, Bunkyo-ku, Tokyo, 133-0033, Japan.

We have investigated Soret effect of colloidal particles. Soret effect, one of the non-equilibrium transport phenomena, is a transport of particles caused by a temperature gradient. Since it is known that addition of polymers can change the Soret effect of colloidal particles in the solution[1], we measured the motions of silica particles in polyethylene glycol solution under non-uniform temperature in detail. We used focused infrared laser to make an inhomogeneity of temperature, and determined the formed temperature distribution by fluorescence microscopy[2].We extract steady distributions of the particles, as in figure 1, for several concentrations of polymer solution by image processing technique. The exponent of distribution change with the polymer concentration. This corresponds to a change of a mobility of Soret effect, called Soret coefficient, S_T. We also discover that the change of Soret coefficient can be described by Langmuir adsorption equation.

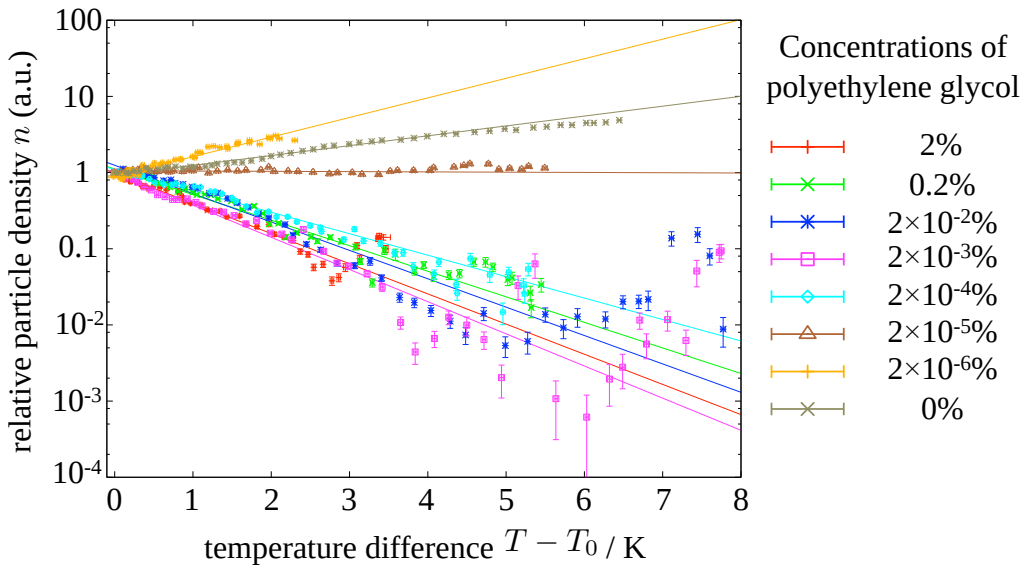

Fig. 1: The steady distributions of silica particles with respect to temperature differences with several concentrations of polymer solution. Fitting lines are given by $n \propto \exp(-S_T(T - T_0))$. Fitting parameters are S_T and normalization factors. The functional form (1) is obtained as a steady state distribution of $J = -D\nabla n - nD_T\nabla T$, which is a fundamental equation of linear non-equilibrium thermodynamics, called ``phenomenological equation'' of particle flow. (D, D_T are diffusion coefficient and thermal-diffusion coefficient, respectively.)

REFERENCES

1. M. Braibanti, D. Vigolo, and R. Piazza, Physical Review Letters **100**, 1-4 (2008).
2. S. Duhr, S. Arduini, and D. Braun, Euro. Phys. J. E, Soft Matter **15**, 277-86 (2004).
3. Jan A van Heiningen and Reghan J Hill, Lab on a Chip **11**, 152-62 (2011).
4. H. Ning, J. Buitenhuis, J. Dhont, and S. Wiegand, J. Chem. Phys. **125**, 204911 (2006).

Combination of Discrete and Finite Elements for the microscopic simulation of particle-loaded flows

Shi Han Ng Hans-Georg Matuttis

Department of Mechanical Engineering and Intelligent Systems,
Graduate School of Informatics and Engineering,
The University of Electro-Communications, Chofugaoka 1-5-1, Chofu-shi, Tokyo, Japan

To analyze two-phase flows of fluid-solid problems, we develop a two-dimensional microscopic simulation (fluid flows around, not "through the particles, as in macroscopic simulations") of Newtonian fluid in which granular particles are suspended. We combined a discrete element method (DEM) for polygonal particles with a finite element method (FEM) for incompressible fluids. The flow field is obtained from the differential algebraic equation-form for the Navier-Stokes equation in the FEM-formulation via Newton-Raphson's method.[1] The time integration for both particles and fluid is done with Backward-Difference Formula of 2^{nd}-order (BDF2)The velocities of the particles are used as the boundary conditions of the flow around them. Force from the fluid acting on the particle is obtained by integrating the fluid stress tensor over the particle's surface. The simulation would become unstable by replacing BDF2 with BDF5, for the particles, which shows that the time integration schemes for particles and fluids cannot be selected independently.

For the grid generation, we introduced a relaxation algorithm[2] in order to improve the quality of our triangular mesh ("more equilateral" triangles) systematically. By treating the sides of a triangular mesh as linear springs, we are able to relax it towards "force equilibrium" (equilateral triangle) using a zeroth-order time integration. Grid adaption is possible by stiffening the springs in regions of high gradients. We verified our fluid-particle code by comparing wall correction factors of dodecagons with values in the literature for circles[3].

Sedimentation of ten polygons of different shapes in a mesh with 1700 triangles. The Reynolds number, obtained from the particle size and the velocity is up to 1000, which is consistent with the relatively long lifetime of the vortices (see Fig. 1 (c)). The area of a single particle corresponds to the area of about 15 triangles of the mesh. The simulation is stable without "tricks" like upwinding or manipulating the viscosity.

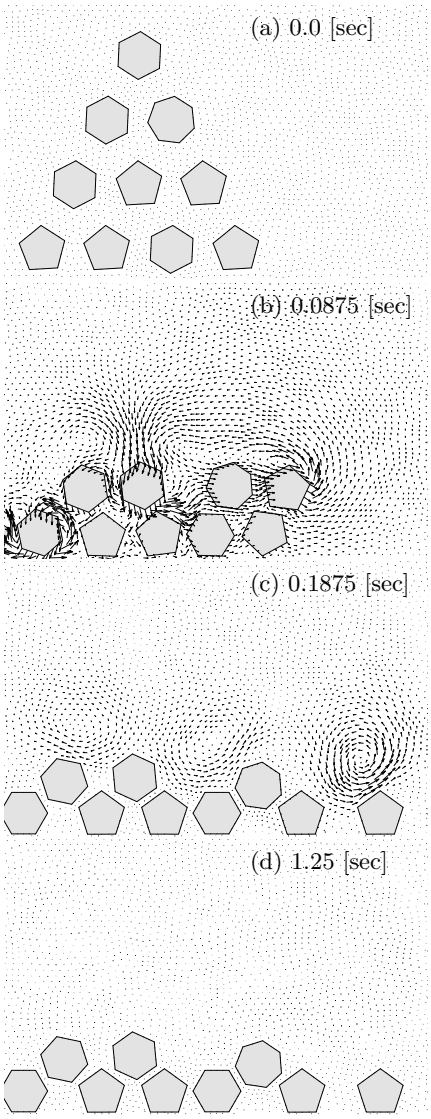

Fig. 1 Snapshots of simulation of fluid with suspending particles.

References

[1] Gresho, P.M., Sani, R.L., *Incompressible Flow and the Finite Element Method: Isothermal Laminar Flow*, vol. 2, John Wiley and Sons, Ltd. (2000).

[2] Ng, S.H., Matuttis, H.G., "Adaptive Mesh Generation for Two-Dimensional Simulation of Polygonal Particles in Fluid", *Theoretical and Applied Mechanics Japan*, 59, 323–333 (2010).

[3] Ng, S.H., Matuttis, H.G., "Two-dimensional Microscopic Simulation of Granular Particles in Fluid", *Theoretical and Applied Mechanics Japan*, 60 (2011).

Pattern formation and bifurcation of *Euglena* in strong optical field

Shuhei Noda, Nobuhiko J. Suematsu[1], Akinori Awazu, Hiraku Nishimori

Department of Mathematical and Life Sciences, Graduate School of Science, Hiroshima University, Kagamiyama 1-3-1, Higashihiroshima-shi, Hiroshima, Japan

[1]Graduate School of Advanced Mathematical Sciences, Meiji University, Higashimita 1-1-1, Tama-ku, Kawasaki-shi, Kanagawa, Japan

Euglena gracilis is a photosensitive unicellular flagellate with a body length of approximately 100 μm. Its response to light illumination depends on the light intensity that means the cell exhibits both positive and negative phototaxis. When the light intensity is stronger than a critical value (0.2 kW/m^2), the *Euglena* tend to swim away from the light source, otherwise the cells swim toward the light source. Furthermore, the cells are sensitive to a gradient of light intensity, and, as a result, the cells assemble in the weakly- illuminated region.

This phototactic behavior of Euglena induces bioconvection. Suematsu et al. reported a novel bioconvection pattern of Euglena, i.e., a localized pattern. In their system, a suspension was prepared in a sealed container, where the surface effect was negligible, that was illuminated from below with a strong light to induce negative phototaxis. [1]

In this study, we discuss the detail structures and dynamical aspects of this bioconvection of *Euglena* through the experiments, image analysis and mathematical model.

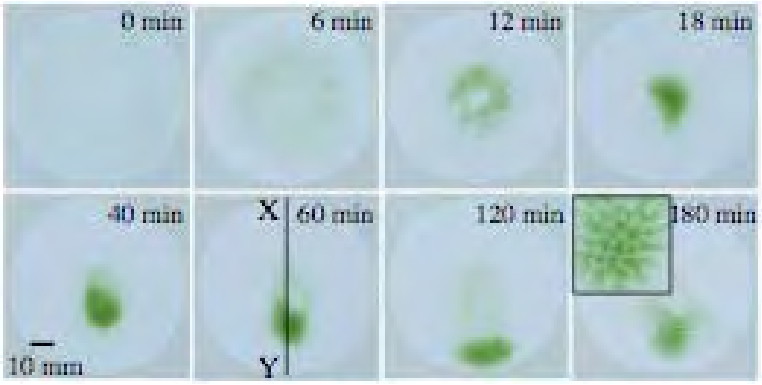

Fig.1 Snapshots during the process of pattern formation by *Euglena*.The diameterof the circular container was 50mm and the suspension depth was 2mm.

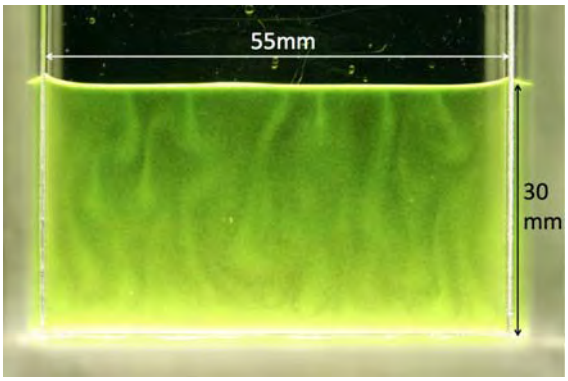

Fig.2 Side view of bioconvection in the vertical-placed chamber.

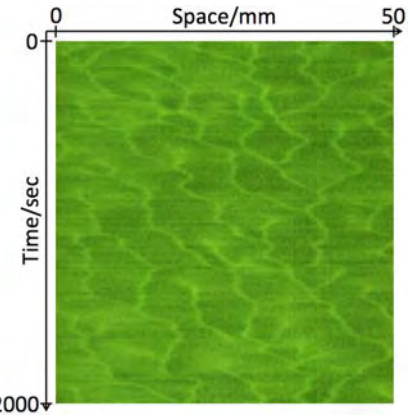

Fig.3 A space-time diagram of a lateral slice at the top of chamber.

REFERENCES

1. Suematsu J. N. *et al.* "Localized Bioconvection of *Euglana* Caused by Phototaxis in the Lateral Direction", *J. Phys. Soc. Jpn.*, 80, 064003 (2011).

Pattern formation of colloids in a polymer solution under a temperature gradient

Kenta Odagiri[1], Kazuhiko Seki[2], Kazue Kudo[1]

1. *Ochadai Academic Production,Ochanomizu University, Otsuka 2-1-1, Bunkyo-ku, Tokyo, Japan*
2. *National Institute of Advanced Industrial Science and Technology, AIST Tsukuba Central 5 Higashi 1-1-1, Tsukuba, Japan*

The migration of particles in fluids induced by a temperature gradient is known as thermophoresis (or the Soret effect). The nonuniform distribution of particles driven by the temperature gradient also influences the migration of particles of another species, which is called diffusiophoresis. Recently, it has been found that colloid particles in a polymer solution localize to a hot region formed by a focused laser [1]. The temperature gradient by the laser drives the polymer's thermophoresis, and as a result, causes the concentration gradient of the polymer. The resulting concentration gradient of the polymer drives the colloids towards the hot region by exceeding the effect of colloids' thermophoresis. More recently, a ring-like distribution of colloids has been reported by using focused laser heating and varying systematically polymer concentrations [2]. Furthermore, separation of the different size of colloids has been observed.

We here introduce the simple model for pattern formation of colloids in a polymer solution under a temperature gradient by considering the entropic effect caused by excluded volume interactions and the effect of thermophoresis of polymers and colloids. The entropic effect by the excluded volume interactions is taken into account by applying a lattice random walk model and taking the continuous limit afterward.

We denote the fraction of lattice points occupied by minor species (colloids) by $c(\vec{r},t)$ and the fraction of lattice points occupied by major species (polymers) by $n(\vec{r},t)$. The size of minor species is assumed to be the same as that of major species for simplicity. Under the assumption, the current of colloids $j^c(\vec{r},t)$ obtained by taking the continuum limit of a lattice random walk model is obtained as,

$$j^c(\vec{r},t) = -D\left\{\left[1-n(\vec{r},t)\right]\left(\vec{\nabla}c(\vec{r},t) + c(\vec{r},t)S_T^c\vec{\nabla}T(\vec{r},t)\right) + c(\vec{r},t)\vec{\nabla}n(\vec{r},t)\right\} \qquad (1)$$

where D and S_T^c are diffusion constant and the Soret coefficient of colloids, and $T(\vec{r},t)$ is spaciotemporal distribution of temperature. In the steady state, we have $j^c(\vec{r},t)=0$ and assume that the system is two-dimensional isotropic medium and the heating region by the focused laser is also isotropic. Thus, we consider the special distribution of all parameters as a function of radius r from the center of laser focus. By solving $j^c(\vec{r},t)=0$ and ignoring the influence of the minor species on the concentration of major species, we have

$$c(r) = c(\infty)\exp\left[-S_T^c\Delta T(r)\right]\frac{1-n(\infty)\exp\left(-S_T^n\Delta T(r)\right)}{1-n(\infty)}, \qquad (2)$$

where S_T^n is the Soret coefficient of polymers and $\Delta T(r) = T(r) - T(\infty)$.

By using the above equation, we discuss the conditions for ring formation and also show phase diagram of depletion, ring formation, and aggregation for colloids.

REFERENCES

1. H.R. Jiang, H. Wada, N. Yoshinaga, and M. Sano, "Manipulation of Colloids by Nonequilibrium Depletion Force in a Temperature Gradient", *Phys. Rev. Lett.*, **102**, 208301 (2009).
2. Y.T. Maeda, A. Buguin, and A. Libchaber, "Thermal Separation: Interplay between the Soret Effect and Entropic Force Gradient", *Phys. Rev. Lett.*, **107**, 038301 (2011).

Quantitive analysis of foraging of the Lasius Japonicus using chemical cues and visual cues

Yusuke Ogihara[A], Kazuki Maeda[A], Katsunori Naka[A],
Shunsuke Izumi[A], Toshiharu Akino[B], Akinori Awazu[A], Hiraku Nishimori[A]

Department of Mathematical and Life Sciences,
Hiroshima University[A], Kagamiyama 1-3-1,Higashihiroshima shi, Hiroshima ken
Department of Materials and Life Science,
Kyoto Institute of Technology[B], Matsugasaki, Sakyou ku, Kyouto shi, Kyouto fu

Ants are representative example among social insects, which form colonies and live as groups. By using communication tools, each colony shows various group behaviors. For example, in foraging, ants that found food secrete pheromone, and by following the pheromone, ants could form trails. In this way, by the exchange of chemical information, ants can carry food to the nest efficiently [1]. Previous research has clearly shown that certain types of ants know the location of their nest during their foraging trip by various cues that include the angle of sunlight, the number of steps from a nest, the landscape, etc. [1] [2]. In the present study we set a conflicted situation for ants such that the relative angle(β) between the homing directions obtained from chemical cues and visual cues is varied as a control parameter, with using a video image analysis, we found that:

i) If the relative angle is small, ants preferentially rely on chemical cues.

ii) If the relative angle is large, ants preferentially rely on visual cues.

The ecological meaning of these results is discussed.

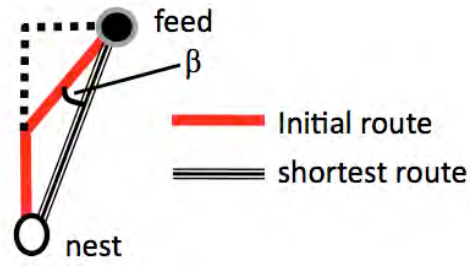

Fig.1：Initial state of experiment

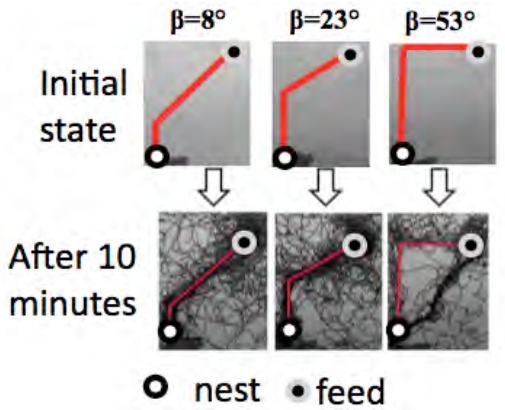

Fig.2：Trail built by Lasius Japonicus
The figure shows the trajectory of Lasius Japonicus 10 minutes after the start of experiment.

REFERENCES

[1] S. E. F. Evison, O. L. Petchey, A. P. Beckerman and F. L. W. Ratnieks , 2008, Behav Ecol. Sociobiol.63: 261-267 (2008)

[2] R. Wehner, F. Raber, Experientia. 35:1569-1971(1979)

Community Dynamics under Indirect Reciprocity Norms

Koji Oishi, Takashi Shimada, and Nobuyasu Ito

Department of Applied Physics, School of Engineering, University of Tokyo, 7-3-1 Hongo, Bunkyo, Tokyo 113-8656, JAPAN

Since mutual help of people often plays important roles in our society, the question how such cooperative relationship can be maintained even if one have to take cost to help another, has long history of research. One of proposed solutions is indirect reciprocity [1], which means if you help someone, one of those who watch your helping will help you back, so it gives you the incentive to help others. Under the mechanism, people assess others as "good" person or "bad" person based on their action. Moreover they decide whether help their counterpart or not, based on whether the counterpart is "good" person or "bad" person.

For now, theoretical studies of indirect reciprocity have mainly paid attention to what kind of assessment rule, that is the definition of "goodness", can promote the cooperation [2]. Few studies were done, however, about community structures of the mutual assessment, that means who think who is "good". In actual human societies, it is often observed that people form groups and cooperate only inside of their own groups, which sometimes can be a cause of serious social problems. Therefore we studied what kind of community structures appear in the model of indirect reciprocity. As the result of numerical simulations, we found that "people" in the model spontaneously split into different communities under some definition of "goodness". On my poster presentation, I will explain the detail of our results and discuss the implication of them on the relationship between reciprocity norms and community structure in our society.

REFERENCES

1. R. D. Alexander, *The Biology of Moral Systems*, Aldine de Geruter, New York (1987)
2. H. Ohtsuki and Y. Iwasa, *J. Theor. Biol*. **231**, 107-120 (2004)

Morphological aspects of carcinogenesis

N. B. Ouchi

Research Group for Radiation Effect Analysis,
Japan Atomic Energy Agency, Tokai, Ibaraki 319-1195, Japan

Cancer, in a broad sense, is the leading cause of death for both men and women in Japan today; about 30% of people have died of cancer. It would be considered that half of the people will suffer from cancer in their lifetime, considering the five-year survival rate for all cancer is about 50%.
Commonly, the definition of cancer is; aggregates of cells with malignancy that normal cells gradually develop precancerous changes by the accumulation of mutations. Here, the word "malignancy" generally implies invasive and metastatic features. Thus the process of carcinogenesis is considered as follows: 1) transformation of normal cell to cancer cell by acquiring mutations, 2) proliferation of cancer cells via clonal expansion, i.e. tumorigenesis, 3) tumor acquire malignancy by malignant transformation. This process is known as genetic multistage process. Fig. 1 is the well-known example of carcinogenesis process of colorectal cancer [1].

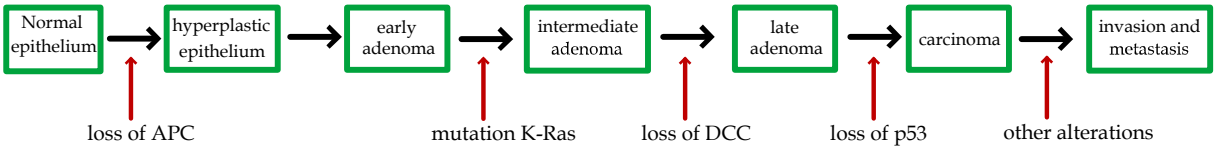

Fig.1 Genetic multistage model of colorectal cancer.

As a mathematical expression of tumor growth process, initiation, promotion and progression (IPP) concept is used for modelling carcinogenesis (Fig.2) [2]. Ionizing radiation is thought to be one of the sources of IPP.

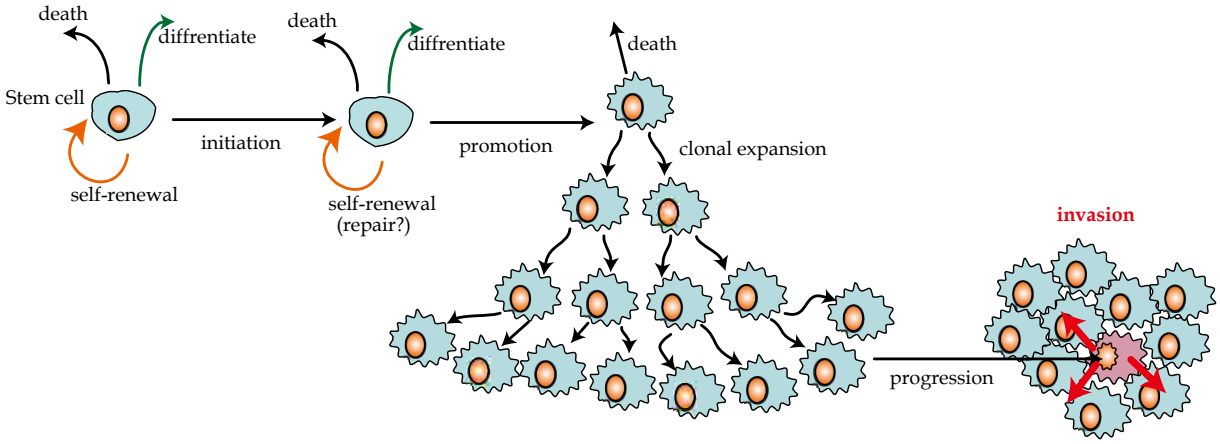

Fig.2 Schematic explanation of tumorigenesis based on IPP concept.

In this presentation, cellular based mathematical model of tumorigenesis is shown and its dynamical aspects, especially based on morphological viewpoint are introduced. The morphological aspect of tumor seems to have important contribution to the progress of invasion because different shape of tumor has different perimeter.

REFERENCES

1. Fearon, E. R. and Vegelstein, B. "A Genetic Model for Colorectal Tumorigenesis", *Cell*, 61, 759-767 (1990).
2. Ouchi, N. B. "Modelling Radiation Health Effects", *Ionizing Radiation / Book 1*, ISBN 979-953-307-345-2, InTech (in press)

The role of phenotypic fluctuation in evolutionary rate

Nen Saito[1], Kunihiko Kaneko[1], Shuji Ishihara[1,2]

1 Graduate School of Arts and Sciences, University of Tokyo, Komaba, Tokyo, Japan,
2 PRESTO, Japan Science and Technology Agency, Kawaguchi, Saitama, Japan

In biological systems, it is known that phenotypic fluctuations or plasticity sometimes play important role. In the context of population genetics, such example is known as Baldwin effect, which claims that phenotypic plasticity speeds up evolutionary process. However, the validity of this effect is still elusive; advantages of phenotypic plasticity in ever-changing environment have been well discussed, whereas there are few models, which deal with advantages of non-responsive phenotypic fluctuation in a static environment [1].

We consider evolutionary dynamics in a model of asexual haploid species in a static environment. In this model, each organism has both genetic trait (g) and phenotypic fluctuation (Σ), which are heritable to next generation. Suppose fitness (reproduction rate) in phenotype space is given as V(x), average fitness $f(g,\Sigma)$ for each individual that has g and Σ, is determined through genotype-phenotype mapping;

$$f(g,\Sigma)=\int \frac{V(x)}{\sqrt{2\pi\Sigma}} e^{-\frac{(x-g)^2}{2\Sigma}} dx .$$

This indicates that larger phenotypic fluctuation provides smaller value of fitness but wider range of its landscape (see Fig.1) . Despite the decreasing fitness, we show phenotypic fluctuation is advantageous for evolutional rate under some conditions.

We study evolution under an unimodal $V(x)$ (Fig.1) and a ragged $V(x)$ (Fig.2). In the latter case, large phenotypic fluctuations provide remarkable expediting effects in evolutionary rate. We show that, depending strength of phenotypic fluctuation and mutation rate, the extended-localized transition in genotype space appears (Fig.3).

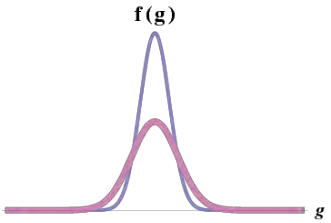

Fig.1 (Color Online) Fitness landscapes for larger (blue) and smaller (red) phenotypic fluctuation.

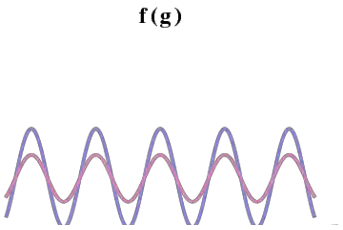

Fig.2 (Color Online) The ragged landscape of fitness. Larger phenotypic fluctuation smoothen valleys in fitness landscape (red).

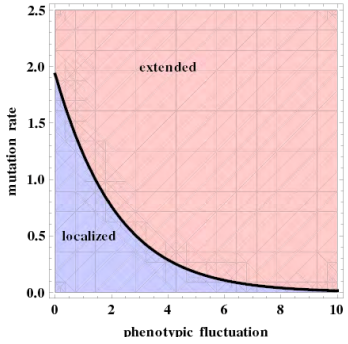

Fig.3 (Color Online) Phase diagram of the extended-localized transition in genotype space. Horizontal axis: strength of phenotypic fluctuation. Vertical axis: mutation rate.

REFERENCES

1. Ancel, L.W. "Undermining the Baldwin Expediting Effect: Does Phenotypic Plasticity Accelerate Evolution ?", *Theor. Pop. Biol.,* **58**, 307 (2000).

Branching Patterns and Stepped Leaders in a Simple Discharge Model

Hidetsugu Sakaguchi and Sahim M. Kourkouss

Department of Applied Science for Electronics and Materials,
Interdisciplinary Graduate School of Engineering Sciences,
Kyushu University, Kasuga, Fukuoka, Japan

Discharge patterns such as lightning often take a branching structure. Fractal-like patterns appear in the creeping discharge. In the creeping discharge, a strong voltage is applied at a point electrode on the surface of dielectric materials. Discharge patterns appear around the point electrode at the interface between the dielectric materials and the surrounding gas or liquid. In a suitable range of voltages, densely branched patterns are observed, that are called Lichtenberg figures. Fractal analysis was performed for the Lichtenberg figures obtained in experiments by several groups. It was found that the fractal dimension decreases with increasing thickness of dielectric materials. The growth dynamics was also studied experimentally using a high-speed camera. When the electric voltage is increased over its threshold value, surface corona appears locally around the central electrode. The corona discharge is a weak discharge that appears locally around a sharp electrode. When the voltage is beyond a second threshold, surface leaders appear. A surface leader shows a stronger discharge than the surface corona. The surface corona grows further around the tips of surface leaders. The growth of surface leaders is not always smooth in time, but sometimes intermittent in time. A similar intermittent growth of the leaders is well known in the lightning discharge. When a leader goes down from a thunder cloud to the ground, it moves in steps of about 30 m with a pause of about 40 ms between steps. This is called the stepped leader. When the leader reaches the ground, a flashover occurs and a strong flash called a return stroke appears, which we observe as lightning.

We propose a simple deterministic model of resistors and capacitors for the creeping discharge on a triangular lattice. A two-step function is used to represent the change of resistance owing to the discharge, which corresponds to the two types of discharge: surface corona and surface leaders. Branching patterns appear in this model. Discharge patterns become more densely branched as the capacitance is larger as shown in Fig.1. We find that the time evolution is not smooth but the surface leaders exhibit a behavior similar to the stepped leader. We construct a simpler one dimensional model to understand the stepped motion.

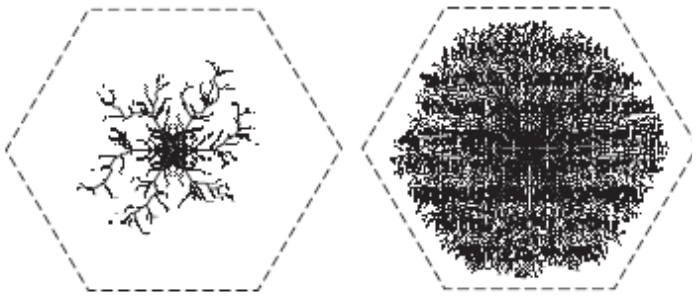

Fig.1 Branching patterns at C=0.024 (left) and 0.054 (right).

REFERENCES
1. H.Sakaguchi and S.M.Kourkouss, *J.Phys.Soc.Jpn.,* 79, 064802 (2010).
2. H.Sakaguchi and S.M.Kourkouss, *J.Phys.Soc.Jpn.,* 80, 094003 (2011).

Mode Analysis of Granular Jet Scattering with Rectangular Cross Section

Tomohiko Sano, Hisao Hayakawa

Yukawa Institute for Theoretical Physics, Kyoto University,
Kitashirakawa Oiwake-Cho, 606-8502 Kyoto, Japan

Granular jet experiments[1] are interesting experiments not only for granular physicists but also for nuclear physicists[2]. Granular physicists are interested in the granular jet experiment because many questions are left concerning contact flows. Nuclear physicist regarded this experiment as a classical version of non-central collision experiment of heavy ions at RHIC. We performed DEM simulation of granular jet scattering in 2D & 3D, and analyzed the results, such as a differential cross section, numerically.

The motivation of the granular jet experiment was the similar scattering experiment. It was the scattering of water columns[3][4]. After water column drops onto a fixed target, it forms a thin sheet after the impact. The shape of the sheet can be bell-like or cone-like structure. Then here is one question, '**When can a jet of discrete particles to be modeled as a liquid, and how do the liquid patterns emerge out of individual particle scattering events from a target?'[1]** Chen *et al*. [1] found that '**as the ratio of the diameter of granular particles and that of the jet increases, particle-like behaviour of the scattering pattern emerges**.' This result was studied by Discrete Element Method(DEM) in 2D[5]. But Y. J. Huang, *et al*.[5] studied this particle-like behaviour only in the case '0.1 < e < 0.9' (e : Coefficent of Restitution). **We found that particle-like behaviour may emerge even in the elastic limit by DEM in 2D**(see Fig. 1).

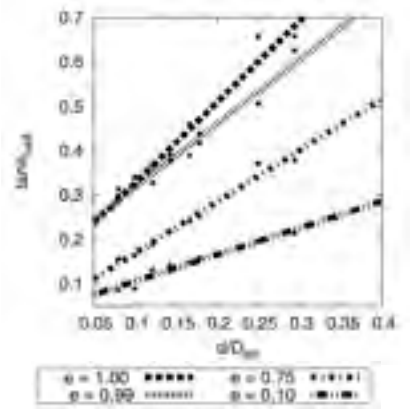

Fig.1 emergence of particle-like behavior

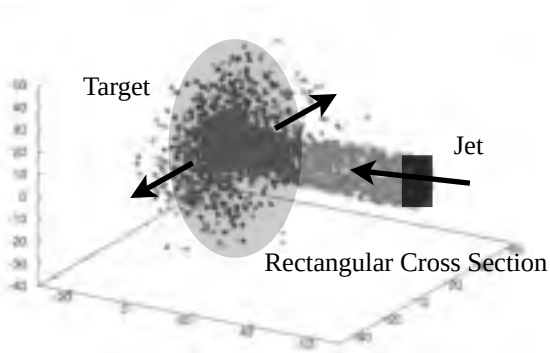

Fig. 2 : snapshot of granular jet scattering with rectangular cross section (by DEM)

The mode analysis of the differential cross section(DCS) has not been studied in the previous study[5]. **We studied DCS of the granular jet experiment by DEM in 3D.** DCS describes the angular distribution of scattered particles. We found that as the ratio of the diameter of granular particles and that of the jet increases, the scattering peak becomes smaller and its variance does larger in 3D. This is the emergence of particle-like behaviour as mentioned above. Recently we are studying **"the scattering with rectangular cross section."** This geometry is familiar with nuclear physicist, because collisions of atomic nuclei are usually non-central collisions, which means its cross section is not circle, but ellipse. X. Cheng, *et al*.[1] found "elliptic flow" in the granular jet experiment with rectangular cross section. We will report the results of the simulation under this geometry.

REFERENCES

1. X. Cheng, *et al*. Phys. Rev. Lett. **99** 188001 (2007)
2. I. Arsene, *et al*. Nucl. Phys. A. **757**, 1 (2005)
3. F. Savart, Ann. de Chim. **54**, 56 (1833)
4. C. Clanet, J. Fluid Mech. **430**, 111 (2001)
5. Y. J. Huang, *et al*. Phys. Rev. E **82**, 031307 (2010)

Scaling Properties and Markovian Nature of Equilibrium Interfaces

Shin-ichi Sato

Department of Physics, Faculty of Science, Shizuoka University,
Ohya 836, Suruga-ku, Shizuoka 422-8529, Japan

We focus on the Markov property of height fluctuations to consider the interfacial problem. The Markov property here means that surfaces with a similar statistical property can be regenerated by a Markov process compared with the original one. By concentrating on a specific class of systems exhibiting the Markovian nature of height fluctuations, an important simplification arises on describing the fluctuations. Let $p(\Delta h, r)$ be the probability of finding a height difference Δh between two points separated by r. If the height fluctuations have the Markovian nature, then the n-joint probability can be expressed by

$$p(\Delta h_1, r_1;\ \Delta h_2, r_2\ ; \cdots ; \Delta h_n, r_n) = p(\Delta h_1, r_1) \prod_{i=1}^{n-1} p(\Delta h_{i+1}, r_{i+1} | \Delta h_i, r_i), \tag{1}$$

which yields a Fokker-Planck equation for $p(\Delta h, r)$ [1]. The Markov property by itself does not prescribe a specific value for the roughness exponent. Hence we consider the system in which height fluctuations can be described by using a surface energy or a Hamiltonian in order that the roughness exponent is determined in a self-organizing manner. In this work, such a discrete equilibrium system is introduced for rough surfaces and the scaling properties of height fluctuations showing the Markov property of Eq. (1) are studied.

Simulations of the introduced system were carried out in 2+1 dimensions. In the simulations, the Markov property of height fluctuations is verified by the Chapman-Kolmogorov equation, which is a necessary condition for the process being Markovian. It is also found that the interface width obeys the Family-Vicsek scaling in terms of the number of simulation-steps instead of time. Figure 1 shows the roughness exponent α and the growth exponent β as a function of K, where K is a dimensionless parameter proportional to the inverse of temperature. The interface is always rough and the scaling exponents change continuously as K varies. Our equilibrium system shows infinitely many universality classes in 2+1 dimensions, which is contrast with the behavior of showing a unique value of $\alpha = 1/2$ in 1+1 dimensions [2].

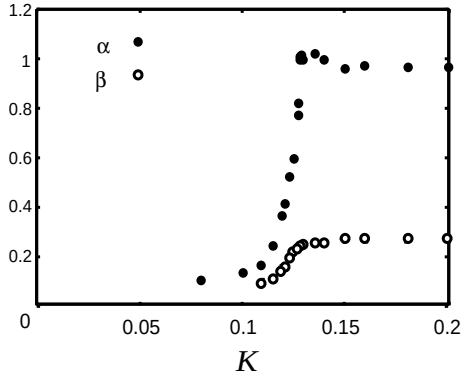

Figure 1: Scaling exponents as a function of K. α and β are denoted by filled and open circles, respectively.

REFERENCES

1. G. R. Jafari, *et al.* Phys. Rev. Let. **91**, 226101 (2003).

2. S. Sato and T. Kitamura, Phy. Rev. E **73**, 026119 (2006).

Characteristics of Statistical Distributions of Height and Weight

Yuta SATO, Jun-ichi WAKITA, Mitsugu MATSUSHITA

Department of Physics, School of Advanced Science-and-engineering,Chuo Univ

[Introduction]

Human's physique is affected by an economic situation, change of a life style, etc. Especially indices such as "height" and "weight" are treated as most fundamental data, when checking our physical condition. Therefore we focus on the statistical distributions of height and weight, and elucidate the characteristics of the distributions from the view of physics.

Here, the time developments of the distributions which are classified by year of birth are analyzed from 5 to 17 years old, and how the body mass index (BMI), which shows the physical feature, changes with age.

The statistical data of height and weight are obtained from the researches by the Ministry of Education, and BMI is calculated by the following equation

$$BMI = \frac{Wieght\ [kg]}{(Height\ [m])^2}.$$

The time developments of BMI from 5 to 17 years old are performed from the year 1954 to 2010.

[Result]

Figure 1 and Figure 2 show the results that the time developments of BMI are different between male and female. In the case of male, the increasing dependency of BMI is recognized as a function of year and age, while in the case of female, the dependency of BMI is similar to the case of male except the age over 15 years old after the year 1985 where BMI seems to be constant. These results indicate that female in the age from 15 to 17 years old may be affected by the social trend in recent years which prefers the delicate type.

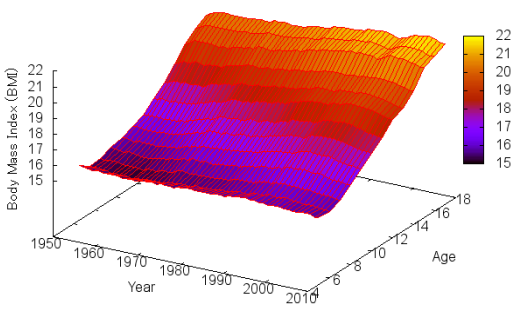

Fig.1 The male's body mass index

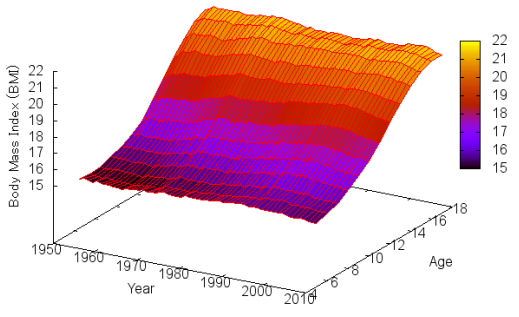

Fig.2 The female's body mass index

Statistical Physics Approach to Understanding Universal Patterns in Ecosystem

Takashi Shimada

Department of Applied Physics, Graduate School of Engineering, The University of Tokyo, Hongo 7-3-1, Bunkyo-ku, Tokyo, 113-8656 Japan

Ecosystem is a prominent example of complex and open systems. Especially, "universal" aspects in its dynamics and statistics in evolutionary time scale have attracted much interest including physicists. Statistical physics approach: Seeking relevant features of the system to reproduce observed characteristics by proposing and investigating minimal models, is a promising way to getting better understanding.

Based on that idea, we proposed a simple population-dynamics-based model to study systems those spontaneously grow to rich and realistic food web structure under successive invasion of new species. We found that the model reproduces several different characteristic statistics found in fossil data such as the skewed distribution (q-exponential or stretched exponential like distribution) of the life span of species [1-4]. This suggests that some empirically found patterns can be relating each other.

We next focused on the distribution of the species life span to understand the origin of the characteristic statistics. For this we studied an individual-based model, and found that this totally different model also provides the skewed distribution of the lifespan under successive invasion, while it shows broader tail when there is a correlation between the newly coming species and the resident species [5]. These findings suggest that the characteristic form of the species life span is universal, since those appear independently from the details of the underlying community dynamics.

Therefore we next consider a further simplified graph dynamics model. Simulations with fixed interaction density among species are again found to reproduce the skewed distribution, which is close to a stretched exponential function with the exponent 1/2. This distribution stems from an age-independent mortality of the species and a system-size independence of the fluctuation of the diversity [6]. Results on a system with fixed number of interactions, which shows much larger fluctuation in diversity, will be also presented on the poster.

REFERENCES

1. T. Shimada, S. Yukawa & N. Ito, *Artificial Life and Robotics*, Vol. 6 (2002) 78-81
2. T. Shimada, S. Yukawa & N. Ito, *Int. J. of Mod. Phys. C*, Vol. 14 (2003) 1267-1271
3. T. Shimada, Y. Murase, N. Ito, & K. Aihara, *Artif. Life and Robot.*, Vol. 11 (2007) 153-156
4. Y. Murase, T. Shimada, & N. Ito, *Artif. Life and Robot.*, Vol. 13 (2009) 460-463
5. Y. Murase, T. Shimada, N. Ito & P. A. Rikvold, *J. of Theo. Biol.* (2010) Vol. 264, (2010) 663-672
6. Y. Murase, T. Shimada, and N. Ito, *New J. of Physics*. Vol. 12, (2010) 063021

Surface pattern formed in Rayleigh-Taylor instability

Michiko Shimokawa

Center for Frontier Science, Chiba University
Chiba University, Yayoi-cho 1-33, Inage-ku, Chiba 263-8522, Japan

When a coffee droplet is put on milk silently, a fractal pattern is observed at the surface of milk as shown in Fig. 1 [1]. The densities of coffee and milk are 1.71 g/ml and 1.03 g/ml, respectively. Rayleigh-Taylor instability occurs in this experiment. The similar fractal pattern, shown in Fig. 2 (a), is also formed in the experiment using magnetic fluid and glycerine solution instead of coffee and milk. The densities of magnetic fluid and glycerine solution are 1.4 g/ml and 1.2 g/ml, respectively. They give the condition for the formation of the fractal structure: (1) the heavier solution is insoluble with the lighter solution, (2) a density of a droplet left on a base solution is larger than that of the base solution.

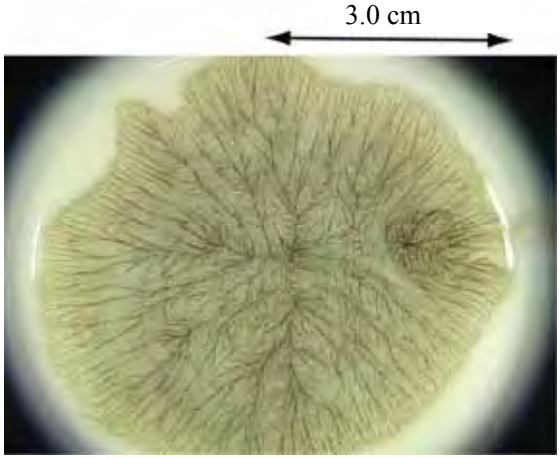

Fig.1 (Color Online)
Coffee fractal observed at the surface of milk

Next, a dependence of the surface pattern is investigated in varies of aspect ratio r / h, where r and h are radius of beaker and the height of glycerine solution. In this experiment, not only a fractal pattern in Fig. 2 (a) but also a cell pattern in Fig. 2 (b) is observed. The cell pattern emerges at $r > h$. On the other hand, the fractal pattern emerges at $r < h$. When the pattern transfers, the vertical convection also changes as shown in Figs. 2 (c) and (d). The comparison between these convections leads that the process, which magnetic fluid gathers at the center of the beakers, is important for the formation of fractal structure.

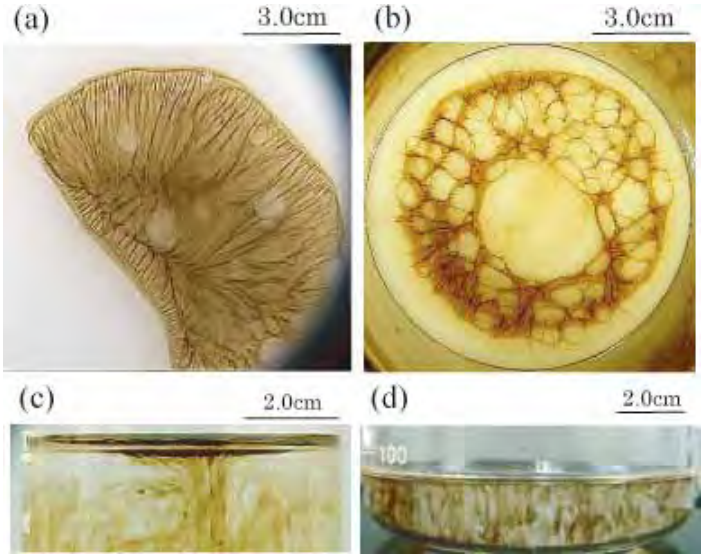

Fig.2 (Color Online) (a) Fractal pattern. (b) Cell pattern. (c) and (d) Vertical flows, which correspond to (a) and (b), respectively.

1. Shimokawa, M. and Ohta, S. “Annihilative fractals formed in Rayleigh-Taylor instability”, *Fractals*, 19, 1-8 (2011).

A minimal model of homing behaviors of homing pigeons

Masashi Shiraishi, Yoji Aizawa

Department of Physics, School of Advanced Science and Engineering,
Waseda University, Okubo 3-4-1, Shinjuku-ku, Tokyo, Japan

We propose a minimal model of homing behaviors of homing pigeons including the effects of the environment and communication, parameterized by an attraction affinity, a positional local force, and an interaction. In the biological study [1], the geomagnetism and solar compasses are famous for a sense of direction. And the senses of sight and olfactory are well-known perceptions to cognize their own local situation. We assume that homing pigeons incorporate the all senses and the incorporating perceptions are composed of the global perception like the geomagnetism and solar compasses and the local perceptions like the senses of sight an olfactory. Our model includes the perceptional force $\boldsymbol{F}_i^p(t)$ as a sum of the effect of the two perceptions. We distinguish the interaction between individuals in a flock from the homing behavior mechanism and represent the effect as the interaction force $\boldsymbol{F}_i^s(t)$. And we regard that the individuals keep their speed constant. We introduce the following equation as the minimal model:

$$\dot{\boldsymbol{v}}(t) = (1 - \|\boldsymbol{v}(t)\|^2)\boldsymbol{v}(t) + \boldsymbol{F}_i^p(t) + \boldsymbol{F}_i^s(t)\,, \tag{1}$$

$$\dot{\boldsymbol{x}}(t) = \boldsymbol{v}(t), \tag{2}$$

$$\boldsymbol{F}_i^p(t) = -w_g \boldsymbol{N}[\boldsymbol{x}_i(t) - \boldsymbol{x}_G] - w_l \boldsymbol{N}[\boldsymbol{k}] \sin(2\pi \boldsymbol{k}\cdot\boldsymbol{x}) \tag{3}$$

$$\boldsymbol{F}_i^s(t) = \sum_{\{j\neq i\}} \boldsymbol{N}[\boldsymbol{r}_{ij}] \left(-\frac{C_r}{l_r}\exp\frac{r_{ij}}{l_r} + \frac{C_a}{l_a}\exp\frac{r_{ij}}{l_a}\right) \tag{4}$$

where $\boldsymbol{x}_G$ is the goal, $\boldsymbol{k}$ is a wave vector. $\boldsymbol{N}[\boldsymbol{u}] = \boldsymbol{u}/\|\boldsymbol{u}\|$, and $\boldsymbol{r}_{ij} = \boldsymbol{x}_j(t) - \boldsymbol{x}_i(t)$. The first term on the right-hand side of the velocity eq. (1) is a speed conservation term. The second term corresponds to the perceptional force which affects each individual. The last term represents that the interaction force between *i*-th individual and other individuals. Eq. (2) is a normal position update equation. The perceptional force is represented in eq. (3). The first term corresponds to the global perceptions and the second one means the local perceptions. The perceptional forces are parameterized by the weighting parameters w_g and w_l respectively. And we adopt molecular attraction-like force as the interaction force for simplicity in eq. (4). Fig. 1-(a) is the snapshot of a single individual's trajectory.

First we analyzed the dependence of the parameters for return ratio of homing for a single individual model. We calculated return ratio for an initial ensemble and present that the parameters, w_g and w_l, can represents the individual behaviors. (Fig. 1-(b)) In the yellow domain, $w_g > w_l$, the individual home perfectly and in the black domain, $w_g < w_l$, the one cannot home. Then we study the collective behaviors in the case of N = 2 and the effect of the interaction. In the numerical calculation, one individual has the fixed parameters and the other adjust parameters in the same way as a single individual. As a result, we showed the group behaviors depend on the parameters of the individuals.

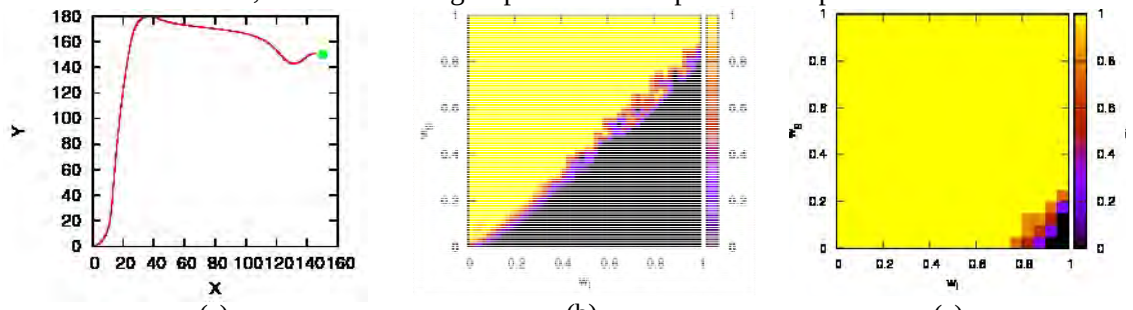

(a) (b) (c)

Fig. 1 (a) The snapshot of the trajectory with, $w_g = 0.5$ and $w_l = 0.5$. (b) The phase diagram of return ratio for a single individual. (c) The phase diagram of return ratio of an individual with fellow that parameterized as $w_g = 0.8$ and $w_l = 0.2$. The fellow can home perfectly if he is alone.

REFERENCES

1. Hans G. Wallraff, Avian Navigation: Pigeon Homing as a Paradigm, Berling, Germany, Springer, (2005)
2. R. Freeman, R. Mann, T. Guilfford, and D. Biro, "Group decisions and individual differences: route fidelity predicts flight leadership in homing pigeons (Columba livia)", Biology letters, vol 7, 63-66, (2010)

Allometries in the Cell Motility of the *Physarum* Plasmodium

Tomohiro Shirakawa

Department of Computer Science, School of Electrical and Computer Engineering, National Defense Academy of Japan, Hashirimizu 1-10-20, Yokosuka, Kanagawa, Japan

Exploration for the living space is a fundamental activity for the survival of living organisms. In fact, there has been many studies on the exploratory behaviors of many species including mammals, birds, insects and so on. Even a unicellular organism, the plasmodium of *Physarum polycephalum*, shows an adaptive behavior in their exploration.

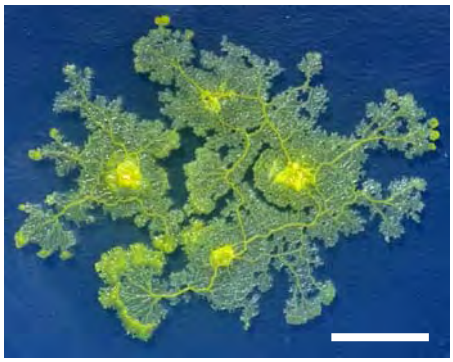

Fig.1 The *Physarum* plasmodium crawling on a 1.5 % non-nutrient agar plate. (Bar: 1 cm)

The plasmodium is a unicellular and multinuclear giant amoeba that grows up to the macroscopic scale (Fig. 1). Recent studies indicated that the plasmodium can solve a maze [1], optimize a network between multiple nodes [2], and find a solution for some graph theoretical problems [3]. However, these studies pursue the optimization by the organism after the full search for the space. For example, in the maze-solving by the plasmodium, the organism first fills out the maze space and then the solution for the maze is found. However, it seems to be more important to study the exploratory behavior for the unknown space in terms of biology and information science.

To study how the plasmodium explores the unsearched space, we focused on the two allometric laws in the cell motility of the plasmodium from our previous studies. In the plasmodium, for the coverage area S, mass M, velocity of cell motility v, cell body length l, the equations below hold,

$$S \sim M^{3/4} \quad (1)$$

$$v \sim l\ (\sim M^{1/3}) \quad (2)$$

In this study, these equations are integrated into one schema in terms of the dynamics of the cell motility of the *Physarum* plasmodium, shedding new light on how such allometries arise in the exploratory behavior of the organism.

REFERENCES

1. Nakagaki, T. *et al.* “Maze-solving by an Amoeboid Organism”, *Nature*, 407, 470 (2000).
2. Shirakawa, T. and Gunji, Y.-P. “Emergence of Morphological Order in the Network Formation of *Physarum polycephalum* ”, *Biophys. Chem.*, 128, 253-260 (2007).
3. Shirakawa, T. and Gunji, Y.-P. “Computation of Voronoi Diagram and Collision-free Path using the Plasmodium of *Physarum polycephalum*”, *Int. Journ. Unconventional Computing*, 6, 79-88 (2010).

Behavior of a deformable self-propelled domain in an excitable reaction-diffusion system

K. Shitara[1] and T. Ohta[1]

[1] *Department of Physics, Graduate School of Science, Kyoto University, Kitashirakawaoiwakecho, Sakyo-ku Kyoto 606-8502, Japan*

Solitary structures can be found in many type of dissipative systems. Particularly, a self-propelled solitary domain attracts considerable interest of researchers in nonlinear science. In experiment, a self-propelled domain can be observed as current density in gas-discharge systems, in semiconductor devises, and on electrical oscillators. These systems are expressed in nonlinear reaction-di usion equations. In higher dimensions, a moving domain tend to deform its shape proportionally with the magnitude of its velocity, and the shape of a domain has head-tail asymmetry along the propagating direction[1]. Furthermore, according to recent investigations, it has been revealed that a deformable self-propelled particle exhibit complex behaviors like a circular and a helical motion [2, 3]. However, there is few study considering the e ect of deformation of a moving domain in a reaction-di usion system.

Quite recently, we have derived, by a singular perturbation method, the set of time-evolution equations of a deformable self-propelled domain starting from an excitable reaction di usion system both in two and three dimensions [4, 5]. As the result, each term of the derived equations agree with one of the equations of a deformable self-propelled particle derived from the symmetry consideration[2, 3]. We have found that the shape of a domain propagating at a constant velocity are determined by evaluating the sign of coe cients in the time-evolution equations, and have obtained the phase diagram for the motions of a domain given in the parameter space of the original reaction-di usion equations.

References

[1] K. Krischer and A. Mikhailov: Phys. Rev. Lett. **73**, 3165 (1994).
[2] T. Ohta and T. Ohkuma: Phys. Rev. Lett. **102**, 154101 (2009).
[3] T. Hiraiwa, K. Shitara and T. Ohta: Soft Matter **7**, 3083 (2011).
[4] T. Ohta, T. Ohkuma, and K. Shitara: Phys. Rev. E **80**, 056203 (2009).
[5] K. Shitara, T. Hiraiwa, and T. Ohta: Phys. Rev. E **83**, 066208 (2011).

Multiscale Complexity of Exotic Statistical Physics Systems

Zbigniew R. Struzik

Graduate School of Education, The University of Tokyo, 7-3-1 Hongo, Bunkyo-ku, 113-0033, Tokyo, Japan

In the poster, I will look into three classical examples of real-life complex systems, which have been extensively analysed by physicists over the past couple of decades: cardiac regulatory system, neural system and financial market. Using my favourite, multiscale approach to the analysis of complex time series, in all the three 'exotic' domains, heart rate [1], financial [2] and neural activity [3], I will illustrate how this kind of analysis helped to uncover physical complexity characteristics.

Email: zbigniew.struzik@p.u-tokyo.ac.jp.

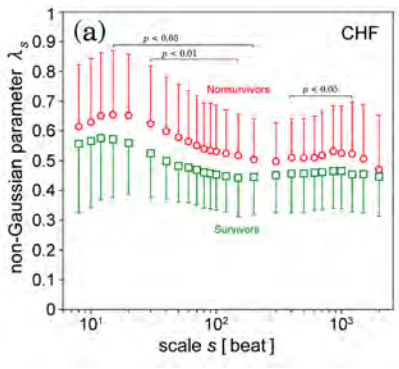

Fig.1 (Color Online) Scale dependence of the non-Gaussian parameter λ for heart rate of congestive heart rate failure patients. (a) Significant differences between the survivors and non-survivors are observed in the range of [15, 200] beats and [400, 1200] beats ($p<0.05$ by 2-tail 2-sample t-test). The squares represent the averages for 69 survivors, and the circles those for 39 non-survivors. The error bars are the standard deviation [2].

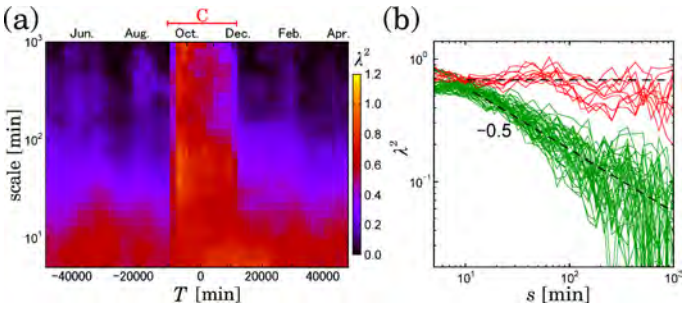

Fig.2 (Color Online) (a) The temporal and scale dependence of λ, where the λ is estimated for each two-month term (~2 × 10^4 data points at sampling intervals at Δt = 1 min) for the S&P500 index. The color scales represent values of λ. The terms in region C include data of black Monday in October 1987. (b) The scale dependence of λ. Red lines correspond to the results in region C of (a). The data before black Monday (disjoint from region C) is represented by green lines [3].

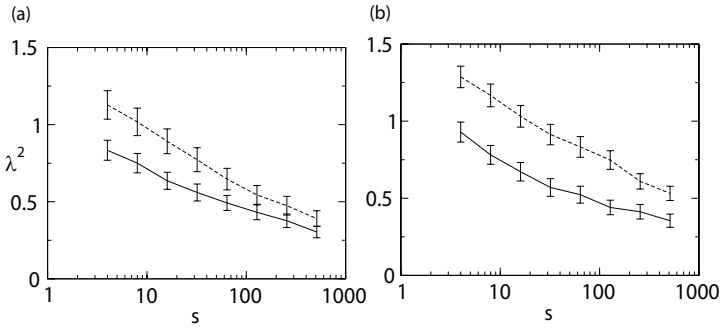

Fig.3 λ for a single tetrode and a single neuron from in vivo recordings in rats. (a) The λ value of single-tetrode spike train (defined precisely in the text) is calculated for each tetrode. The mean value of λ thus calculated over 23 tetrodes is plotted along with the standard deviation. (b) λ value of a single-neuron spike train is calculated for each neuron and the mean value of the λ over 49 neurons is plotted along with standard deviation [4]

REFERENCES

1. Struzik, Z.R. *et al*. “Increased Heteroscedasticity of Heart Rate in Fatal Heart Failure”. *Europhys. Lett.* 82, 28005, (2008).
2. Kiyono, K. *et al*. “Criticality and Phase Transition in Stock Price Fluctuations”, *Phys. Rev. Lett.*, 96, 068701 (2006).
3. Safonov, L.A. *et al*. Near scale-free dynamics in neural population activity of waking/sleeping rats revealed by multiscale analysis, *PLoS ONE*, 5:e12869, (2010).

Large scale nematic vortex of self-propelled microtubules induced by local interaction

Yutaka Sumino[1], Ken H. Nagai[2], Kazuhiro Oiwa[3], Hugues Chaté[4]

[1]Department of Education, Division of Physics, Aichi University of Education, Hirosawa 1, Ogayacho, Kariyashi, Aichi, Japan .[2]Department of Physics, The University of Tokyo, 7-3-1 Hongo, Bunkyo, Tokyo, Japan. [3]Advanced ICT Research Institute, National Institute of Information and Communications Technology, 588-2, Iwaoka, Nishi-ku, Kobe, Japan., and Graduate School of Life Science, University of Hyogo, Harima Science Park City, Hyogo, Japan [4]Service de Physique de l'Etat Condensé, CEA-Saclay, 91191 Gif-sur-Yvette, France.

Pattern formation out of equilibrium is intensively studied topic for its potential relation with living organisms or group of biological objects. One of emerging topic is collective motion of self-propelled objects, such as fish schooling and bird flocking, without leaders or external guides. In addition to abundant examples found in natural fields, many physicists find it interesting after the work by Vicsek et al. [1], which extended well-known XY-model for the motionless spin to the model for a group of self-propelled particles. Up to know, many theoretical works has been done so far despite that clear experimental works without hidden variable have not been done.

In this study, we present an experimental system where large scale pattern formed with self-propelled particles with local interaction. The system is *in vitro* motility assay with motor protein, dynein c, and microtubules. Setting microtubules on a glass surface coated with dynein c, microtubules are propelled by dynein c with a consumption of ATP. With high enough density of microtubules and dynein c, the microtubule formed vortex pattern (Fig.). The vortex structure was composed of group of microtubule moving both clockwise/counterclockwise directions. Furthermore, the group of generated vortex formed lattice structure. Pair interaction between independent microtubule was revealed to be a collisional steric interaction, which make microtubules to have temporal parallel and anti-parallel alignment. We further elucidated the motion of isolated microtubule is persistently curved, without interaction. Adopting these measured features, we propose a simple mathematical model based on the Vicseck model [1, 2]. The model successfully reproduced the observed dynamic patterns when we used parameters obtained from experimental measurements. This system is similar to that reported recently by Schaller et al. [3], but our experiments allow for a clear understanding of the elementary mechanisms at the origin of the phenomena observed, such as pair interaction as well as isolated microtubule motion.

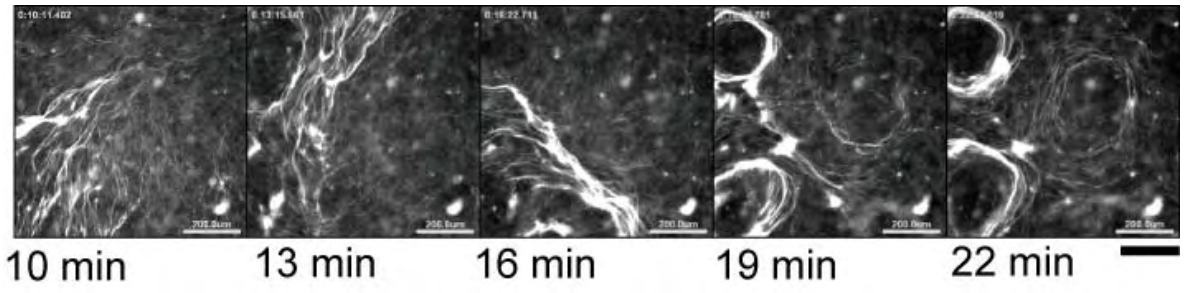

Fig.: Emergence of vortex pattern of microtubules, bar:200 μm.

Reference

1. T. Vicsek, et al., *Phys. Rev. Lett.* **75**, 1226-1229 (1995).
2. G. Grégoire and H. Chaté, *Phys. Rev. Lett.* **92**, 025702 (2004).
3. V. Schaller, C. Weber, C. Semmrich, E. Frey & A. R. Bausch, *Nature* **467**, 73-77 (2010).

Self-Propelling Asymmetric Colloids in AC Electric Field

Ryo Suzuki[1], Hong-Ren Jiang[2], and Masaki Sano[1]

[1]*Department of Physics, the University of Tokyo, 7-3-1 Hongo, Bunkyo-ku, Tokyo, Japan*

[2]*Institute of Applied Mechanics, National Taiwan University, Taipei City 106, Taiwan*

How the motion of colloidal particles that self-propel differs from those of normal Brownian motion is an intriguing question, especially in the context of nonequilibrium statistical mechanics. Over the past decade, a variety of self-propelling colloids have been devised and synthesised, and used in order to experimentally apprehend "self-propelling motion" at microscopic scales. However, particle motion and/or information on particle motion were limited. Therefore, a good understanding of the motion proved problematic.

Asymmetrical colloidal particles (Janus particles) that we used in our experiments are known to self-propel by applying AC electric field [1]. Janus particles (polystyrene beads half coated with metal) of few micrometres in size self-propel in the direction of the non-coated side and the motion is orientated perpendicular to the applied electric field. Such motion is understood to originate from an asymmetry in the flow at the dielectric and metal surface (Fig. 1), which is induced by AC electric field [2]. In our experiment, like is illustrated in Fig. 2, we applied AC electric field to the Janus particles in the vertical direction and observed planar particle motions.

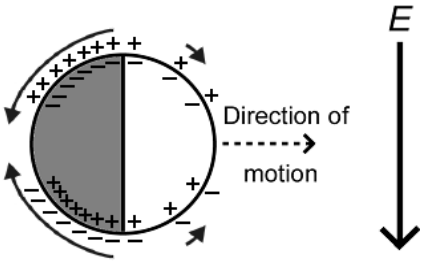

Fig. 1 Flow at metal side (grey) is stronger, resulting in asymmetric flow that induces self-propulsion.

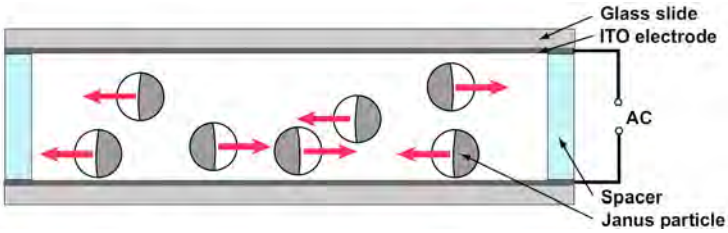

Fig. 2 Schematic figure of experimental system (side view). Janus particles move in the direction of the non-coated side (white), and perpendicular to the applied electric field.

These Janus particles show interesting behaviours and interactions. Since the asymmetrical flow induced in the vicinity of the particle changes due to differences in the AC frequency, we observed 3 characteristic frequency regions. In these regions, not only do the direction of motion change but also the interaction differs too. We show detailed results. Further, we show the measuring of force acting on the Janus particles at the time of self-propulsion. Although direct measurements are beyond being strenuous due to the particle's self-propelling nature, force can be estimated indirectly using fluctuation theorem. We present results and examine the validity of this method. Moreover, we look at how Janus particles behave when the number density is relatively high. We show that particles demonstrate polar alignment and anomalous number/density fluctuations are seen. Details are discussed.

REFERENCES

[1] S. Gangwal, O. J. Cayre, M. Z. Bazant, and O. D. Velev, *Phys. Rev. Lett.* 100, 058302 (2008).

[2] M. Z. Bazant and T. M. Squires, *Phys. Rev. Lett.* 92, 066101 (2004).

Self-propelled motion of a composite induced by interfacial instability: spontaneous symmetry breaking and mode-bifurcation

Fumi Takabatake[1], Nobuyuki Magome[2], Masatoshi Ichikawa[1], and Kenichi Yoshikawa[1]

[1] Department of Physics, Graduate School of Science, Kyoto University, Kitashirakawa Oiwake-cho, Sakyo, Kyoto 606-8502, Japan
[2] Institute for Integrated Cell-Material Sciences (iCeMS), Kyoto University, Yoshida Ushinomiya-cho, Sakyo, Kyoto 606-8501, Japan

Currently, the spontaneous motions of liquid droplets, solid particles and gels under non-equilibrium conditions have been actively investigated [1]. Among the phenomena of spontaneous motions, the self-agitation of a fluid interface is well known and has been studied for over a century, especially in the field of chemical engineering in terms of the chemical Marangoni effect. The chemical Marangoni effect is induced by local variations in interfacial tension, which are caused by a chemical concentration gradient under isothermal conditions. Recently, it was found that irregular interfacial agitation caused by the Marangoni instability exhibits bifurcation into a regular motion by choosing a suitable physical or chemical boundary condition.

In the present paper, we report [2] that a solid/liquid composite exhibits regular spontaneous motions under isotropic boundary conditions, driven by chemical Marangoni effect. When an oil droplet of oleic acid merged with a solid sodium oleate is placed on a water phase, the composite undergoes specific spontaneous motion, such as translational, spinning, or orbital motion (shown in Fig. 1). The results showed that a composite assumes a certain mode of spontaneous motion depending on the relative size of the solid sodium oleate with respect to that of the oil droplet. The essential features of such mode-switching are reproduced by using ordinary differential equations by taking into account of the spontaneous symmetry breaking on the composite under a dissipative condition.

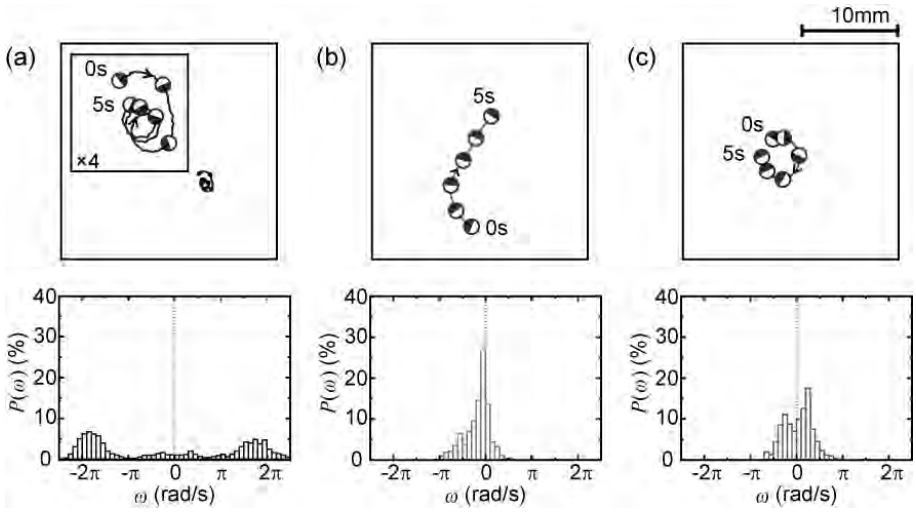

Fig. 1 Representable examples of the spontaneous motion of a solid/liquid composite floating on an aqueous phase, where the volume of the droplet was kept constant at 100 μl. Top: Trajectory of the center of the droplet. Bottom: Histograms of the angular velocity. (a) The long axial length of the solid column, $l \simeq$ 1 mm. The composite exhibits spinning motion. (b) $l \simeq$ 3 mm. Translational motion is observed. (c) $l \simeq$ 5 mm. Orbital motion is generated together with rotational motion around its centroid with the same periodicity.

REFERENCES

1. Tersoff, J. *et al.*, "Running Droplets of Gallium from Evaporation of Gallium Arsenide", *Science*, **324**, 236 (2009).
2. Takabatake, F. *et al.*, "Spontaneous mode-selection in the self-propelled motion of a solid/liquid composite driven by interfacial instability", *J. Chem. Phys.*, **134**, 114704 (2011).

Predictability of conversation partners in Japanese company offices

Taro Takaguchi[1], Mitsuhiro Nakamura[1], Nobuo Sato[2], Kazuo Yano[2], and Naoki Masuda[1,3]

[1] *Department of Mathematical Informatics, The University of Tokyo, 7-3-1 Hongo, Bunkyo, Tokyo, Japan*

[2] *Central Research Laboratory, Hitachi, Ltd., 1-280 Higashi-Koigakubo, Kokubunji, Tokyo, Japan*

[3] *PRESTO, Japan Science and Technology Agency, 4-1-8 Honcho, Kawaguchi, Saitama, Japan*

Recent developments of sensing technologies have enabled us to examine the nature of human social behavior in great details. By applying an information theoretic method to the spatiotemporal data of cell-phone locations, Song *et al*. (2010) found that human mobility patterns are remarkably predictable [1]. Inspired by their work, we ask a similar predictability question in a different kind of human social activity: conversation events [2]. The predictability in the sequence of one's conversation partners is defined as the degree to which one's next conversation partner can be predicted given the current partner; we quantify it by using the mutual information.

We examine the predictability of conversation events for each individual using the longitudinal data of face-to-face interactions collected from company offices in Japan [3,4]. The data were collected by World Signal Center, Hitachi, Ltd. Each subject wears the name tag equipped with an infrared sensor node, and conversation events are marked when signals are exchanged between close sensor nodes. We find that the conversation events are predictable to some extent. Much of the predictability is explained by the bursty pattern of human activity, characterized by long-tailed distributions of interevent intervals [5]. However, a predictability also exists in the data, apart from the contribution of their bursty nature. In addition, the degree of the individual's predictability is correlated with the position in the static social network derived from the data. Finally, we discuss our results in relation to the community structure of the social network.

REFERENCES

1. Song, C., Qu, Z., Blumm, N., and Barabási, A.-L., “Limits of predictability in human mobility”, *Science*, 327, 1018 (2010).

2. Takaguchi, T., Nakamura, M., Sato, N., Yano, K., and Masuda, N., “Predictability of conversation partners”, *Physical Review X*, 1, 011008 (2011).

3. Wakisaka, Y., Ara, K., Hayakawa, M., Horry, Y., Moriwaki, N., Ohkubo, N., Sato, N., Tsuji, S., and Yano, K., “Beam-scan sensor node: Reliable sensing of human interactions in organization”, in *Proceedings of Sixth International Conference on Networked Sensing Systems (INSS)*, (Carnegie Mellon University, Pittsburgh, 2009) p. 1-4.

4. Yano, K., Ara, K., Moriwaki, N., and Kuriyama, H., “Measurement of Human Behavior: Creating a Society for Discovering Opportunities”, *Hitachi Review*, 58, 139 (2009).

5. Barabási, A.-L., “The origin of bursts and heavy tails in human dynamics”, *Nature*, 435, 207 (2005).

Dynamical Pattern Formation in Motile Cyanobacteria

Atsuko Takamatsu, Yuki Fukazawa, Keita Tanaka, Hideo Iwasaki

Department of Electrical Engineering and Bioscience, School of Advanced Science and Engineering,
Waseda University, Okubo 3-4-1, Shinjuku-ku, Tokyo, Japan

Systems of self-propelled particles have widely attracted physicists. A number of the mathematical models have been proposed for the systems, e.g., from a swarm of bugs, a school of fish, a flock of birds, to a group of person or artificial vehicles [1]. These provide perspective of their behavior; however, experimental evidences especially with well-controlled environment are insufficient. Here we introduce the motile filamentous (multicellular) cyanobacterium, *Pseudoanabaena* sp. (Fig. 1a), newly isolated from a pond at Waseda University [2], to investigate the behavior of the group of elements during their dynamical pattern formation by systematic and synthetic way.

The cells form a variety of colony patterns depending on culture conditions. By focusing on the cell movement under a standard culture condition, we found coexistence of two types of collective movement such as rotating disc (Fig.1b) and comet-like movement (Fig.1c). The time-lapse sequential images were analysed with the Particle Image Velocimetory (PIV) method, which enabled us to capture velocity vectors at every locations. The analysis revealed that the velocity of the collective movement depends on the cell density. It suggests that there exists a certain interaction among the cells, which would affect positively feedback to collective cell motility. Furthermore, the velocity finally saturates against the density but not decelerate at higher density, like traffic jam.

To be compared with the experimental results, a simple 1-dim cellular automaton model [3] was tested, which mimics ants considering evaporation rate of pheromone. It is known that the system behaves like cars or ants where the evaporation rate is slow or fast, respectively. In contrast, the motile cyanobacterium seems to behave as their intermediate states, suggesting more effective collective motion.

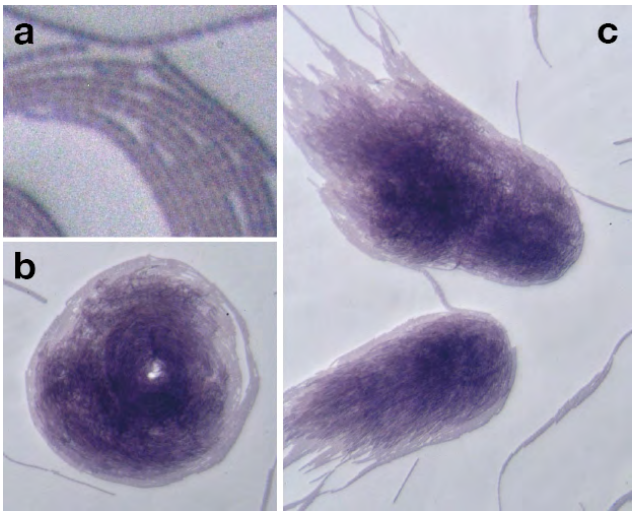

Fig.1 (Color Online) Pattern formation of collectives of *Psuedoanabena*cells. (a) A magnified image of *Psuedoanabena* cells in chains, (b) Rotating disc, (c) Comet-like movement.

REFERENCES

1. T. Vicsek et al. (1995) Phys. Rev. Lett. 75 1226; G. Grégorie and H. Chaté (2004) Phys. Rev. Lett. 92 025702; N. Shimoyama et al. (1996) Phys. Rev. Lett. 76 3870; D. Helbing (2001) Rev. modern phys. 73, 1067-1141; Bando et al., (1994) Phys.Rev.E, 51, 1035; Tadaki et al. (1998) J. Phys. Soc. Jp. 67, 2270; Nakayama et al. (2005) Phys. Rev. E 71 036121
2. A. Kubota, H. Iwasaki (2009) Tama Art University Ronshu24 (in Japanese); H. Iwasaki (2010) Kagaku, Iwanami, Vol. 7pp.747-754 (in Japanese); H. Iwasaki (2011) Jikken Igaku29 (7) 1188-1196 (in Japanese).
3. Chowdhury, Schadschneider, Nishinari. (2005) Phys. Life Rev. 329, 199-329.

Growth of Gold Nanorods in Gelled Surfactant Solutions

Yoshiko Takenaka[1)], Hiroyuki Kitahata[2,3)], Norifumi L. Yamada[4)] and Hideki Seto[4)]

[1)]NanoSystem Research Institute (NRI), National Institute of Advanced Industrial Science and Technology (AIST), 1-1-1, Higashi, Tsukuba 351-8565, Japan. [2)]Department of Physics, Graduate School of Science, Chiba University, 1-33 Yayoi-cho, Inage-ku, Chiba 263-8522, Japan. [3)] PRESTO, JST, 4-1-8 Hon-cho, Kawaguchi 332-0012, Japan. [4)]KENS & CMRC Institute of Materials Structure Science, High Energy Accelerator Research Organization, 1-1 Oho, Tsukuba 305-0801, Japan.

A gold nanorod is a one-dimensional crystal of gold, which is among the objects generating the most interest for new nanotechnological materials and industrial applications. One of the most important parameters on the shape of a gold nanorod is aspect ratio (ratio between length and diameter). Low-aspect-ratio gold nanorods (<10) can be applicable to a chemical sensor and a cancer attacker, and high-aspect-ratio gold nanorods (>20) can be applicable to the probes of microscopy, nano-gap electrodes, catalytic substances. As for the synthesis, however, few high-yield syntheses for high-aspect-ratio gold nanorods have been reported, while such methods for low-aspect-ratio gold nanorods have been established. In general, gold nanorods grow in a cationic surfactant solution. Recently, we have reported that the gelation of the surfactant solution strongly affects the shape of gold nanorods [1]. Actually the nanorods grown in a gelled surfactant solution exhibit high aspect ratio of over 50. Moreover the yield of nanorods in this method is over 90%. Therefore to clarify the effect of gelation on the growth of gold nanorods is important to control their aspect ratio. In this study, we reveal the detailed structure of gelation and present a model how the gelation affects the aspect ratio of gold nanorods, especially on the diameter.

Gold nanorods were synthesized through seeding method with octadecyltrimethylammonium bromide (OTAB). The growth process was observed with scanning electron microscopy (SEM) by stopping the growth at any instant [2]. The structure of a surfactant solution was observed with small angle neutron scattering (SANS) and was determined by fitting the scattering profiles. All of these experiments were done for both solutions with and without gelation, and we compared both results.

By the observation of SEM, thin and thick nanorods coexisted in some period; from 8 to 40 min after starting the growth. This time period corresponded to that of gelation indicated by the decrease in the light transmittance of the solution. Thus we concluded that the structural change of a surfactant solution from 8 to 40 min after starting the growth affects the diameter of gold nanorods. By the fitting of SANS profiles, we could regard the gelation in this period as the structural change in self-assembly of surfactant molecules from micellar to lamellar structure. We also revealed that the lamellar structure shows the interdigitation. With these results, we presented a model of the growth mechanism of gold nanorods in a gelled surfactant solution.

It is well known that gold nanorods are covered with bilayer of surfactant molecules in a solution. We focused on the outer layer of the bilayer, because the outer layer is stabilized by the spontaneous curvature while the inner layer binds strongly to the gold surface. The structural transition from micelle to lamellae would induce the decrease in the spontaneous curvature of the outer layer, which leads to the increase in the diameter of gold nanorods. In addition to this effect, the bilayer around gold surfaces would interdigitate and it would become rigid. This effect also induces the increase in the diameter. We concluded that the diameter of gold nanorods grown in a gelled surfactant solution is determined by these two effects as shown in Fig. 1 [3].

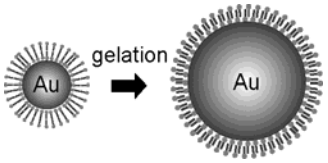

Fig. 1 Effect of the gelation on the diameter of a gold nanorod.

1. Takenaka, Y. *et al.* "High-aspect-ratio gold nanorods synthesized in a surfactant gel phase", *Chem. Phys. Lett.*, 467, 327 (2009).
2. Takenaka, Y. *et al.* "Analysis of the growth process of gold nanorods with time-resolved observation", *Phys. Rev. E*, 80, 020601 (2009).
3. Takenaka, Y. *et al.* "Growth of gold nanorods in gelled surfactant solutions", *J. Colloid Interface Sci.*, 356, 111 (2011).

Growing interfaces uncover universal fluctuations behind scale invariance

Kazumasa A. Takeuchi and Masaki Sano

Department of Physics, the University of Tokyo,
7-3-1 Hongo, Bunkyo-ku, Tokyo, Japan

To what extent can fractal or self-affine phenomena be universal in systems driven out of equilibrium? We know that such scale invariance can lead to a variety of scaling laws expected to be universal, but is this all we can have? As an important case study to address this problem, we present our experimental results on growing interfaces in electrically-driven turbulent liquid crystals, which turns out to show unprecedented universality beyond the scaling laws [1]: Growing interfaces of topological-defect turbulence exhibit not only the universal scaling laws of the Kardar-Parisi-Zhang (KPZ) class, which is the basic class for stochastic surface growth problems, but even universality in the distribution and correlation functions for the interface fluctuations, in agreement with theoretical models for growing interfaces [2]. The asymptotic distribution agrees quantitatively with the one studied in the completely different context of random matrix theory – namely the largest-eigenvalue distribution of Gaussian random matrices, or the Tracy-Widom (TW) distribution [3]:

$$\boldsymbol{h(t) = v_\infty t + (\Gamma t)^{1/3} \chi}, \tag{1}$$

with local height or radius $\boldsymbol{h}$ of the interface, time $\boldsymbol{t}$, constant parameters $\boldsymbol{v_\infty}$ and $\boldsymbol{\Gamma}$, and a random variable $\boldsymbol{\chi}$ obeying the TW distribution. Moreover, we find that the distribution and the correlation depend on whether the growing interfaces are curved or flat on average, albeit universal in each case. Specifically, for the curved (flat) interfaces, $\boldsymbol{\chi}$ obeys the TW distribution for the Gaussian unitary (orthogonal) ensemble, or the largest-eigenvalue distribution of large complex Hermitian (real symmetric) matrices with Gaussian-distributed elements. This indicates that the KPZ class should be split to two (or more) sub-classes according to different geometries of the problem. Altogether, we provide a strong experimental evidence for the detailed yet geometry-dependent universality underlying scale-invariant growth processes driven out of equilibrium [1,2].

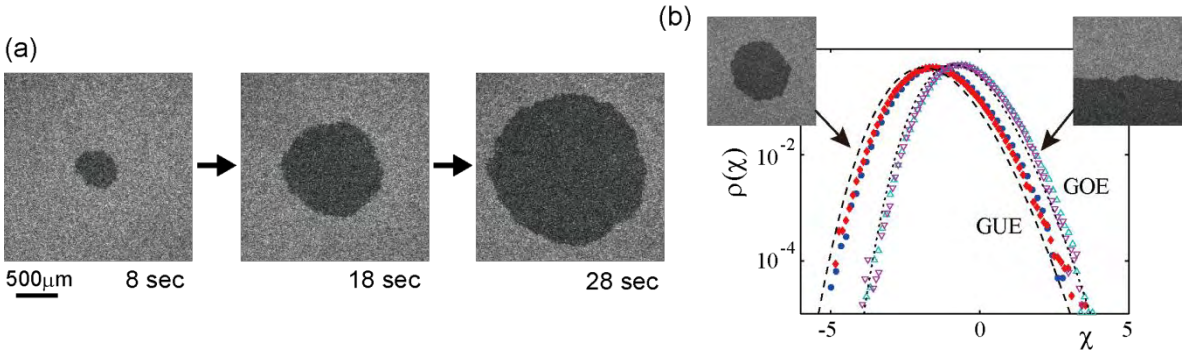

Fig.1 (a) Growing circular cluster of the topological-defect turbulence. (b) Distribution of the rescaled height $\boldsymbol{\chi \equiv (h - v\ t)/(\Gamma t)^{1/3}}$ for the circular (full symbols) and flat (open symbols) interfaces. The dashed and dotted lines are theoretical curves for the TW GUE and GOE distributions.

REFERENCES

1. Takeuchi, K. A., Sano, M., Sasamoto, T., and Spohn, H. "Growing interfaces uncover universal fluctuations behind scale invariance", *Sci. Rep. (Nature)*, 1, 34 (2011); Takeuchi, K. A. and Sano, M. "Universal Fluctuations of Growing Interfaces: Evidence in Turbulent Liquid Crystals", *Phys. Rev. Lett.*, 104, 230601 (2010); a forthcoming paper is in preparation.
2. For a recent review on remarkable theoretical progress marked in the last decade, see, e.g., Kriecherbauer, T. and Krug, J. "A pedestrian's view on interacting particle systems, KPZ universality and random matrices", *J. Phys. A*, 43, 403001 (2010).
3. Mehta, M. L. "Random Matrices", 3rd ed. (Elsevier, Amsterdam, 2004).

Complementary pictures of traction stress field of migrating cell

Hirokazu Tanimoto and Masaki Sano

Department of Physics, School of Science, the University of Tokyo,
Hongo 7-3-1, Bunkyo-ku, Tokyo, Japan

Background:
Motility of living cells is a long-standing subject in biophysics [1]. Although the traction forces, the forces exerted by migrating cells to its substrate, have been regarded as an important key to understand the migratory behavior physically [2], quantitative characterizations of this forces are still lacking.

Results:
With improving both experimental and calculating protocols, we measured the traction forces of migrating Dictyostelium cells with a better spatial resolution and for a longer time. Observed highly localized forces (force spots, Fig.1 A) were found to show front-rear asymmetry. The birth and death events of the force spots were analyzed statistically. As a complementary approach to this fine-grained picture, we also performed multi-pole expansion of the stress vector field and investigated the dynamic nature of the force dipole (Fig.1 B) which related to the cellular motion.

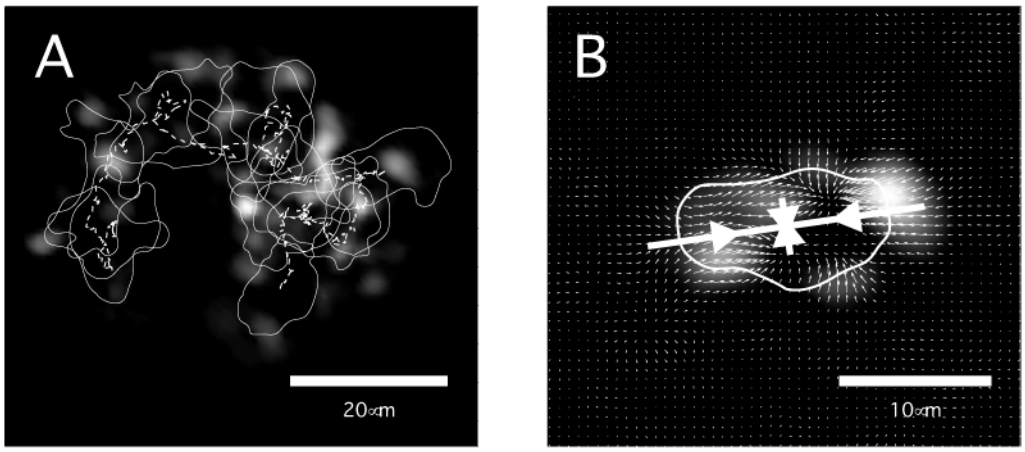

Fig.1 Fine- and course-grained pictures of traction stresses. (A) Cellular traction stresses integrated for 60min in Lab-frame. The traction stresses were measured with a time-interval of 6 seconds. Cellular outlines were plotted with every 4min and the trajectory of the centroid was plotted with broken line. The amplitudes of stresses were represented with the brightness (the same in B). This plot shows highly concentrated nature of the traction stresses. (B) Snap shot of the traction stresses and force dipole. The traction stress vectors were shown with white small arrows and the 1st order moment of the traction stress field was represented with white bold arrows. Because the forces were contractile, the amplitudes of the dipole were negative.

References

1. Oosawa F, "Motility of Living Systems", *Biophysics* **10** 9-23 (1970).
2. Lauffenburger D.A. and A.F. Horwitz, "Cell migration: a physically integrated molecular process", *Cell* **84** 359-369 (1996).

Influence of external forcing on the dynamics of a deformable self-propelled particle

Mitsusuke Tarama and Takao Ohta

Department of Physics, Kyoto University, Kyoto, 606-8502, Japan

We have investigated how the dynamics of a deformable self-propelled particle is changed under the influence of external field in two-dimensional space. Our analysis is based on the model equations constructed by the symmetry argument for the velocity of the centre of mass and a tensor variable characterizing deformation. Here, we have considered two kinds of external force. One is a gravitational force, which enters additively in the time-evolution equation for the centre of mass. The other is an electric force supposing that a dipole moment is induced in the particle. This force is added to the equation for the deformation tensor.

The system we consider is simply a single isolated particle but has internal degrees of freedom due to deformability. It should be noted that, even when the external forcing is absent, there is a bifurcation between a straight motion and a rotating motion [1]. Therefore, by adding an external force, there occurs a conflict or frustration between the rotating motion and the forced straight motion. As a result, non-trivial states of motion and bifurcations are exhibited by changing the magnitude of the external force. We have carried out numerical simulations of the time-evolution equations to obtain a dynamical phase diagram. Analytical study has also been developed to reproduce some of the bifurcations.

REFERENCES

1. T. Ohta and T. Ohkuma, “Deformable Self-Propelled Particles”, *Phys. Rev. Lett.*, **102**, 154101 (2009).
2. M. Tarama and T. Ohta, “Dynamics of a deformable self-propelled particle under external forcing”, *Euro Phys J. B* (in press). DOI: 10.1140/epjb/e2011-20307-7.

Formation of polymer spherulites by branching and re-orientation of lamellar crystallites

Akihiko TODA, Ken TAGUCHI and Hiroshi KAJIOKA

GSIAS, Hiroshima University
Higashi-Hiroshima 739-8521, Japan

As a hierarchical structure, chain-folded lamellar crystals of polymers form a spherical aggregate of crystallites called "spherulite" with space filling branching and non-crystallographic re-orientation (Fig. 1). Spherulite is the basic structure of crystalline polymeric materials, so that the formation mechanism has been one of the fundamental issues in polymer science and technology. We have proposed the following modeling and have been examining it experimentally [1-4].

1. The non-crystallographic re-orientation is most probably caused by the excess surface stresses induced by the steric hindrance among chain folding, as has been extensively discussed [5].
2. For the mechanism of branching, we have supposed the fingering instability of Mullins-Sekerka type caused by a self-induced gradient field upon crystallization [1-5]; the crystallization from viscous polymer melt can easily induce gradient fields near the growth front in the media. The instability sets a critical width of lamellar crystals.
3. The branches grow independently from each other because of the re-orientation of each branch, so that the branches grow in width which will reach the critical width repeatedly, resulting in the repetition of branching and re-orientation enough to fill in the three-dimensional space. The critical width λ is given as,

$$\lambda \propto (\gamma / a)^{1/2} \propto (\gamma D / V)^{1/2} \quad : \text{compositional}$$
$$\propto (\gamma / \eta V)^{1/2} \quad : \text{pressure} \qquad (1)$$

where γ represents the surface tension, a the gradient in chemical potential, D the diffusion coefficient, V growth rate, η viscosity; the compositional gradient is supposed for multi-component systems (Keith-Padden's original proposal) and the pressure gradient is for the melt flow to sustain the stationary growth compensating the crystal-melt density gap (Schultz's conjecture). In addition, experimentally, we have found that the lamellar width, namely the size of the building blocks of spherulite, determines the characteristic sizes of the inner structure of spherulite, such as the band spacing, P, shown in Fig. 2.

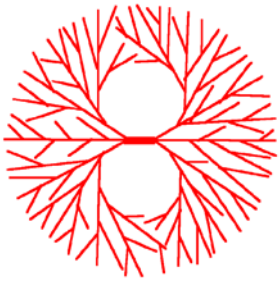

Fig. 1 Schematic drawing of a spherulite.

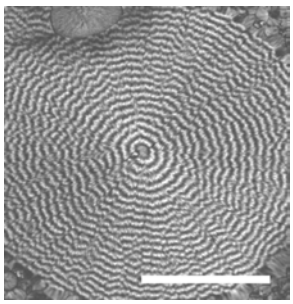

Fig. 2 Polarizing optical micrograph of a ringed spherulite of PVDF.

In order to confirm the instability-driven branching, we have examined the followings.

1. Temperature and molecular weight dependences of λ, P, V, and η (or D) in spherulites.
2. Effect of external gradient field of temperature on the inner structure of spherulite, *i.e.* P.
3. Cellular structure of lamellar crystals formed from ultra-thin film.

All the results support the self-induced gradient field driven by the mobility in the media of bulk melt.

REFERENCES

1. Toda, A. *et al.* "Branching and higher order structure in banded polyethylene spherulites", *Macromolecules*, 41, 2484 (2008).
2. Toda, A. *et al.* "Instability-driven branching of lamellar crystals in polyethylene spherulites", *Macromolecules*, 41, 7505 (2008).
3. Kajioka, H. *et al.* "Branching and re-orientation of lamellar crystals in non-banded poly(butene-1) spherulites", *Polymer*, 49, 1685 (2008).
4. Kajioka, H. *et al.* "Morphology and crystallization kinetics of it-polystyrene spherulites", *Macromolecules*, 43, 3837 (2010).
5. Lotz B, Cheng SZD "A critical assessment of unbalanced surface stresses as the mechanical origin of twisting and scrolling of polymer crystals", *Polymer*, 46, 577 (2005).

Synchronization of weakly perturbed Markov chain oscillators

Ralf Toenjes and Hiroshi Kori

Ochadai Academic Production, Ochanomizu University, Tokyo 112-8610, Japan

Rate processes are simple and analytically tractable models for many dynamical systems that switch stochastically between a discrete set of quasi stationary states; however, they may also approximate continuous processes by coarse-grained, symbolic dynamics. In contrast to limit-cycle oscillators that are weakly perturbed by noise, in such systems, stochasticity may be strong, and topologies more complicated than a circle can be considered. In [1], we apply a second-order time-dependent perturbation theory to derive expressions for the mean frequency and phase diffusion constant of discrete-state oscillators coupled or driven through weakly time-dependent transition rates. We also describe a method of global control to optimize the response of the mean frequency in complex transition networks.

REFERENCES

1. R. Toenjes and H. Kori, *"Synchronization of weakly perturbed Markov chain oscillators"*, accepted for Phys. Rev. E., available at http://arxiv.org/abs/1108.3690

Phase description of nonlinear dissipative waves under space-time-dependent external forcing

Yousuke Tonosaki[1], Takao Ohta[1], Vladimir Zykov[2]

[1]*Department of Physics, Graduate School of Sciences, Kyoto University, Kyoto, Japan*

[2]*Institut fuer Theoretische Phtysik, Technische Universitaet Berlin, Berlin, Germany*

We investigate the dynamics of the propagating dissipative waves under the external forcing, based on the model system undergoing phase separation and chemical reactions as

$$\frac{\partial u}{\partial t} = \nabla^2\left[-\nabla^2 u - \tau u + u^3\right] + a_1 u + a_2 v + a_3 + \Gamma, \qquad \frac{\partial v}{\partial t} = b_1 u + b_2 v + b_3 + \Gamma \qquad (1)$$

where u and v are the order parameters related with the local concentrations of the chemical species [1]. The parameters τ, a_i, b_i specify the phase separation and chemical reactions and Γ is the external force.

In order to investigate synchronization and modulation of the traveling waves under external forcing, we consider the case that $\Gamma = \varepsilon \cos(q_f x - \Omega t)$ where ε, $2\pi/q_f$ and Ω is the magnitude, the spatial period and the frequency of the forcing, respectively. A phase diagram for the entrained and non-entrained states under the external forcing is obtained numerically (Fig.1). Theoretical analysis in terms of phase description of the traveling waves is carried out to show that the transition between the entrained and the non-entrained states by changing the external frequency occurs either through a saddle-node bifurcation or through a Hopf bifurcation and that these two bifurcation lines are connected at a Bogdanov-Takens bifurcation point [2].

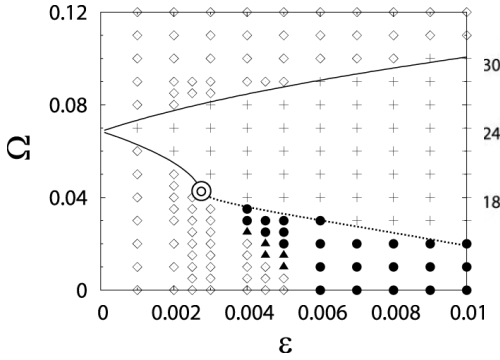

Fig.1: Phase diagram of the traveling waves under the external forcing on the $\varepsilon - \Omega$ plane. Each symbol indicates asymptotic behaviour of the traveling waves. Symbol +, ◇ and ● correspond to (a), (b) and (c) in Fig.2, respectively. The solid lines are the saddle-node bifurcation thresholds whereas the dotted line is the Hopf bifurcation threshold. The Bogdanov-Takens bifurcation point is indicated by the double circle.

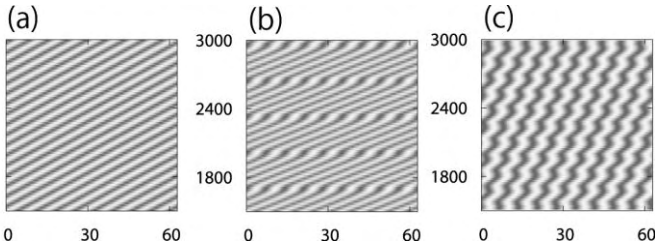

Fig.2: Space (horizontal)-time (vertical) plot of the propagating waves for $\varepsilon = 0.007$ (a) in the synchronized state for $\Omega = 0.07$, (b) near the saddle-node bifurcation for $\Omega = 0.1$ and (c) near the Hopf bifurcation for $\Omega = 0.02$. The gray scale indicates the magnitude of the variable u.

REFERENCES

1. Okuzono, T. and Takao, O. "Traveling waves in phase-separating reactive mixtures", *Phys. Rev. E.*, **67**, 056211 (2003).
2. Tonosaki, Y. , Takao, O. and Zykov, V. "Phase description of nonlinear dissipative waves under space-time-dependent external forcing", *Physica D*, **239**, 1718 (2010).

Two-teeth rotary ratchet and its unidirectional rotation under linearly polarized ac-field

Hiroki Tutu

Department of Applied Analysis and Complex Dynamical Systems, Graduate School of Informatics, Kyoto University, Kyoto 606-8501, Japan

A theoretical model for an artificial molecular rotor mounted in a biological membrane [Fig. 1(a)], which can serve for unidirectional rotation in response to a weak periodic pumping with linearly polarized ac-field, is studied. The dynamics of the rotor unit is modeled by a Langevin equation for a particle in a two dimensional bistable potential of a two-teeth ratchet structure [Fig. 1(b)]. Unlike well-known one dimensional Brownian ratchet models, the presented model can easily extract an effect due to two dimensionality of the ratchet and polarization of the applied field. First, I shall demonstrate that a unidirectional rotation appears with stochastic resonance exhibiting a bell-shaped peak on the noise intensity in mean angular momentum (MAM) of the rotor. An analytical expression for the expectation value of MAM, $\langle L \rangle$, is obtained on the basis of a four-state transition model. Second, a significant effect due to torsion (ratchet like structure) of the potential geometry will be elucidated: in the absence of torsion, MAM depends on the polarization angle ϕ of the applied field as $\langle L \rangle \propto \sin(2\phi)$, on the other hand, in the presence of torsion, it yields an additional bias to the dependence $\sin(2\phi)$ in MAM. It is found that the emergent bias can be utilized to make the rotor system robust for maintaining a unidirectional rotation against uncertainty about the mount condition. On the basis of this utility, I shall discuss an architectural design for an artificial molecular rotor system.

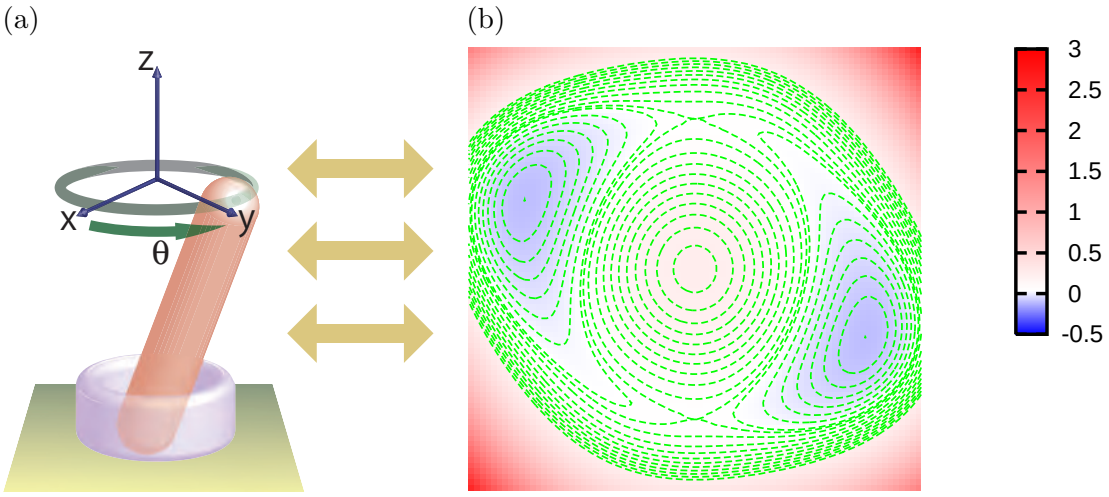

Figure 1: (a) A sketch of a conceptual illustration for an artificial molecular rotor: The rod like object is softly binded its end on the inner side of the cylinder like object, its contact with the cylinder edge is retained, and it can also freely rotate around the z-axis with its tilt loosely maintained in the rotation. The body of the cylinder object is partially embedded in biological membrane. The arrow indicates a direction of the linearly polarized ac-field. (b) A two dimensional contour graph of the potential landscape $V_0(\boldsymbol{X})$ assumed for the rod and the cylinder interaction: The motion of the rotor tip is regarded as a motion of a particle obeying $\dot{\boldsymbol{X}} = -\partial V_0(\boldsymbol{X})/\partial \boldsymbol{X} + h\cos(\Omega t)\boldsymbol{N} + \boldsymbol{R}(t)$, where $\boldsymbol{R}(t)$ is a two components vector of the Gaussian white noises, Ω and $\boldsymbol{N}$ are an angular frequency and polarization of the applied field. The horizontal (vertical) direction corresponds to the x (y) direction, and the dashed curves indicate contour levels.

Minimal Models of Hydrodynamic Synchronization at Low Reynolds Number

[*]Nariya Uchida and [†]Ramin Golestanian

[*]*Department of Physics, Tohoku University, Aramaki Aoba 6-3, Sendai 980-8578, Japan*
[†]*The Rudolf Peierls Centre for Theoretical Physics, University of Oxford, 1 Keble Road, Oxford OX1 3NP, UK*

Coordinated motion of cilia and flagella facilitate self-propulsion of cells in viscous environment. For example, the surface of a *Paramecium* is covered by several thousands of cilia that beat in synchrony to form a propagating wave on the cell surface (metachronal wave). An *E. Coli* has several helical flagella that are autonomously bundled in the swimming mode and unbundled in the tumbling mode. The emergent collective pumping by such active organelles has potential application to microfluidic devices, as recently demonstrated by the bacterial carpet. It is a dense monolayer of flagellated bacteria that are attached to an elastomeric substrate with their heads (cell bodies), while their tails (flagella) can freely rotate in the fluid. The flagella are spontaneously and orientationally ordered, and create non-trivial flow patterns that enhance fluid mixing near the surface. These systems provide interesting examples of synchronization mediated by long-range hydrodynamic interaction.

The mechanism of hydrodynamic synchronization has been the subject of extensive theoretical studies since the pioneering work of G. I. Taylor [1], who modelled the beating pattern of a flagellum by a sinusoidal traveling wave. Recent studies incorporate elastic deformations of cilia and flagella and resolve their intricate conformations by numerical simulations. At the same time, minimal approaches with a small number of dynamic variables have been also pursued to clarify the essential conditions for synchronization [2]. Here we present a couple of such minimal models and discuss its implications to collective dynamics of biological and artificial microfluidic machineries.

In both models, we consider a rigid sphere making a fixed trajectory, which represents the center-of-mass motion of cilia or flagella. In Model 1, the driving force acting on the sphere is a periodic function of its phase, while a hydrodynamic drag force is exerted by the sphere on the surrounding fluid. For arbitrary trajectory shape, we derive sufficient and necessary conditions on the force profile to make two parallel rotors synchronize. In particular, we show that the non-constantness of the driving force is necessary [3]. In Model 2, the rigid sphere makes a circular orbit driven by a constant torque, and at the same time exerts a radial pumping force on the surrounding fluid, which mimics the action of flagella in bacterial carpets. The model exhibits various collective behavior such as macroscopic phase ordering, turbulent spiral waves, traveling waves, and frustrated disorder [4]. A model of bacterial carpet is obtained by making the driving torque randomly distributed around zero. The system undergoes gradual order-disorder crossover as the randomness is increased, which is characteristic of coupled oscillators with long-range interactions [5].

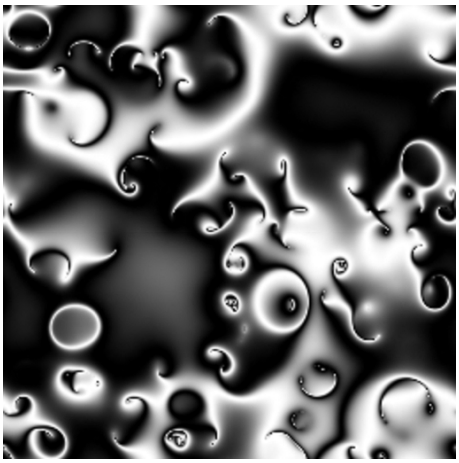

Fig.1 Turbulent spiral waves (Model 2).

REFERENCES

[1] G. I. Taylor, Proc. R. Soc. London, Ser. A, **209**, 447 (1951).
[2] For a review, see: R. Golestanian, J. M. Yeomans and N. Uchida, Soft Matter, 7, 3074 (2011).
[3] N. Uchida and R. Golestanian, Phys. Rev. Lett., **106**, 058104 (2011)
[4] N. Uchida and R. Golestanian, Phys. Rev. Lett., **104**, 178103 (2010).
[5] N. Uchida and R. Golestanian, Europhys. Lett. **89**, 50011 (2010).

Fracture strength and toughness in a disordered lattice system

Chiyori Urabe

FIRST, Aihara Innovative Mathematical Modelling Project, Japan Science and Technology Agency, Collaborative Research Center for Innovative Mathematical Modelling, Institute of Industrial Science, The University of Tokyo 4-6-1 Komaba, Meguro-ku, Tokyo, 153-8505, Japan

Shinji Takesue

Department of Physics, Graduate School of Science, Kyoto University, Kitashirakawa Oiwake-cho, Sakyo-ku, Kyoto, 606-8502, Japan

It is found numerically that a kind of disorder can enhance the fracture toughness and the maximum stress σ_{max}. The model considered in this paper consists of particles of equal mass which are initially arranged on a triangular lattice and Hookean springs connecting each nearest-neighbour pair of particles. Spatial disorder is introduced into the spring constants. A given fraction r of the springs is soft ones with a spring constant and the remaining are hard ones with a larger spring constant. The soft and hard springs are randomly located. Moreover, every spring is cut if the force on it exceeds a threshold value, which is common to all the springs. Thus the model mimics a composite of soft and hard materials. Numerical simulations of an overdampd equation of motion for the model with various r and the length of an initial crack, a_0, reveal that when the initial crack is sufficiently long, the disordered systems have larger σ_{max} than the uniform systems (r = 0 or 1) do as shown in Fig. 1. In contrast, σ_{max} in the disordered systems with a short initial crack is smaller than those in the uniform systems. A theory for quasi-brittle materials by Bažant [1] is successfully applied to the results and the critical stress intensity factor K_c and the size of the fracture process zone (FPZ), ξ, are found to be increased in the disordered systems compared with the uniform cases. Namely, the stress concentration near the crack tip is mitigated in the disordered systems by formation of the FPZ. This also leads to the enhancement of the fracture toughness (Fig. 2). [2]

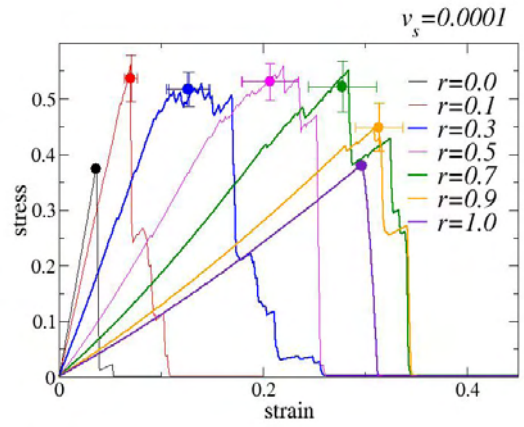

Fig.1 Stress-Strain Curves for several r.

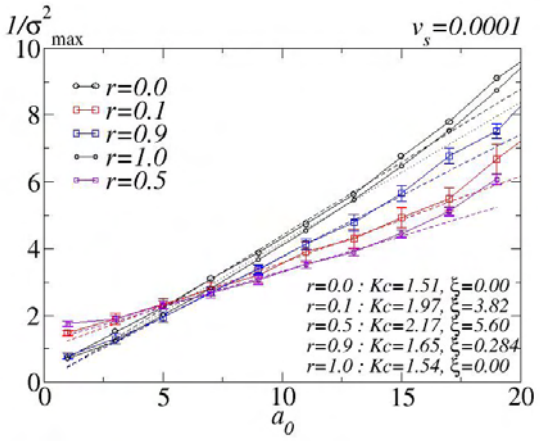

Fig.2 Dependence of $1/\sigma^2_{max}$ on initial crack length a_0.

REFERENCES

1. Z. P. Bažant, "Scaling theory for quasibrittle structural failure", *Proc. Natl. Acad. Sci. U.S.A.* 101, 13400 (2004).
2. Urabe, C. and Takesue, S., "Fracture toughness and maximum stress in a disordered lattice system", *Phys. Rev. E* 82, 016106 (2010).

Size Distributions of Branch Widths and Gaps of DBM pattern Formed by *Bacillus subtilis*

Jun-ichi Wakita, Mina Arima, Ryuto Kumata, Tohey Matsuyama, and Mitsugu Matsushita

Department of Physics, Chuo University, Kasuga, Bunkyo-ku, Tokyo 112-8551

Bacterial colonies which are formed on agar plates exhibit a variety of patterns depending on bacterial species and environmental condition. In the case of *Bacillus subtilis*, colony patterns are classified into five types by changing both nutrient and agar concentrations: diffusion-limited aggregation (DLA), Eden, concentric ring, homogeneously spreading disk, and dense branching morphology (DBM) (Fig.1). DBM pattern is formed under the condition where the concentrations of agar and nutrient are both low. The characteristics of this colony formation are that many thin branches grow densely and ramify complicatedly, but the outermost tips of the branches form a smoothly rounded circumference (Fig.2). DBM pattern is observed for various physical systems such as viscous fingering, electro deposition and crystal growth. However, the growth mechanism for DBM pattern is not clearly understood yet. In this presentation, we investigate the size distributions of branch widths and gaps of DBM pattern, and show the results that the distribution of branch widths is power-law (Fig.3), while the distribution of branch gaps is lognormal (Fig.4). The growth process of the branches of DBM pattern will be discussed paying an attention to the spatiotemporal characteristics of both the distributions.

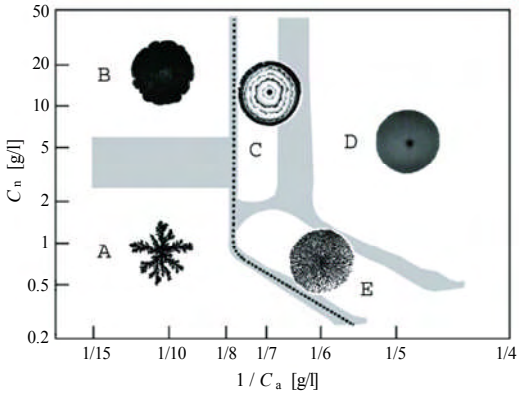

Fig.1 Morphological diagram of *B. subtilis* colonies as a function of nutrient concentration C_n and the inverse of agar concentration C_a.

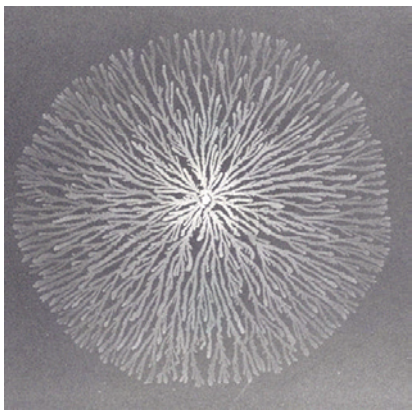

Fig.2 DBM pattern of *B. subtilis* colonies. C_a = 5 g/l, C_n = 0.5 g/l. The diameter of the colony is about 5 cm.

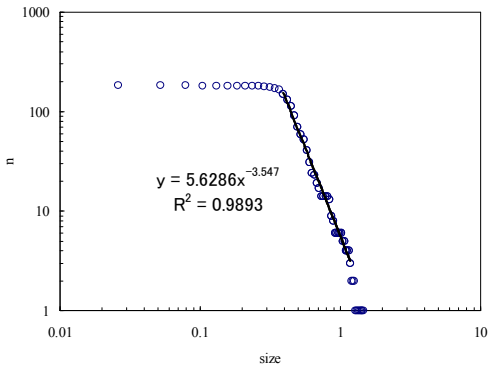

Fig.3 Cumulative size distribution of branch widths.

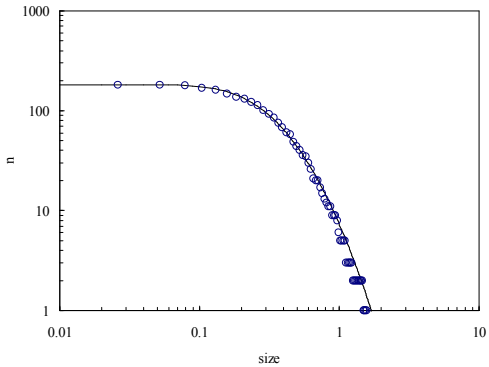

Fig.4 Cumulative size distribution of branch gaps.

Self-propelled motion of a fluid droplet under chemical reaction

Shunsuke Yabunaka

Department of Physics,
Kyoto University, Kyoto 606-8502, Japan

Self-propelled motion of particles has attracted much attention from the viewpoint of non-linear physics far from equilibrium. There are several experiments of self-propulsion of a fluid droplet[1]. It has been known in numerical simulations of a reaction-diffusion equations that there is a bifurcation from a motionless state to a propagating state by changing system parameter[2]. The domain dynamics near the drift bifurcation in a reaction-diffusion system was investigated theoretically[3].

We studied self-propelled dynamics due to a Marangoni effect and chemical reaction by extending the previous studies in the reaction-diffusion systems [4]. We introduced a model system of phase separating binary mixture where a chemical reaction takes place inside a droplet. The free energy of this model is given in terms of $\phi = \phi_A - \phi_B$ by

$$F\{\phi\} = \int d\vec{r}\left[\frac{B(c)}{2}(\nabla\phi)^2 + f(\phi) + c\ln c\right], \tag{1}$$

where $\phi_A(\phi_B)$ is the local concentration of the component A(B). c is the density of the third dilute component. $f(\phi)$ is a free energy density such that phase separation takes place at low temperatures. $B(c) = B_0 + B_1 c > 0$ and the surface tension $\sigma = \sigma_0 + c\sigma_1 > 0$ is assumed to depend linearly on c. The time-evolution equation for ϕ is given by

$$\frac{\partial\phi}{\partial t} + \nabla\cdot(\vec{v}\phi) = \nabla^2\frac{\delta F}{\delta\phi} \tag{2}$$

$$\frac{\partial c}{\partial t} + \nabla\cdot(\vec{v}c) = D\nabla^2 c - \gamma c + A\theta\left(R - |\vec{r} - \vec{r}_G|\right) \tag{3}$$

The third component diffuses away from the droplet and influences the interfacial energy. The coefficient A stands for the strength of the production of the component c inside a droplet.

We derived the following equation of the time evolution of the center of the mass of the droplet [4].

$$m\dot{u}^\alpha = (-1+\tau)u^\alpha - g u^\alpha |u|^2 \tag{4}$$

Here m, τ, and g are positive coefficients when $A\sigma_1 > 0$. Equation (4) clearly indicates that there is a bifurcation from a motionless state to a propagating state by changing the strength of the Marangoni effect. The bifurcation parameter τ is given as

$$\tau = -M\left.\frac{\partial Q_2}{\partial s}\right|_{s=R}, \tag{5}$$

where $M = \frac{2\sigma_1}{15\eta_0}$, $Q_n(s) = A\int_{\vec{q}} G_q S_q e^{-i\vec{q}\cdot\vec{s}}$, $G_q = \frac{1}{D(q^2+\beta^2)}$, $\beta = \sqrt{\frac{\gamma}{D}}$, and $S_q = \int d\vec{r} e^{-i\vec{q}\cdot\vec{r}}\theta(R-(\vec{r}-\vec{r}_G))$.

REFERENCES

1. A. Shioi, T. Ban and Y.Morimune, *Entropy* **12,** 2308 (2010).
2. K. Kricher and A. Mikhailov *Phys. Rev. Lett.* **73** 3165 (1994).
3. T. Ohta *Physica D* **151** 61 (2001).
4. S. Yabunaka, T. Ohta, and N. Yoshinaga (in preparation).

Velocity correlations of a discrete-time TASEP in stationary state on a circle

Yasuyuki Yamada, Makoto Katori

Department of Physics, Faculty of Science and Engineering, Chuo University, Kasuga Bunkyo-ku, Tokyo 112-8551, Japan

Totally asymmetric simple-exclusion process (TASEP) is a minimal statistical-mechanics model for driven diffusive systems of many particles with hardcore exclusive interaction. The discrete-time version of TASEP in a stationary state on a finite one-dimensional lattice is studied with the periodic boundary condition [1]. We consider the parallel update rule for hopping.

The hopping probability is denoted by p. Let L and N be the numbers of particles and vacancies, respectively, and $1 \le k \le L$. We pick up k distinct particles arbitrarily. We define the k-particle velocity correlation function $F_{L,N}(k)$ as the expectation value of a product of velocities of k particles in stationary distribution. We obtained the expressions

$$F_{L,N}(k) = \frac{p^k}{Z_{L,N}} \sum_{s=0}^{k} (-1)^s \binom{k}{s} Z_{L-s,N}$$

$$= \frac{p^k}{LF(L+1,N+1;2;1/(1-p))} \sum_{s=0}^{k} (L-s) \binom{k}{s} \left(\frac{1-p}{p}\right)^s F\left(L-s+1, N+1; 2; \frac{1}{1-p}\right),$$

where $Z_{L,N}$ is the partition function studied by M. Kanai *et al.* [2] and $F(\alpha,\beta;\gamma;z)$ is the Gauss hypergeometric function. The result does not depend on the choice of particle positions, but depends only on the total number k of particles, whose velocity correlation is calculated. This special property comes from the fact that the distribution function in the stationary state is given by a factorized form.

Then covariance of velocities of two particles is obtained from $F_{L,N}(k)$ with $k = 1$ and 2. Let V and V' denote velocities of two particles at different sites. The result is given by [1]

$$\mathrm{Cov}_{L,N}[V,V'] = (1-p)^2 \left\{ \frac{(L-2)F(L-1,N+1;2;1/(1-p))}{LF(L+1,N+1;2;1/(1-p))} - \left(\frac{(L-1)F(L,N+1;2;1/(1-p))}{LF(L+1,N+1;2;1/(1-p))} \right)^2 \right\}.$$

We have checked the validity of this result by comparing it with the numerical simulation data as shown by Fig. 1. We proved that the covariance of velocities becomes zero asymptotically in the thermodynamic limit

$$\lim_{\substack{L\to\infty, N\to\infty; \\ \rho=\text{const.}}} \mathrm{Cov}_{L,N}[V,V'] = 0,$$

where $\rho(= L/(L+N))$ denotes the density of particles. Fig. 2 shows the numerical data demonstrating $\mathrm{Cov}_{L,N}[V,V'] \to 0$ as $K(= L+N) \to \infty$. In the presentation, we will report these results in detail.

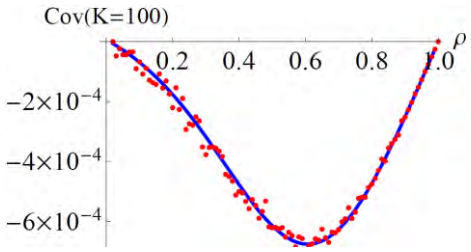

Fig. 1 The covariance of velocity plotted versus the density for $K = 100, p = 0.5$.

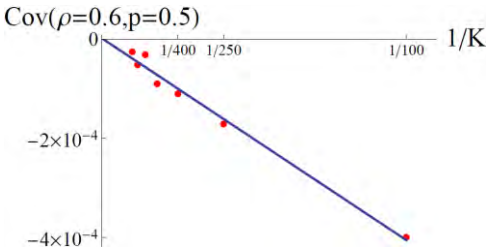

Fig. 2 Numerical fitting of the covariance of velocities evaluated by computer simulation versus $1/K$ for $p = 0.5$, $\rho = 0.6$.

REFERENCES

1. Y. Yamada, M. Katori, *Phys. Rev.* E **84,** 041141 (2011).
2. M. Kanai, K. Nishinari, T. Tokihiro, *J. Phys.* A **39**, 9071 (2006).

Large stress fluctuations in sliding friction of polymer gels

Tetsuo Yamaguchi

Department of Applied Physics, School of Engineering,
The University of Tokyo, 7-3-1 Hongo, Bunkyo-ku, Tokyo, Japan

We report on experimental studies of spatio-temporally heterogeneous stick-slip motions in the sliding friction between a hard polymethyl methacrylate (PMMA, plexiglass) block and a soft poly-dimethyl siloxane (PDMS, silicone) gel plate. We observe large and rapid slip events preceded by an alternation of active and less active periods. The probability distributions of the force drop, a quantity analogous to seismic moment, obey a power law similar to Gutenberg-Richter's empirical law for the frequency-size statistics of earthquakes, and the exponents of the power law vary with the plate velocity. We propose a simple model to explain this velocity dependence. Finally, we introduce our preliminary results on the visualization of shear stress fields during stick-slip cycles. We observe a significant change in spatial patterns of the stress field towards a large slip event.

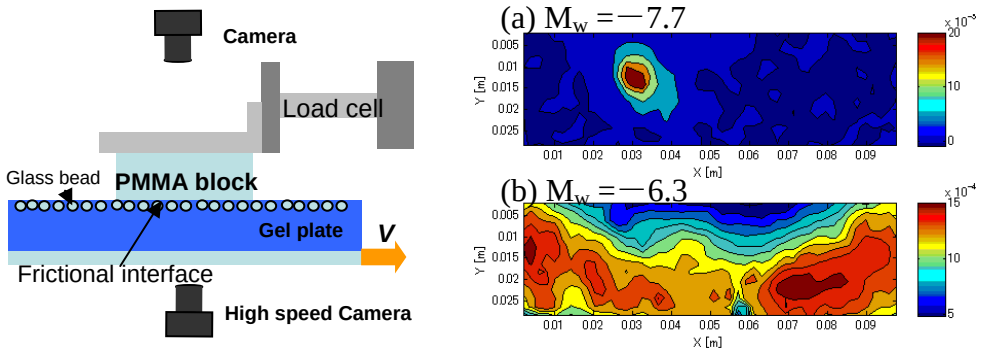

Fig.1 (a) Experimental setup, (b), (c) slip distributions of two events.

REFERENCES

1. T. Yamaguchi, S. Ohmata, M. Doi, J. Phys.: Condens. Matter 21, 205105 (2009).
2. M. Morishita, M. Kobayashi, T. Yamaguchi, M. Doi, J. Phys.: Condens. Matter 22, 365104 (2010).
3. T. Yamaguchi, M. Morishita, M. Doi, T. Hori, H. Sakaguchi, J.-P. Ampuero, J. Geophys. Res., in press.

Lognormal behavior in crease patterns of origami

Ken Yamamoto and Yoshihiro Yamazaki

Department of Physics, School of Advanced Science and Engineering,
Waseda University, Okubo 3-4-1, Shinjuku-ku, Tokyo, Japan

Origami is Japanese traditional arts of paper folding, and now it is familiar to many people around the world. One way to illustrate how to make an origami work is a crease pattern, where all or most of the creases are projected into one image. In a crease pattern, a sheet of paper is divided into many „cells" by the creases. In this presentation, we show that the size distribution of the cells in a crease pattern is close to a lognormal distribution, and explain its reason.

We selected four origami works in our analysis: Goliath Beetle, Roosevelt Elk (both designed by Robert Lang), Angel (designed by Satoshi Kamiya), and Shrimp (designed by Jason Ku); the numbers of cells are respectively 262, 690, 499, and 648. The crease patterns of them are available online as electronic figure files [1], and the size of a cell can be measured by simply counting the pixels inside the cell. Figure 1 is the cumulative cell-size distribution of Shrimp, and a lognormal distribution is drawn. The other three works also have lognormal behavior of the cell-size distributions in common.

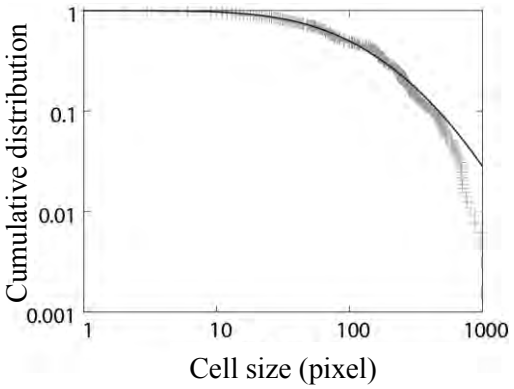

Fig.1 The cumulative cell-size distribution of the origami Shrimp. The solid curve is a lognormal distribution.

A lognormal distribution normally appears in a system exposed to multiplicative effect [2]. In origami, a sheet of paper usually becomes compact and multi-folded as the making process gets along. Multi-folded sheets are further folded at once, and it gets thicker and thicker. We think that this feature acts as a multiplicative effect in origami so that the cell sizes obey a lognormal distribution. Figure 2 illustrates a making process of a simple origami of „waterfowl," and the evolution of the creases [panel (b)] is similar to a multiplicative fracture.

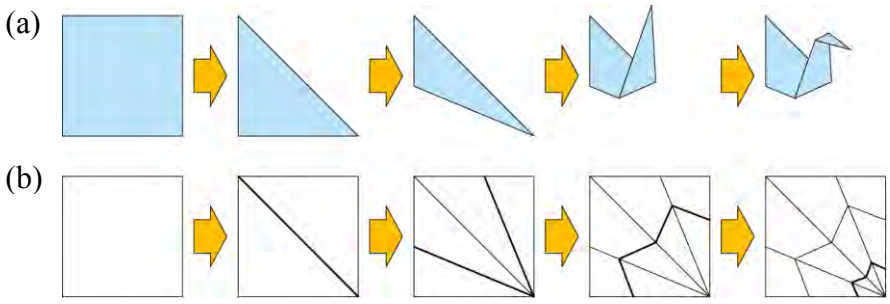

Fig. 2 The process of making an origami „waterfowl": (a) a folding diagram, and (b) evolution of creases (the new creases in each stage are indicated as the bold lines).

REFERENCES

1. The crease patterns can be obtained from the following web pages:
   a) http://www.langorigami.com (Robert Lang)
   b) http://www.folders.jp (Satoshi Kamiya, in Japanese)
   c) http://scripts.mit.edu/~jasonku (Jason Ku)
2. Kobayashi, N. *et al.* "Statistical Features of Complex Systems –Toward Establishing Sociological Physics–", *J. Phys. Soc. Jpn.*, 80, 072001 (2011).

Hierarchical mechanism of development of local society
- statistical mechanics study of premodern local society-

Miki Yamamoto

Institute for Research on Earth Evolution, JAMSTEC,
Yokohama Institute for Earth Sciences, Kanazawa-ku, Yokohama, Japan

Dynamics of society is one of the most familiar everyday phenomena that Terada explored. In society, many social phenomena self-organize from the interactions between a large number of individuals. When a social community is sufficiently large, the collective behavior of individuals should be independent of the details of interactions and individual attributes, and therefore statistical physics considerations can be applied to understand social phenomena. Under these considerations, various statistical data analyses and modeling studies of the society have recently been conducted. However, the pitfall of such approaches is that it often assumes unmeasurable parameters in mathematical models such as human attributes. Therefore, the comparison with real-world social phenomena is often merely qualitative, while models are studied quantitatively in great detail. Moreover, it is not possible to discriminate meaningfully between competing models. These difficulties weaken attempts to apply mathematical consideration to social dynamics.

To achieve a quantitative study of society, we must pay attention of the observable social parameters. For example, the behavior of people is not restricted to economic actions, but also includes various important social actions such as marriage, parenting, living together, and working. Traditional sociology has clarified that these nonecnomic activities also depend on economics, and economic behavior and noneconomic behavior interact. To understand all the related human activities, some sociologists developed a method to rely not only on statistical indices but also microscopic components of society. For instance, in the first attempt, Henry demonstrated that it is possible to reconstruct a life trajectory of an individual in the past using old documents, which contained information about people living in the municipality such as name, age, sex, and sometimes special events such as marriage, birth, and death [1]. His technique might contribute to compensating the pitfalls of the previous model-based studies

In this presentation, we combine Henry's techniques with statistical physics. We study the development of the wealth distribution of a Japanese premodern society, which is the first investigation of premodern Japanese society by using statistical physics consideration. Data analysis shows that the wealth distribution has a well-known universal power-law tail throughout the observed period, while the Pareto index gradually decreases with time. We further show that the noneconomic social properties, such as the household number, average family size, and number of collaterals in a household, of the local society, also have decreasing or increasing trends throughout the observed period. We propose a hierarchical model of social development composed of two associated hierarchies, each of which describes economic and noneconomic activities in society, respectively. The model is designed to explain the development of wealth distribution and social structure over 50 years in a premodern Japanese local society. We show that the hierarchical model consistently demonstrates the correlations of these economic and noneconomic properties [2].

REFERENCES

1. L. Henry and A. Blum, eds., "*Techniques d'Analyse en Demographie Historique"* (INED, Paris, 1988).
2. Miki Y. Matsuo "Hierarchical mechanism of development of wealth and structure for a premodern local society", PHYSICAL REVIEW E 83, 066110 (2011).

Collective behavior of bistable units with global and asymmetric local interactions

Yoshihiro Yamazaki

Department of Physics, School of Advanced Science and Engineering, Waseda University, Okubo 3-4-1, Shinjuku-ku, Tokyo, Japan

Collective behaviors of coupled units have been studied extensively from the viewpoint of nonlinear dynamics and non-equilibrium statistical physics, for example synchronization in coupled oscillators, collective motion in interactive self-propelled particles, and so on. Recently, we have found that the dynamics in peeling an adhesive tape can be also described by the collective dynamics of coupled units showing the state of peeling front[1, 2]. In our experiment, it is found that there exists two types of peeling front depending on the stability of a characteristic structure, called tunnel structure, formed in peeling front . The size of the tunnel structure is quite regular, and peeling front can be represented by a group of the units aligning one dimensionally. From our experimental results, we can extract the following features for the dynamics of the units.

(1) The unit determines the relation between the state and the adhesive force, and has bistability with respect to the state (stable state and unstable state for the tunnel structure) for a fixed adhesive force.
(2) At the interface between the two different peeling states coexisting in the peeling front, the tunnel structure has a tendency to break up, and the interface moves to increase the region of unstable state. On the other hand, the reverse motion to increase the stable state region does not occur at the interface. This means that the interface motion can be described by a local asymmetric interaction between the units.
(3) The unit affects the peel force as an external effect. The peel force depends both on the stiffness of the peeling system and peel speed, and this effect can be represented by global interaction of the units.

Based on these features, we have proposed a simple dynamical model for the collective dynamics of the units. When the peeling front is composed of N units, and the state variable of j-th unit is denoted by ϕ_j ($j = 1 \sim N$), the model is described as

$$\begin{cases} \tau \dot{u} = (\overline{\phi} - V) - u, \\ \dot{\phi}_j = f_0(\phi_j) + f_{\mathrm{sp}}(\{\phi_j\}) - u + \xi_j, \end{cases}$$

where τ is the constant representing the stiffness of the system, u corresponds to the peel force, $\overline{\phi}$ means the average of ϕ_j ($j = 1 \sim N$), V corresponds to the peel speed. Moreover, $f_0(\phi_j)$ shows the response of the bistable unit ϕ_j to the peel force, $f_{\mathrm{sp}}(\{\phi_j\})$ shows the local interaction between the units, and ξ_j is a noise term. Especially, in the hard limit case of the system (i.e. $\tau \to 0$), this model turns out to be written as

$$\dot{\phi}_j = f_0(\phi_j) + f_{sp}(\{\phi_j\}) - \left(\overline{\phi} - V\right) + \xi_j.$$

This equation shows the collective dynamics of the bistable units with global and asymmetric local couplings. And the essence of this dynamics is competition between regulation of ratio of the two unit states by the global coupling and directional transition from stable to unstable states by the asymmetric local coupling.

REFERENCES

1. Y. Yamazaki, A. Toda, *Physica D*, 214, 120-131 (2006).
2. Y. Yamazaki, *Prog. Theor. Phys.* 125, 641-652 (2011).

Collective motion of hooded gull

Makoto Yomosa[1], Tsuyoshi Mizuguchi[1, 2] and Yoshinori Hayakawa[3]

[1] *Department of Mathematical Sciences, School of Engineering, Osaka Prefecture University, 1-1 Gakuen-cho, Nakaku, Sakai, Osaka, 599-8531, Japan*

[2] *JST, PRESTO, 4-1-8 Honcho, Kawaguchi, Saitama, 332-0012, Japan*

[3] *Center for Information Technology in Education, Tohoku University, 41 Kawauchi, Aoba-ku, Sendai, Miyagi, 980-8576, Japan*

Recently, with the development of measurement devices such as GPS or stereo camera systems, it becomes possible to obtain time series of three-dimensional position data of several kinds of birds. And studies on the collective motions of birds in flocks based on real data are increasing [1][2][3].

We focus on flocks of hooded gull (*Larus ridibundus*) which come and go between colony aggregation site along Yamatogawa river in Osaka. Three-dimensional positions of individuals in flocks are reconstructed from movies taken by portable stereo camera system. By analysing the data, two flight modes, i.e., flapping and gliding mode, are observed, which are distinguished by an oscillation amplitude of the vertical velocity component of each individual.

The correspondence between the oscillation and the flapping motion is confirmed by comparing the time series of individual's shape changing and the vertical velocity component. The shape of an individual is characterized by the aspect ratio of its image as shown Fig. 1. Figure 2 shows time series of the vertical velocity component (top) and the aspect ratio (bottom) of one individual which flies alone. Switching between the flapping mode and the gliding mode represented by the aspect ratio well coincides with the change of oscillation amplitude of the vertical velocity component.

We also analyse collective behaviour of the flocks such as flapping frequency dependence on the number of individuals in flocks.

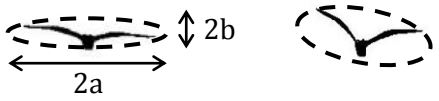

Fig.1 The aspect ratio, a/b, obtained from an ellipse which fits the individual image. Left and right figures represent different timings of flapping motion.

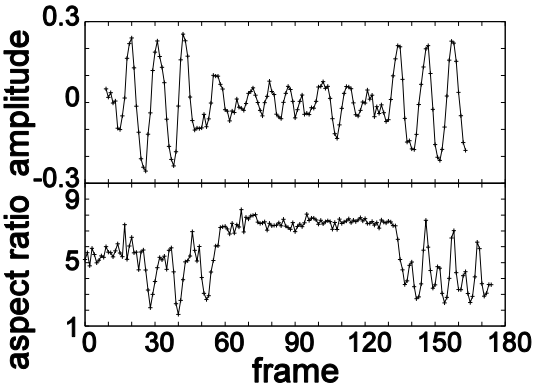

Fig.2 Time-series of oscillating motion in the vertical velocity component (top) and the aspect ratio (bottom).

REFERENCES

1. M. Ballerini *et al.* "Interaction ruling animal collective behavior depends on topological than metric distance: Evidence from a field study", *PNAS* **105**, 1232 (2008).
2. Y. Hayakawa "Spatiotemporal dynamics of skeins of wild geese", *Europhys. Lett*. **89**, 48004 (2010).
3. M. Nagy *et al.* "Hierarchical group dynamics in pigeon flocks", *Nature* **464**, 890 (2010).

Spontaneous Reverberation in a Growing Neuronal Network

Yu-Ting Huang[1,2], Yu-Lin Cheung[1], Chun-Chung Chen[3], Pik-Yin Lai[2] and C. K. Chan[1,2],

[1] *Institute of Physics, Academia Sinica, Nankang, Taipei, Taiwan*,

[2] *Department of Physics, National Central University, Chungli, Taiwan*,

[3]*Physics Division, National Center for Theoretical Sciences, Hsinchu, Taiwan*

Firing patterns of a growing neuronal network are studied in a multi-electrode array system to understand the mechanism of spontaneous generation and termination of network activities. Synchronized bursting is observed in the cultures a few days after plating. We find that the synchronization of spikes within the bursts can be understood as network reverberations which have a time scale of 100 ms while the time scale of the synchronization of the network is set by the depletion of neuronal vesicles which can be of the order of seconds. However, as the cultures mature, the synchronization of the spikes within the burst disappear indicating that there is either a change of dynamics or a change in structure of the network. Results from simulation of reverberation model suggest that the disappearance of spike synchronization is probably due to a change in the network structure.